Distribution Statement

Distribution A: Public Release.

The views presented here are those of the author and are not to be construed as official or reflecting the views of the Uniformed Services University of the Health Sciences, the Department of Defense or the U.S. Government.

F. Edward Hébert School of Medicine
Uniformed Services University of the Health Sciences

Neuroinflammation and Sensorimotor Dysfunction in a Mouse Model of Mild Cortical Contusion Traumatic Brain Injury and the Therapeutic Potential of Human induced Pluripotent Stem Cell-Derived Neural Cell Transplantation

Dissertation submitted to the
Faculty of the Neuroscience Graduate Program
in candidacy for the degree of
Doctorate of Philosophy, Ph.D.

Department of
Anatomy, Physiology & Genetics

By
Michael Denzel Nieves

Bethesda, Maryland
July 2021

UNIFORMED SERVICES UNIVERSITY OF THE HEALTH SCIENCES
SCHOOL OF MEDICINE GRADUATE PROGRAMS
Graduate Education Office (A 1045), 4301 Jones Bridge Road, Bethesda, MD 20814

APPROVAL OF THE DOCTORAL DISSERTATION IN THE NEUROSCIENCE GRADUATE PROGRAM

Title of Dissertation: "Neuroinflammation and Sensorimotor Dysfunction in a Mouse Model of Mild Cortical Contusion Traumatic Brain Injury and the Therapeutic Potential of human induced Pluripotent Stem Cell-Derived Neural Cell Transplantation"

Name of Candidate: Michael Nieves
Doctor of Philosophy Degree

DISSERTATION AND ABSTRACT APPROVED:

DATE:

ARMSTRONG.REGINA.C.1228898755 Digitally signed by ARMSTRONG.REGINA.C.1228898755 Date: 2021.07.26 15:37:05 -04'00' 7/26/21

Dr. Regina C. Armstrong
DEPARTMENT OF ANATOMY, PHYSIOLOGY & GENETICS
Committee Chair

[redacted] 6/25/21

Dr. Martin L. Doughty
DEPARTMENT OF ANATOMY, PHYSIOLOGY & GENETICS
Dissertation Advisor

[redacted] 6/25/21

Dr. Joseph T. McCabe
DEPARTMENT OF ANATOMY, PHYSIOLOGY & GENETICS
Committee Member

[redacted] 6/25/21

Dr. Kimberly R. Byrnes
DEPARTMENT OF ANATOMY, PHYSIOLOGY & GENETICS
Committee Member

[redacted] 6/25/21

Dr. Andrew L. Snow
DEPARTMENT OF PHARMACOLOGY & MOLECULAR THERAPEUTICS
Committee Member

ACKNOWLEDGEMENTS

I am grateful for every interaction I've had that's culminated in this piece of work: for the grand sacrifices and minute gestures alike. Every kindness is indelible.

To my PI and chief mentor Dr. Martin Doughty: Thank you for accepting me into your lab and continually pushing me toward excellence. Thank you for your patience, honesty, trust, and wisdom as I defined and grew into my role. I believe we both learned our lessons.

To members of my thesis and qualifying exam committees: Dr. Kimberly Byrnes, Dr. Joseph McCabe, Dr. Regina Armstrong, Dr. Andrew Snow, and Dr. Sharon Juliano. Thank you for your insights, encouragement, and advocacy as I made my way. Thank you for the small conversations that allowed my curiosity to flourish. My committee choices were some of the few decisions that did not disappoint. I am proud to have received mentorship and guidance from each of you.

To the colleagues that I knew as teachers: Qiong Zhou, Anastasia Efthymiou, Dr. Fritz Lischka, Dr. Krislaine Radomski, Dr. Orion Furmanski; and to the experts I knew as tutors: Amanda Fu, Laura Tucker, Dr. Dennis McDaniel, and Dr. Cara Olsen. Thank you for helping me climb steep learning curves. Every original finding within these pages derives from your generosity.

To the bodies that made my presence at USUHS possible: the Graduate Program in Neuroscience, the Center for Neuroscience and Regenerative Medicine, the Henry M. Jackson Foundation, and the Graduate Education Office. Thank you to Tina Finley, Laura Cutler, Danielle Hawkins, and Gale Morgan for going above and beyond to accommodate uncommon circumstances.

And ultimately, to the family—through blood or bond—who've shared with me courage like a flame. Thank you Mom & Dad for your loving support. Thank you Dr. Edwin Obaña and Dr. Maria Sanchéz for your kindred embrace. Thank you to my sisters Gabby, Alicia, and Xiomara for lifting my spirit and grounding my head. And thank you to my brother Daniel for awakening the academic in me. Thank you all for your exemplary tenacity, audacity, grit.

DEDICATIONS

For my *abuela* Juanita and my young aunt Jeannie, who I could've known better had neuroregenerative therapies been available in their times.

And for every educator that gave this kid from the Bronx a chance—

for every kid that deserves one too.

COPYRIGHT STATEMENT

The author hereby certifies that the use of any copyrighted material in the dissertation entitled: **Neuroinflammation and Sensorimotor Dysfunction in a Mouse Model of Mild Cortical Contusion Traumatic Brain Injury and the Therapeutic Potential of human induced Pluripotent Stem Cell-Derived Neural Cell Transplantation** is appropriately acknowledged and, beyond brief excerpts, is with the permission of the copyright owner.

Michael Denzel Nieves

July 2021

DISCLAIMER

The views presented here are that of the author and are not to be construed as official or reflecting the views of the Uniformed Services University of the Health Sciences, the Department of Defense, or the U.S. Government.

ABSTRACT

Traumatic brain injury (TBI) remains a significant health and economic burden as a major contributor to death and disability. The failure to generate effective therapies is often attributed to the heterogeneous nature of injury mechanisms and outcomes which challenge preclinical modeling. In addition to injury severity and pre-existing vulnerabilities to brain damage, biologic sex represents a significant yet complex variable in TBI pathogenesis. Acute trauma to the brain initiates a cascade of metabolic and biochemical changes directed by neuroinflammatory processes that can prolong injury, hinder restoration, and lead to chronic neurodegeneration. Stem cell (SC)-based therapies are a promising approach to address neuroinflammation following brain injury and promote neuro-restorative processes, yet treatment strategies remain to be optimized for clinical use.

We have modified and characterized a focal cortical contusion impact (CCI) model of trauma to the left forebrain in adult C57BL/6 male and female mice. Behavioral observations of sensorimotor integration and gait-adjusted ambulation indicated dysfunction of topographically defined neurological circuits cognate to the impacted cortical area. Immunohistochemical staining and unbiased stereological counting confirmed robust astroglial and microglial activation without significant neuronal loss or tissue cavitation. Multiplex electrochemiluminescent immunoassays of the impacted cortical area further revealed elevation of cytokines and chemokines (C/Cs) indicative of innate but not adaptive immune processes.

We further used our model of sensorimotor brain injury to optimize cell transplantation strategies of isogenic human induced pluripotent SC (hiPSC)-derived

neural stem cells (NSCs), neuroblasts (Nbs), and astrocytes. Immunohistochemistry revealed survival, adaptation, and integration of transplanted NSCs and Nbs, but not astrocytes into the host parenchyma along white-matter tracts. Histology and behavioral testing further demonstrated that the effects of engrafted cells on host gliosis, neuronal survival, and sensorimotor recovery depend on the interactions of injury severity, transplant cell phenotype, and host sex; female mice exhibited superior functional recovery compared to their male counterparts in an injury-dependent manner.

These data serve to provide a framework through which rodent models of TBI can be developed and characterized to recapitulate unique pathology, to optimize promising therapeutic strategies, and to determine the role of sex as a biologic variable in brain injury.

TABLE OF CONTENTS

LIST OF TABLES

LIST OF FIGURES

LIST OF ABBREVIATIONS

ALM	Anterior-lateral motor area
ALS	Amyotrophic Lateral Sclerosis
AP	Anterior-posterior
ART	Adhesive Removal Test
BBB	Blood-brain barrier
BM-MSC	Bone Marrow-MSC
BW	Beam Walk Test
C/C	Cytokines and chemokines
CCI	Controlled cortical impact
CFA	Caudal forelimb area
GCS	Glasgow Coma Scale
CHI	Closed-head injury
CNS	Central Nervous System
CsA	Cyclosporin A
CSF	Cerebrospinal fluid
CT	Computed Topography
D	Day
DAB	Diaminobenzidine
DAI	Diffuse axonal injury
DAMP	Damage-associated molecular patterns
Dcx	Doublecortin
EPO	Erythropoietin
FrA	Frontal association are
GFAP	Glial fibrillary acidic protein
h	hour
HA	Hindlimb area
hiPSC	Human induced pluripotent stem cell
HLA	Human leukocyte antigen
hNA	Human nuclear antigen
hNSC	Human neural stem cell
HR	Hazard ratio
Iba1	Ionized calcium-binding adapter protein-1
ICP	Intracranial pressure
IL	Interleukin

iPSC	induced pluripotent stem cell
LOC	Loss of consciousness
M1	Primary motor area
M2	Secondary motor area
ML	Medial-lateral
MRI	Magnetic Resonance Imaging
mRNA	Messenger ribonucleic acid
MSC	Mesenchymal stem cell
mTBI	Mild traumatic brain injury
NeuN	Neuronal Nuclei
NVU	Neurovascular unit
OPC	Oligodendrocyte progenitor cell
PCA	Principal Component analysis
PI	Post-injury
PTA	Post-traumatic amnesia
RFA	Rostral forelimb area
ROI	Region of interest
ROS	Reactive oxygen species
S1BF	Primary somatosensory barrel field area
S1FL	Primary somatosensory forelimb area
S1HL	Primary somatosensory hindlimb area
S1J	Primary somatosensory jaw area
S1Sh	Primary somatosensory shoulder area
S1Tr	Primary somatosensory trunk area
S1ULp	Primary somatosensory upper lip area
S2	Secondary somatosensory area
SC	Stem cell
SCI	Spinal cord injury
TAI	Traumatic axonal injury
TBI	Traumatic brain injury

CHAPTER ONE

INTRODUCTION

TRAUMATIC BRAIN INJURY AS A DEVASTATING BRAIN DISEASE

Traumatic brain injury (TBI) is a significant health and economic burden globally and within the United States specifically (28; 32). As a leading cause of morbidity and disability in young people (less than 45 years), TBI is a hallmark injury of US uniformed service members. Between the years 2002-2006, the overall incidence rate of TBI in the US was approximately 1.7 million cases per year and the approximate death count was upwards of 52,000 US citizens annually (45). As recently as 2017, injury to the head represented a quarter (24.5%) of all emergency department visits (152). Additionally, moderate to severe TBI disables 80,000 persons annually (48) and the total annual cost of TBI was estimated to be 60.43 billion US dollars for the year 2000 (45). Despite decades of research and clinical trials, pharmacological efforts to treat TBI have not been approved. The standard of care for acute TBI remains monitoring and maintaining physiological intracranial pressure (ICP), systemic blood pressure, and caloric intake to prevent secondary injuries (21; 115).

The failure to develop more effective treatments is often credited to the multifaceted and heterogeneous nature of TBI pathophysiology (168). Primary injury to the brain can result from blunt force trauma (possibly with skull fracture), penetration of brain tissue, blast-induced deformation of brain tissue, or rapid acceleration or rotational forces acting upon the head. Blunt force to the head or rapid acceleration/torsional forces

can cause focal contusion damage to the parenchyma as well as diffuse axonal injury (DAI) and diffuse vascular injury due to stretching and shearing forces. Hemorrhagic events may present immediately in TBI or evolve over minutes to hours later, necessitating rapid assessment of intracranial bleeding and stabilization of ICP. Scattered or diffuse axonal injury (DAI) is a consistent component of most forms of TBI and a key contributor to morbidity lasting long after the injury (121). Indeed, even a single mild-severity TBI can lead to symptoms such as headache, fatigue, depression, anxiety, irritability, and post-concussive syndrome beyond 1 year post-injury, and increasing injury severity holds increased risk of long-lasting cognitive impairments (122).

Damage to neurons, glial cells, and cerebrovascular epithelia instigates cascades of biochemical and metabolic events collectively termed "secondary injury" involving cellular excitotoxicity, energy failure, oxidative stress, neuroinflammation, blood-brain barrier (BBB) dysfunction, and influx of fluid and blood components (123). These cascades foster neurotoxic or life-threatening acute conditions such as brain edema, ischemia, vasospasms, unregulated ICP, and cerebrovascular accidents (121). Secondary injuries can present at any time post-trauma and may be short-lived or persist long-term, contributing to chronic and evolving neuropathology (123). TBI increases the risk of accelerated cognitive decline and the development of chronic neurological and psychiatric disorders such as epilepsy (132), memory deficits (138), chronic headache (7), dementias (123) (94), stress disorders (76), sleep disorders (156), and sensorimotor impairments with associated balance problems (146; 212).

CLINICAL PRESENTATION OF TBI

Despite the delayed nature of chronic TBI pathology, mitigating negative outcomes can be challenging due to diagnostic and prognostic limitations. Injury severity assessment considers neuroimaging findings, length of loss of consciousness (LOC), length of post-traumatic amnesia (PTA), and the neurological function composite score Glasgow Coma Scale (GCS). Clinical neuroimaging using CT and MRI may identify gross structural injury (e.g., hemorrhage, lesion) yet cannot predict the extent of cognitive impairment. Additional experimental neuroimaging techniques may detect microstructural axonal damage or metabolic alterations following TBI, yet their utility within the clinical setting remains to be determined. Despite these advances in neuroimaging techniques, many patients with TBI do not show evidence of injury on clinical scans (100). For these and other reasons, the initial assessment of injury severity cannot rule out occult or evolving damage and does not predict the extent of morbidity or the recovery trajectory resulting from TBI (135).

Although the initial injury severity has a major influence on acute functional decline, sustained impairment or recovery within the subacute and chronic post-injury phases is further influenced by the presence of comorbidities, neurological or psychiatric resilience, and cognitive reserve (78; 114; 186). Susceptibility to injury, outcomes, and risk of comorbid conditions in TBI has been linked to biological sex as well as hormonal and reproductive status (12; 148). Additional factors influencing recovery or cognitive decline include age at the time of injury (59) and genetic predispositions (226). The multitude of factors influencing the presentation of brain trauma—and their interacting

effects on pathology—are determinants of the recovery process and contribute to the heterogeneity of TBI outcomes (Figure 1).

Blood-based biomarkers are currently sought to aid in clinical management, namely for: diagnosis of mild TBI (mTBI), identification of expanding intracranial damage, prognosis of impaired recovery in mTBI, and outcomes in severe TBI (52). Cellular constituents of brain cells and their metabolic derivatives released into circulation as a result of injury have been explored, as have stress-response proteins, damage-associated molecular patterns (DAMPs), and inflammatory mediators. Elevated cytokines and chemokines have been measured within bio-fluids after TBI, some of which correlate with injury severity, patient outcomes, and post-TBI comorbidities (67; 194). Neuroinflammation within the CNS as well as TBI-induced peripheral inflammatory events may therefore be detected using blood-based biomarkers and could provide prognostic or even therapeutic utility.

CELLULAR AND IMMUNOLOGICAL RESPONSE TO TBI

Post-traumatic neuroinflammation emerges immediately and can evolve over months to years following the initial insult (173). Damaged or permeabilized brain cells, including non-neural perivascular and meningeal cells, release DAMPs, glutamate, cytokines, and ions capable of inciting a robust acute inflammatory response (215). These activating signals also attract glial and peripheral immune cells to the injured area, and drive upregulation and release of additional soluble inflammatory mediators such as cytokines and chemokines (C/C), proteases, and extracellular vesicles (215). Glial cells of the CNS, namely astrocytes and microglia, undergo reactive gliosis in response to injury and serve as resident mediators of neuroinflammation. Additionally, infiltrating

neutrophils and monocytes appear acutely after injury followed later by T-cells, dendritic cells, and natural killer cells (173)(Figure 2). Neuroinflammatory events initiated at the time of injury can evolve over time depending on a number of interacting factors and therefore contribute to chronic neurological and cognitive disability. Enhancing our understanding of TBI-induced neuroinflammation and its effects on secondary pathology may open avenues of therapeutic and diagnostic applications to optimize patient recovery and well-being.

A significant initiating event in neuroinflammation is impairment of the BBB, a selectively permeable barrier composed of vascular epithelia connected via intercellular tight-junctions. The integrity of the tight junctions and proper regulation of selective membrane transporters is supported by additional cells collectively termed the neurovascular unit (NVU), including pericytes, astrocytes, and neurons (88). Damaged cerebrovascular epithelia contribute cytokines to the inflammatory milieu and are unable to maintain barrier function. Spillage of blood materials into the parenchyma catalyzes pro-inflammatory signaling (29) and fosters vasogenic brain edema, driving increased ICP, ischemia, or cerebral herniation (214). Cerebrovascular damage can evolve diffusely within the brain and facilitate continued and renewed neuroinflammation through long-term impaired barrier function. Therefore, chronic neurovascular dysfunction from a traumatic event may support cognitive decline and neurodegenerative pathology through vascular insufficiency, poor barrier integrity, and pro-inflammatory signals emanating from cells of the NVU itself (155; 208). Cerebrovascular remodeling and reformation of the BBB are therefore key events to limit neuroinflammation and preserve cognitive function (185).

Microglia

Microglia respond to danger signals by undergoing dramatic changes in gene expression, morphology, proliferation, and cell function. Similar to peripheral macrophages, microglia become polarized along a spectrum from pro-inflammatory (M1) function to an alternative anti-inflammatory (M2) phenotype (109). A popular hypothesis is that M1-mediated functions and subsequent inflammation are prerequisite events for regenerative and reparative processes later prompted by M2 signals (3)(Figure 2B). However, an exaggerated or prolonged pro-inflammatory disposition can incite a self-propagating hyperinflammatory state and drive secondary injury processes (110).

Importantly, it is now understood that the simplicity of the M1/M2 dichotomy does not capture the multidimensional presentation of brain microglia following neurotrauma (111). Cluster-based analysis of single-cell sequencing has also identified overlapping populations of microglia across the lifespan and during brain injury (63) as well as across brain regions (58), with little or no concordance to the M1/M2 binary. Simultaneous expression of microglial polarization markers has also been found in gene profiling studies of isolated microglia/macrophages taken from the injured brain (130) as well as gene profiling of the perilesional area (131). These studies demonstrate that at any given time point post-injury, microglia/monocytes are not dedicated to any single polar state.

Microglial phenotype plasticity is therefore appreciated as a multi-polar spectrum dependent on immediate microenvironmental cues rather than a linear construct between two extremes. Carefully directing microglial and macrophage cell phenotype toward

neuro-reparative processes is therefore an important yet complex tenet of inflammation-targeting therapeutic strategies (173).

Astrocytes

Astrocytes undergo progressive and heterogeneous changes in gene expression, morphology, proliferation, and cell function collectively termed astrogliosis (18). Astrocytic scarring of the damaged area serves to corral soluble neurotoxic mediators—demonstrated by selective ablation of scar-forming astrocytes or inhibition of scar formation (207)—thereby limiting the spatial and temporal extent of the damage. Interestingly, specific pharmacological manipulations but not prevention of the astroglial scar formation facilitate regenerative processes within the injured spinal cord, suggesting that reactive astrocytes that accrue at the site of CNS trauma are capable of acting in benefit or detriment to recovery dependent on microenvironmental cues (6; 64).

Dysfunctions of reactive astrocytes are acknowledged to exacerbate neuropathology through persistent pro-inflammatory signaling and dysfunction of key homeostatic functions such as BBB maintenance, ionic regulation, and metabolic support to neurons (103). The well-regulated astrocyte response to trauma, however, includes sequestration of cytotoxic mediators, return of normal brain stasis, provision of neurotrophics, and regeneration and remodeling of neuronal circuits and cerebral microcirculation (18). As the most abundant cell type within the CNS and the main producers of chemoattractants, astrocytes are able to reversibly direct the pro-inflammatory response of microglia as well as peripheral immune cells (103).

Peripheral Immune Cells

Peripheral immune cells can appear in contused brain tissue immediately after injury to contribute and propagate inflammation in concert with resident glial and epithelial cells. Neutrophil traffic into the CNS is attracted by damage signals from neural cells and directed by dysregulated epithelia to cross the BBB. The contribution of neutrophils to pathogenesis in experimental TBI varies depending on the experimental model and mechanism of injury (81). Invading peripheral monocytes follow chemokine gradients into the CNS and develop a macrophage phenotype (215). Monocyte-derived macrophages then work with microglia to foster tissue remodeling and regeneration, yet can develop a persistent maladaptive pro-inflammatory disposition as well. Disruption of monocyte recruitment to the brain limits damage and promotes recovery in experimental TBI (161), yet there's evidence that infiltrating monocytes are important for recovery as well in TBI (154), spinal cord injury (167), and stroke (209). The role of T-cells in TBI-related pathology remains controversial. CNS-adjacent T-cells, such as within meningeal spaces and choroid vessels, play an important beneficial role in brain homeostasis via interleukin (IL)-4 signaling (51). After injury, T-cells have been found to benefit the brain through neurotrophic signaling (204) as well as cause long-term neurological impairment and white-matter damage (30). The activation status of T-cells, their surface receptor expression, and prior exposure to CNS injury all influence the effect of T-cells on TBI pathology (40; 87). Infiltrating peripheral immune cell dynamics and their interplay with resident cells of the CNS represent an aspect of TBI pathology potentially amenable to a wide range of approved and novel therapeutic interventions (13).

Glial and immune cells of the CNS determine the magnitude and duration of neuroinflammation consequent to brain injury and thus contribute to long-term neurological dysfunction when chronically activated or dysregulated (18; 109). Furthermore, it is increasingly apparent that immune support plays a crucial role in regenerative and reparative processes after brain injury (56; 81; 129).

THERAPEUTIC TARGETING OF NEUROINFLAMMATION TO TREAT TBI

The normal time-course of glial and immune cell activation has been determined in a number of animal studies (173), however experimental evidence has shown that immune cell phenotype, behavior, and subsequent effect on outcome changes over several incidence and host variables such as injury type and severity, patient sex (173), and experimental species (129). Therapeutic interventions with immunomodulatory agents must also consider timing, duration, and dosage of treatment to accommodate the multifaceted and beneficial role of inflammation (129). Accordingly, the suitability of immune factors as therapeutic targets is not yet well defined, however addressing maladaptive neuroinflammation has become a treatment focus for TBI (129; 142; 215; 220).

Inflammation-targeted treatment strategies for TBI have included broad-acting anti-inflammatory agents as well as agents targeting specific cells, processes, or signaling axes (13). Additionally, experimental studies have employed a number of strategies which modulate the immune response through multifactorial or unclear mechanisms such as cell-based therapies, EPO administration, or nutraceuticals (220) (185). Despite the central role of inflammation in TBI pathology, clinical trials of anti-inflammatory agents have at best demonstrated no benefit of favorable outcomes and at worse even increased

mortality (42; 153; 218). The discrepancies between preclinical and clinical data suggests that efficacy of immune modulators is co-varied by pharmacological factors such as timing of first dose post-injury, dosage amount, and duration (13; 129). For instance, the therapeutic time window to address specific inflammatory targets may not overlap with the actual time of clinical presentation, and furthermore represents a moving target depending on individual pathophysiology (126). Additionally, broad-acting immunosuppressive agents—as opposed to single immune target therapy—may impair beneficial reparative processes necessary for neurorecovery during specific time periods post-injury. Targeting neuroinflammation following TBI is furthermore complicated by several host variables such as genetic variance, age, and biological sex (129; 173; 220).

Heterogeneity of therapeutic targets has led some investigators to suggest alternative therapeutic strategies. Simon et al. (2017) advocate for targeted, single-pathway strategies as part of individualized treatment to address the wide number of patient variables impacting inflammation-mediated damage (173). Drug combinations of inflammation-targeting agents is proposed as a means to extend the therapeutic time window post-injury and increase the number of engaged targets (116). Additionally, many groups have shifted treatment strategies toward enhancement of beneficial neuroinflammation by skewing the functional phenotype of immune cells rather than suppression of detrimental processes to promote regeneration (173; 220). Biopharmaceuticals, or biologics, such as stem cells (SC), SC-derived products, and growth factors tend to have pleiotropic actions as well as maintained efficacy when dosed long after the injury (126; 139), making cell-based biologics an attractive avenue of TBI treatment. An important need of experimental research therefore is modeling the variety

of TBI pathology to best construct and validate treatment strategies. The heterogeneity of TBI calls for experimental modeling over a wide range of injury subtypes and biological variability to determine the impact of these intersecting variables on potential treatment outcomes.

PRE-CLINICAL MODELS FOR THERAPEUTIC DEVELOPMENT

Several animal models of TBI have been developed to interrogate the neuroinflammatory events and test efficacy of potential therapeutics, although no single animal model can fully recapitulate all the features of human TBI (33). Furthermore, as TBI itself is notoriously heterogeneous in mechanism of injury and resulting pathology, as are outcomes in animal studies of brain trauma. Researchers have called for increased standardization of animal models and carefully connecting the model used to research outcomes and objective (33).

Experimental brain trauma pathology is often broadly classified as focal, diffuse, or mixed (112; 172) depending on the spatial extent of injury. Focal injury has traditionally required craniotomy to expose the brain for direct deformation (112), typically resulting in hematoma and tissue cavitation of the impacted cortex and sometimes subcortical gray- and white-matter structures as well (121). Variations of direct impact models allowing for rotational acceleration produce injury predominantly characterized by widespread and severe traumatic axonal injury (TAI), an important feature of human TBI related to cognitive dysfunction (83). A widely used method to produce focal injury, the controlled cortical impact (CCI) model delivers a focused contusion along experimenter-set injury parameters (velocity, depth of deformation, dwell time, impactor diameter). Although craniotomy may not replicate human TBI, the

controlled impact allows for well-defined biomechanical parameters and reproducibility compared to other models and serves as an excellent system for cellular and molecular pathophysiology. Increased severity of CCI injury parameters correlate with enhanced tissue and behavioral pathology (223), but there is not a consensus for mild, moderate, or severe injury parameters to reflect those same designations given clinically (172). Despite the widespread use of the CCI model, relatively few groups have characterized mild CCI injury in mice (<10% of CCI studies) (172).

The approach of our laboratory is to develop a mild-severity model of focal TBI which produces sustained immune-like activation and cognate behavioral deficits while sparing cortical tissue loss. By targeting topographically defined areas of the cortex associated with the sensorimotor control of distinct behaviors, we are able to track impairment of cortical function. Such a model is well-suited to interrogate cellular and molecular pathology within the impacted cortex amongst host variables such as biological sex and age, as well as in response to therapeutic avenues such as cell-based strategies (Figure 3).

STEM CELL TRANSPLANTATION THERAPY FOR BRAIN TRAUMA

Stem cell (SC)-based strategies have emerged as a potential regenerative strategy to treat TBI and are often able to limit pathological processes and accelerate functional recovery. Initially devised as a means to provide cellular replacement, SCs or SC-derived neural cells engrafted after a TBI have been found to take residence within the parenchyma and integrate into host structures. Implanted multipotent neural stem cells have been shown to differentiate toward neuronal or glial fate in a site-specific manner (41). With the exception of engrafted oligodendrocyte precursor cells (OPCs) which

successfully re-myelinate the brain, integration of transplanted cells into damaged circuitry is not considered a major mechanism of treatment benefit in TBI (41). Transplanted cells can secrete a wide variety of immunomodulatory and neurotrophic factors which benefit the injured brain. Experiments have demonstrated that infusion of SC-conditioned media or SC-derived microvesicles containing intracellular proteins and nucleic acids is able to exact the beneficial effects as well, implicating the cells' secretome as key to neuroprotection (220).

Additional host benefit is relayed by cells genetically modified to overexpress neurotrophins or anti-inflammatory cytokines, and transplant survival is enhanced by hypoxic pre-conditioning of cells (15). Cell-based therapy is further advanced with adjuvant pharmacologics to support transplant activity as well as act synergistically on host cell populations to foster regeneration such as host splenocytes and hematopoietic stem cells (228). In instances of cavitating trauma, cell transplants can include biocompatible scaffolding material such as hydrogels to provide physical substrate (96). These and other advancements in SC technology continue to optimize cell-based paradigms and enhance the potential clinical utility of cell-based neurotherapy.

Clinical trials have been performed employing transplantation of bone marrow-derived mesenchymal stem cells (BM-MSCs) in patients with TBI. Safety and feasibility has been demonstrated of transplantation via intraparenchymal, intravenous, and intrathecal routes (165; 227). Furthermore, these studies have demonstrated improved neurologic and systemic outcomes as well as reduced treatment intensity (102). Recently, transfusion of BM-MSC-derived neural-like cells were found to improve neurological outcome and increase serum levels of brain-derived neurotrophic factor and nerve growth

factor in patients with severe TBI (206). Several clinical trials of cell transplantation are also currently recruiting or underway (228).

The majority of stem cell therapy studies for TBI have been conducted using cells with limited neuronal potential when compared to an alternative source of patient-specific stem cells, induced pluripotent stem cells (iPSCs) (189; 219). iPSCs result from phenotype reprogramming of somatic cells through specific transcription factors toward a pluripotent stem cell identity. Improved reprogramming technology has eliminated the need for viral-mediated transduction and incorporated iPSC derivation into good clinical manufacturing methods, thereby enhancing patient safety for clinical potential (164). iPSCs can be generated from patients for autologous transplantation or human leukocyte antigen (HLA)-matched allogenic transplantation (192), expanding their clinical potential. Importantly, technical advances have greatly increased the efficiency and speed of iPSC-derivation (145) and refined differentiation protocols permit iPSCs to recapitulate specific cell phenotypes of the central nervous system (57; 106; 187; 224) for targeted cell replacement strategies.

Preclinical experiments have shown positive results from therapeutic transplantation of human iPSC-derived cells into models of neurologic disorders and degeneration including spinal cord injury, stroke, ALS, and retinal degeneration to name a few, however few studies have done so in rodent models of TBI (1; 4; 65; 95; 166; 195; 225). Despite widespread applicability, inter-laboratory comparisons amongst transplantation studies in TBI can be difficult due to the large number of possible variables inherent within the paradigm. The behavior of transplanted cells and their impact on pathology outcomes are directly influenced by pre-transplantation cell culture

conditions as well as transplantation parameters such as dosage, transplant site, and post-injury timing (54). Host conditions such as injury mechanism and severity as well as species and age also influence transplant and treatment outcomes.

How engrafted cells manipulate host glia and what the ensuing cellular and molecular disposition of glia may be to effect secondary pathology remains unclear. Understanding these parameters will be key towards developing successful cell-based therapeutic strategies for brain repair and regeneration.

SUMMARY

TBI represents a significant health and economic burden for which limited therapeutic avenues exist to reverse its sequelae. Neuroinflammatory processes are common to all types of brain injury and are therefore a common target of therapeutics research to treat TBI. Numerous incidence and patient variables such as injury mechanism and severity, as well as patient sex and age, amongst others, influence the extent of neuroinflammation over time, thereby impacting neurological outcomes and efficacy of treatments. To appreciate the full scope of TBI-induced pathophysiology, animal models over a wide range of injury and subject parameters have been developed and characterized to best define therapeutic opportunities. Furthermore, studies involving cell-based strategies, including stem cell (SC) or SC-derived cell transplantations, have emerged as a strategy to modulate the neuroinflammatory milieu and foster recovery following injury. The purpose of this dissertation is to characterize a mouse model of mild TBI useful for interrogating cellular and molecular dynamics of the impacted cortical tissue, and to use this model to determine the effects of stem cell intervention on behavioral, neurochemical, and histopathological features of TBI (Figure 3).

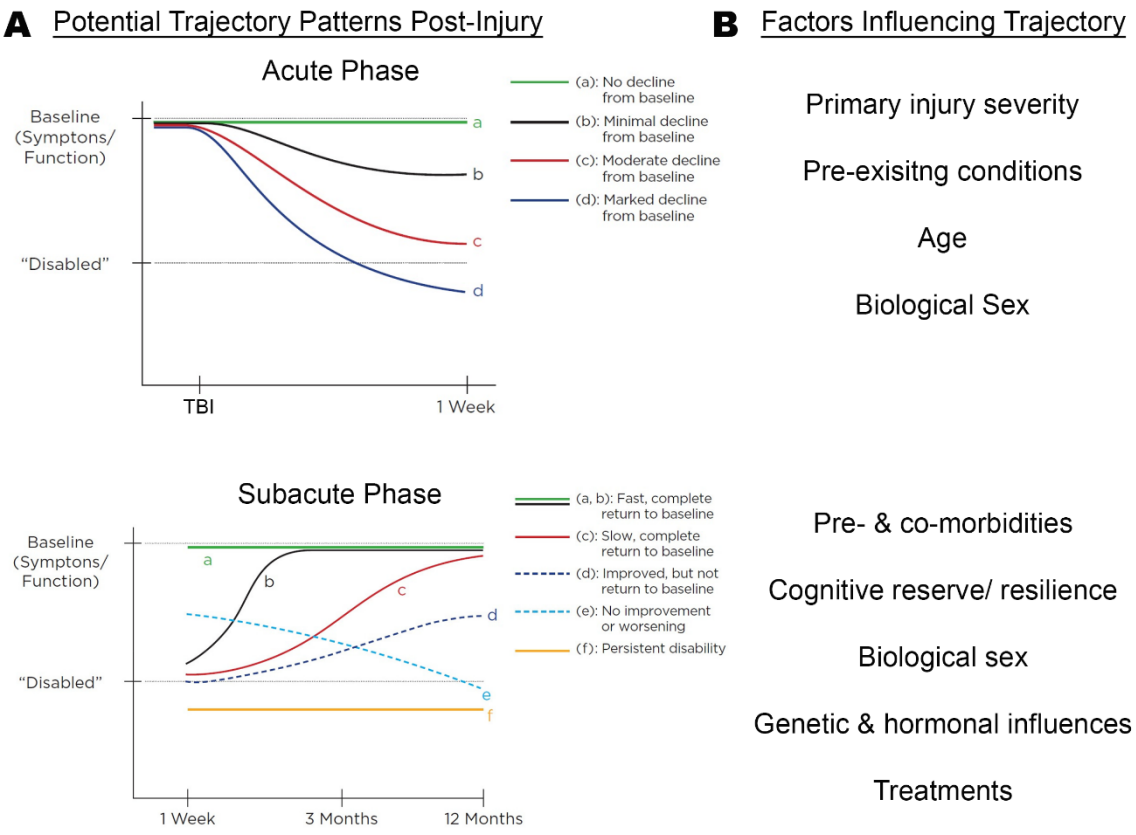

Figure 1. Conceptual model of potential trajectories of functional disability and recovery after a single TBI. **(A)** Trajectories presented during the acute (0-1 week) and subacute (1 week – 12 months) post-injury phases represent a wide range of heterogeneous patient outcomes. **(B)** Subject-level factors compound the injury progression and presentation. Adapted from NAS, 2019 (135)

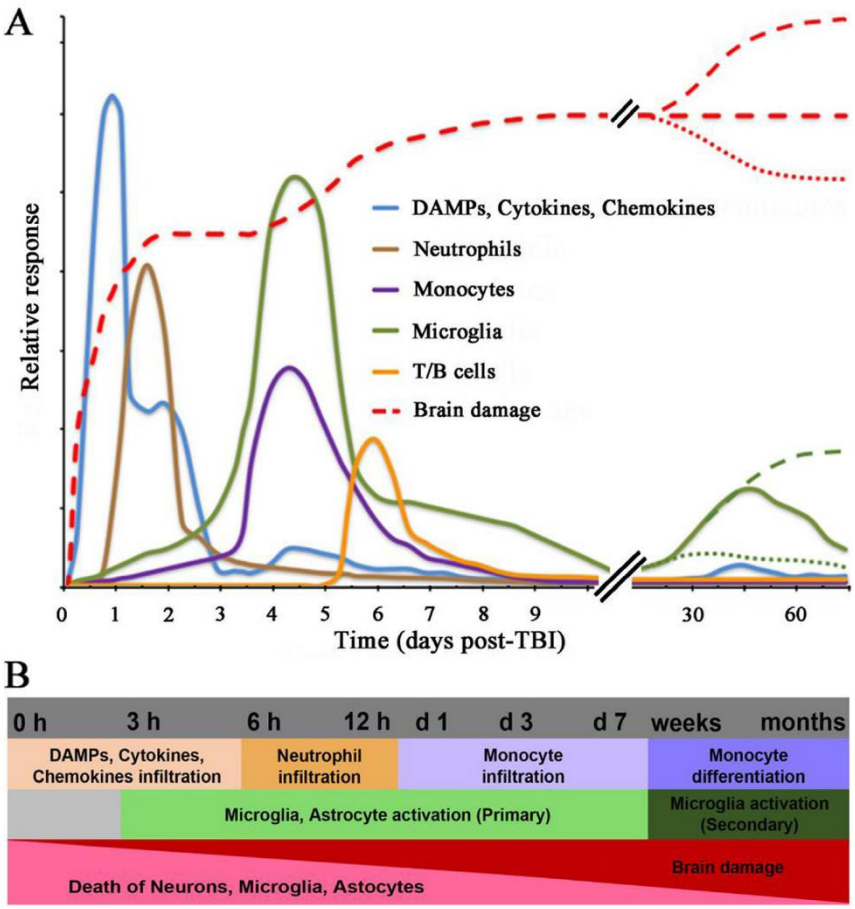

Figure 2. Simplified timeline of cellular response after TBI. **(A)** Following TBI, damaged brain cells release inflammatory activating signals (e.g., DAMPS, cytokines, chemokines) initiating a self-propagating sequence of glial (astrocyte and microglia) activation, peripheral immune cell (neutrophil, monocyte, T/B-cells) infiltration, and further release of inflammatory mediators which drive or limit brain damage. **(B)** Schematic representation to highlight the relative predominance of cellular action after TBI. Adapted from Alam et al., 2020 (3).

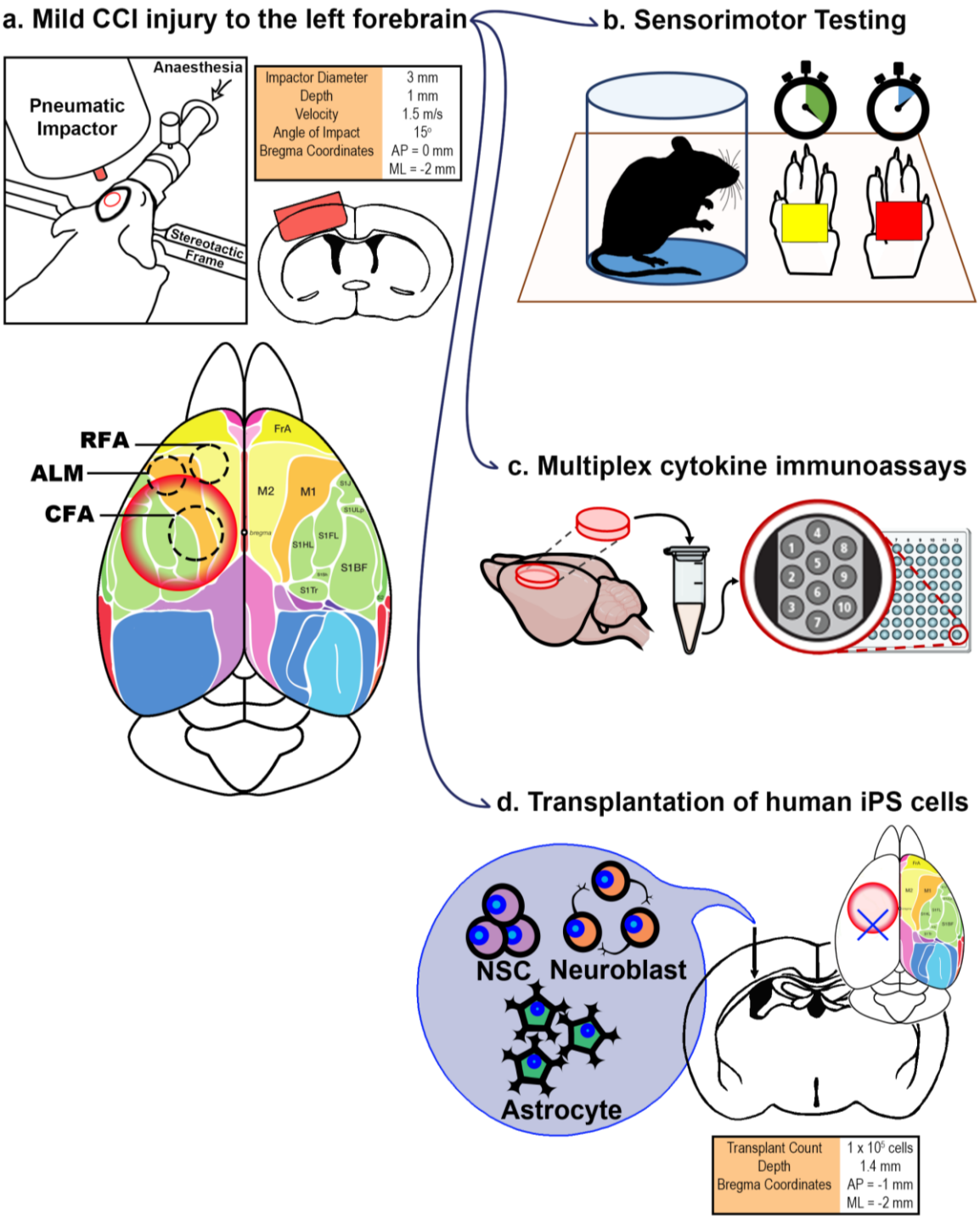

Figure 3. Project overview. **(a)** A single unilateral controlled cortical impact (CCI) contusion injury is delivered to anaesthetized mice using a pneumatic-driven impactor with pre-defined impact parameters. The impacted area (red circle) encompasses functionally defined cortical regions of the motor and somatosensory cortices. RFA, rostral forelimb area; ALM, anterior lateral motor; CFA, caudal forelimb area; FrA, frontal association; M1, primary motor; M2, secondary motor; S1FL, primary somatosensory forelimb; S1HL, primary somatosensory hindlimb; S1Sh, primary

somatosensory shoulder; S1J, primary somatosensory jaw; S1ULp, primary somatosensory upper lip; S1Tr, primary somatosensory trunk; S1BF, primary somatosensory barrel field; S2, secondary somatosensory. Adapted from Kirkcaldie et al., 2012 (90) and Hira et al., 2015 (72). **(b)** Mice were challenged with sensorimotor tasks including the adhesive removal test which quantifies the latency for animals to notice and to remove nuisance adhesives placed on their forepaw while confined to a clear Plexiglas cylinder. **(c)** Biopsy punch (5 mm diameter) of the impacted cortex is homogenized and processed through multiplex immunoassay arrays for notable cytokines and chemokines allowing for simultaneous detection of brain analytes. **(d)** Human induced pluripotent stem (iPS) cell-derived NSCs, neuroblasts, or astrocytes are transplanted via pulled-glass pipette into the deep layers of the impacted cortex at day 1 post-injury.

CHAPTER TWO

SENSORIMOTOR DYSFUNCTION IN A MILD MOUSE MODEL OF CORTICAL CONTUSION INJURY IS ASSOCIATED WITH INCREASES IN INFLAMMATORY PROTEINS WITH INNATE BUT NOT ADAPTIVE IMMUNE FUNCTIONS

ABSTRACT

Traumatic brain injury is a leading cause of mortality and morbidity in the United States. Acute trauma to the brain triggers chronic secondary injury mechanisms that contribute to long-term neurological impairment. We have developed a single, unilateral contusion injury model of sensorimotor dysfunction in adult mice. By targeting a topographically defined neurological circuit with a mild impact, we are able to track sustained behavioral deficits in sensorimotor function in the absence of tissue cavitation or neuronal loss in the contused cortex of these mice. Stereological histopathology and multiplex enzyme-linked immunosorbent assay proteomic screening confirm contusion resulted in chronic gliosis and the robust expression of innate immune cytokines and monocyte attractant chemokines IL-1β, IL-5, IL-6, TNFα, CXCL1, CXCL2, CXCL10, CCL2, and CCL3 in the contused cortex. In contrast, the expression of neuroinflammatory proteins with adaptive immune functions was not significantly modulated by injury. Our data support widespread activation of innate but not adaptive

immune responses, confirming an association between sensorimotor dysfunction with innate immune activation in the absence of tissue or neuronal loss in our mice.

KEYWORDS

Chemokine, Controlled Cortical Impact, Cytokine, Innate Immune Response, Sensorimotor, Traumatic Brain Injury

SIGNIFICANCE

We profile neuroinflammatory protein levels in the motor and sensory cortex of adult mice following a mild contusion that results in sensorimotor dysfunction, gliosis but not loss of neurons. Injury increases levels of cytokines and monocyte attractant chemokines of the innate immune system but not cytokines with adaptive immune functions. Our data demonstrate a strong association between innate immune system activation and impairment of sensorimotor activity. The absence of significant neuronal loss and the expected preservation of sensory and motor circuits in our mouse model make it ideal to investigate specific chemokine and cytokine effects on sensorimotor pathways and behaviors.

INTRODUCTION

As a leading cause of morbidity and disability, traumatic brain injury (TBI) represents a significant health and economic burden globally as well as specifically within the United States (28; 32). Additionally, incidence of TBI has been linked to the development of chronic neurological and psychiatric disorders, including epilepsy (132), memory deficits (138), headaches, dementias (94), stress disorders (76), and chronic neuroinflammation (173). Post-traumatic neuroinflammation mediates both beneficial

and deleterious effects within the brain: immediate activation of astrocytes and microglia (gliosis) limits damage and promotes debris clearance, yet prolonged or dysregulated activity of resident and infiltrating immune cells can impair restoration of normal brain stasis (81; 173). Indeed, the presence of several elevated inflammatory factors in biofluids and brain microdialysate of TBI patients has been linked to poor outcomes (101). Alleviating maladaptive neuroinflammation has therefore become a treatment focus for TBI (129; 142; 215; 220).

Following brain trauma, neuroinflammation is instigated via passive and active signals (215). Injured neural cells can release damage-associated molecular patterns (DAMPs), glutamate, cytokines, and ions capable of inciting a robust acute inflammatory response (215). These activating signals also attract glial and peripheral immune cells to the injured area, and drive upregulation and release of additional soluble inflammatory mediators such as cytokines and chemokines (C/C), proteases, and extracellular vesicles (215). The time-course of infiltrating peripheral immune cells has been determined in a number of animal studies (173), however experimental evidence has shown that immune cell phenotype, behavior, and subsequent effect on outcome changes over several incidence and host variables such as injury type and severity, patient sex (173), and experimental species (129). Therapeutic interventions with immunomodulatory agents must also consider timing, duration, and dosage of treatment to accommodate the multifaceted and beneficial role of inflammation (129). Accordingly, the suitability of immune factors as therapeutic targets is not yet well defined.

Several animal models of TBI have been developed to interrogate the neuroinflammatory events mediating dysfunction and degeneration, although no single

animal model can fully recapitulate all the features of human TBI (33). Experimental brain trauma pathology is often broadly classified as focal, diffuse, or mixed (172; 205) depending on the spatial extent of injury. Focal injury has traditionally required craniotomy to expose the brain for direct deformation (205), typically resulting in hematoma and tissue cavitation of the impacted cortex and sometimes subcortical structures as well (121). A widely used method to produce focal injury, the controlled cortical impact (CCI) model delivers a focused contusion along experimenter-set injury parameters (velocity, depth of deformation, dwell time, impactor diameter). Increased severity of these parameters correlate with enhanced tissue and behavioral pathology (223) but there is not a consensus for mild, moderate, or severe injury parameters to reflect those same designations given clinically (172). Nevertheless, it has been suggested that CCI injuries be considered mild if the depth <1.0 mm, velocity <4.0 m/s (172), and infarct volume measures 5-10% (205). Despite the widespread use of the CCI model, relatively few groups have characterized mild CCI injury in mice (<10% of CCI studies) (172).

Our laboratory has developed a mild-severity, open-skull model of CCI contusion neurotrauma to the left forebrain in mice. By using mild injury parameters within an open-skull model, the injury results in categorically mild tissue pathology including reduced blood-brain barrier (BBB) integrity but without the possibility of uncontrolled skull fracture seen in closed-head injury (CHI) models (172). The low-velocity contusion (1.5 m/s) and shallow depth (1 mm) of the CCI avoids tissue loss in the cortex and underlying structures yet instigates a period of cortical inflammation including astrocyte and microglial activation (gliosis) and BBB compromise (136; 143). Additionally, by

targeting the primary somatosensory and motor cortices, we are able to track cognate sensorimotor deficits up to 8 weeks post-injury (PI). In summary, we have created a novel CCI model for the direct comparison of neuroinflammatory protein dynamics with histological and behavioral changes in sensorimotor CNS circuits.

Here we report the temporal progression of CCI-induced cortical cytokine and chemokine proteins measured using a multiplex immunoassay platform within the immediate early phase and up to 8 weeks post-injury (PI). Our results indicate an immediate and robust neuroinflammatory response within the brain consistent with innate immunity but does not support an evolving T-cell-mediated response post-injury. Temporal increases in innate immune cytokines and monocyte attractant chemokines IL-1β, IL-5, IL-6, TNFα, CXCL1, CXCL2, CXCL10, CCL2 and CCL3 within the contused cortex track closely with injury-associated deficits in sensorimotor function and cortical gliosis. The data links dynamic neuroinflammatory responses at the molecular and cellular level to cognate behavioral outcomes in our CCI mice, making it a reliable pre-clinical model for the interrogation of discrete chemokine and cytokine contributions to TBI pathology.

METHODS AND MATERIALS

Animals

Male and female C57Bl/6J mice were obtained from The Jackson Laboratory (Bar Harbor, ME; Cat. No. 0664) and allowed to acclimate after arrival for 3-10 days before intervention, such that mice were 10-11 weeks-old at the time of surgery. Animals were group-housed (5 same-sex mice per cage) and remained with the same cage-mates for the duration of the study. Male and female cages were housed in the same room in a standard

12:12 h light: dark cycle. Food and water were available *ad libitum*. Animal housing facilitates were accredited by the Association for the Advancement and Accreditation of Laboratory Animal Care and all animal procedures described were approved by the institutional animal care and use committee at the Uniformed Services University of the Health Sciences (Bethesda, MD).

Surgical procedures and behavioral testing were performed during the light phase of the diurnal cycle but not within 2 hours of either lights-on or lights-off time. Mice were handled and treated one sex at a time such that both sexes never occupied the same surgical or behavioral space at the same time. Animal treatment, testing and handling strictly avoided cross-sex interactions and detection to prevent behavioral or hormonal effects of stress or arousal caused by the opposite sex. Rodent equipment and handing utensils were sex-dedicated or thoroughly wiped with 70% ethanol before and after each use.

Study Design

Sample size considerations for behavioral experiments were based on a pilot study of the adhesive removal test. This study of 6 CCI-injured animals per sex yielded effect sizes (male vs. female) of about 0.62 standard deviations and a within-subjects correlation of about .34. Assuming 11 repeated observations per animal (time-points), the required sample size is 16 male and 16 female animals per CCI-injured group, based on two-way repeated measures ANOVA with 80% power and 5% significance level. Sham-injured animals merely served as within-sex controls for the effect of injury (CCI vs. sham), and therefore required a minimal number of animals. For fresh tissue harvest,

3-5 animals of each sex were used for each time-point excluding 8 weeks. 160 animals total were used for this study.

Controlled Cortical Impact (CCI) and Sham procedure

Mice were randomized to dictate the order in which they were to be handled or treated on the day of surgery. Animals were allowed to acclimate to the surgical suite for 30-60 minutes prior to handling. At this point, the randomization outcome for the animal is revealed as either naïve (handled and re-caged) or injured (continue to anesthesia). Mice were anesthetized in a clear induction chamber with 3% isoflurane (Forane, Baxter Healthcare Corporation, Deerfield IL) in O_2 vehicle gas for a total of 3 minutes, during which time the scalp fur was clipped. Mice were then fastened onto a stereotaxic device with an incisor bar and atraumatic ear bars where anesthesia was maintained via a flow-through nose cone and isoflurane reduced to 2%. The scalp was wet thoroughly with betadine, the eyes were applied anti-microbial ophthalmic ointment, and then the scalp wiped clean with 70% ethanol; anesthesia was then reduced to 1.5%.

The scalp was opened via scalpel midline incision and the underlying left fascia cleared with a pre-moistened cotton-tipped swab. At this point, the animal's randomized allocation to sham or CCI treatment was revealed to the surgeon. Sham animals received simple interrupted stitches (silk, 5-0) and remained anesthetized within the stereotactic frame for 18-20 total minutes. In CCI animals, a 5 mm craniectomy centered at 2.0 mm left of Bregma was outlined then cut using a high-speed rotary tool with a 0.6 mm burr drill bit. Cortical impact was performed with the Impact One™ device (Leica Microsystems, Buffalo Grove, IL) using a 3 mm diameter probe at a 15-degree angle relative to the sagittal plane. Impact velocity was set at 1.5 m/s, displacement depth was 1

mm, and dwell time was 100 ms. After impact, the incision site was sutured with simple interrupted stiches (silk, 5-0) without replacement of bone flap. Bleeding events were mitigated with cotton.

Following cessation of anesthesia, mice were allowed to recover in a pre-warmed cage with softened chow until fully alert and ambulatory. All mice received acetaminophen in their drinking water (Children's Mapap, Livonia, MI; 1 mg/ml) from the point of acclimation to the surgical suite until approximately 24 h after the final surgery.

Naïve animals were merely handled on the day of surgery. All mice were randomized to either naïve, sham, or CCI treatment group, as well as the order in which they were handled or treated on surgery day.

Sensorimotor Tests

Mice were subject to sensorimotor testing on the day before surgical injury ("baseline"), on alternate days during the acute phase (up to day 7), and every week until study termination (8 weeks, Figure 4). Animals were allowed 30-60 minutes of acclimation to the testing room prior to each session without food or enrichment shelter. The observer was blinded to each animal's injury status during the testing period.

Adhesive removal behavior testing

The adhesive removal test was performed as previously described (16; 50). Briefly, electrical tape (3mm x 5mm strips) was manually applied with equal pressure to the ventral pads of each forepaw while the mouse was held immobilized. The animal was placed in a clear Plexiglas cylinder of 9.5 cm inner diameter and observed for a

maximum of 2 minutes per trial. Latencies to notice the tape and to remove the tape were recorded for each forepaw. Notice events were indicated by bringing the paw to the mouth or nose. Two trials were performed per testing day and the latencies generated were averaged to yield single latency scores per time point. The color (red, yellow) of the tape applied to each forepaw was alternated between two trials performed per testing day for each mouse. The latencies to notice and to remove the tape were averaged. Mice were familiarized to this procedure for 5 days prior to recording baseline testing data.

Testing for the ART was recorded using a video camera recorder (Canon FS300) along with notice and remove event declarations. These videos were later reviewed by three blinded investigators to verify accuracy and determine latency times.

Beam Walk

Mice were tasked to ambulate across a narrow (1 cm thick) wooden beam suspended 30 cm above the bench-top. The animals' home cage stood at the end of the beam to act as a motivating factor. Focusing on the right hind-paw, the experimenter counted the number of successful steps or slips taken by the animal. A step was denoted by placement of the innermost digit on the dorsal aspect of the beam, whereas a slip was noted as a failure to do so (47). Animals were tried consecutively, for a total of 4 trials per session. The total number of slips per session was analyzed statistically. Mice were trained to traverse the beam in 3 consecutive days prior to baseline measurements.

Tissue Preparation, Histology, and Microscopy

Transcardial perfusion

Mice were induced and maintained in anesthesia with 3% isoflurane in O_2 vehicle gas. After cessation of paw withdrawal reflex, thoracotomy was performed to expose the heart. Using a 25G needle, 20 mL-30 mL of ice-cold 0.1 M sodium phosphate-buffered saline solution (PBS) entered the left ventricle from a peristatic pump, and the right atrium was cut to allow exsanguination. Animals designated for fixation then received 20 mL-30 mL of ice-cold 4% paraformaldehyde in PBS (PFA), and the harvested brain was further post-fixed overnight in PFA at 4° C.

Animals designated for fresh tissue harvest were exsanguinated via transcardial perfusion of PBS as above. The brain was rapidly dissected from the skull, cleared of meninges and debris, and biopsy-punched through the impacted cortex using the pipette-end of a P-200 micropipette tip (Tip One by USA Scientific). The cortex is teased apart from underlying brain tissue along the sheet of white-matter tracts (corpus callosum and external capsule), weighed in the receiving tube, and homogenized in 10 volumes (mL) of T-PER extraction buffer (Thermo Scientific, Rockford, IL) with added Halt protease inhibitor cocktail (Thermo Scientific) per weight (g) of sample using a Biorupter UCD-200 ultrasonic disruptor (Diagenode, Sparta, NH) for 2 minutes at 4° C. Cortical homogenates were centrifuged at 4° C for 20 minutes at 10,000 G, and the resulting supernatant was apportioned into 50 uL aliquots and stored at -80° C.

Histology

PFA-fixed brains were embedded in 4% agarose gel and mounted on a vibratome. Brains were cut into 50 µm sections, and serial sections were collected from anterior to

posterior starting just prior to the anterior commissure. Sections were stored in PBS with 0.04% NaN_3 in 96-well plates.

Tissue sections were permeabilized with 3 successive rinses in PBS with 0.4% Triton X-100 (PBS-T) for 5 minutes, rinsed with isotonic saline, then treated with antigen retrieval buffer (10 mM Sodium Citrate, 0.05% Tween 20; pH 6.0) at 80° C for 30 min. Tissues were rinsed again with diH_2O, then treated with 0.3% hydrogen peroxide in diH_2O for 10 min. Tissues were rinsed in diH_2O, PBS, and PBS-T. Tissues were incubated overnight at 4° C with primary antibody in 1% normal goat serum (NGS) in PBS. Primary antibodies included rabbit polyclonal anti-GFAP antibody (Dako), rabbit polyclonal anti-Iba1 antibody (Wako) and rabbit polyclonal anti-NeuN (Abcam), see table 1. Tissue sections were rinsed with PBS, then processed using Vectastain® ABC kit (Vector Laboratories; PK-4001) according to the manufacturer's instructions: tissues were incubated at room temperature for 1 hour with anti-rabbit biotinylated secondary antibody, rinsed with PBS, then incubated with ABC reagent for 1 hr. All tissues were rinsed again with PBS and immunoreactivity was revealed using Vector Labs DAB Kit. Sections were mounted on poly-L-lysine coated slides and counter-stained in Mayer's Hematoxylin Solution (Millipore-Sigma; MHS1) for 3 minutes, then in 1% sodium-bicarbonate for 3 minutes. Counter-stained sections were then coverslipped for microscopy using Permount mounting medium (Fisher Scientific; #SP-15).

Astrocyte and Microglia Stereological Estimation

Sets of every third section (150 µm interval), were taken from the brain impact region spanning AP +0.3 mm to AP -0.4 mm relative to Bregma, for a total of 5 sections. The sampling grid was set at 400x400 µm, the counting frame 50x50 µm, and the

counting height 10 µm was set to the middle of the mounted section thickness (measured at 16.23 µm, 3.07 (mean, SD)). The impacted cortex was counted under 63x oil immersion magnification (numerical aperture = 0.9). Immunopositive Iba1+ cells where counted at the Z depth of the widest circumference. Iba1+ cells were simultaneously classified based on morphology as "ramified" (small cell body, numerous and thin processes) or "non-ramified" to denote activation status (109). Astrocytes were identified by using GFAP+ processes to find the corresponding hematoxylin-stained nuclei, and were counted at the widest nuclear circumference. The cortical area sampled represents the impacted area. The lateral extent of the traced cortex was determined by the equation: $y = \sqrt{|x| - 1.5^2} + 2$, where x is the anterior-posterior coordinate of the section relative to the anterior commissure (Bregma).

Neuronal Stereological Estimation

Sets of every tenth section (500 µm interval), were taken from the brain impact region spanning AP +1.5 mm to AP -1.5 mm relative to Bregma, for a total of 6 sections. The sampling grid was set at 450x450 µm, the counting frame 30x30 µm, and the counting height 20 µm was set to the middle of the mounted section thickness (measured at 23.86 µm, 1.23 (mean, SD)). The impacted cortex and ipsilateral striatum were counted under 40x magnification (numerical aperture = 0.4). Immunopositive nuclei where counted at the Z depth of the widest circumference. The cortical area sampled represents the impacted area. The lateral extent of the traced cortex was determined by the equation: $y = \sqrt{|x| - 1.5^2} + 2$, where x is the anterior-posterior coordinate of the section relative to the anterior commissure (Bregma).

Bright-field Microscopy

DAB-stained images were captured using a Zeiss Axioscan slide scanner. Tissues were scanned in Z-stacks of 1 µm-thick images and flattened using the extended depth of focus function.

Blood-Brain Barrier Integrity

Two days following CCI surgery, injured and naïve animals received a single injection of 4% Evans Blue dye (2.5 mL/kg; MilliporeSigma) via the lateral tail-vein under isoflurane anaesthesia. Animals were transcardially perfused with 20-30 mL heparinized (10U/mL) saline and de-brained. Freshly harvested hemispheres were homogenized in 50% Trichloroacetic acid (TCA; MilliporeSigma) at 3 times the tissue mass (w/v) using the BeadBug Microtube Homogenizer (Benchmark Scientific). Extravasated dye within the supernatant was quantified using a plate reader with emission equal to 612 nm.

Multiplex Immunoassays

Impacted cortical samples were probed for 19 cytokines and chemokines using the Meso Scale Discovery (MSD, Gaithersburg, MD) V-PLEX (mouse) Cytokine Kit (K15255D) according to manufacturer's protocol. Cortical homogenate aliquots were thawed on ice, re-collected into a single tube per each animal, and applied to each MSD panel as undiluted samples in duplicate. Unknown samples and calibration standards were allowed to incubate overnight in 4° C (alternate protocol 1), and all plate shaking was performed at 700 RPM for single plates or 750 RPM for double-plate runs. Plates were read using a Sector 6000 Imager (MSD) and analyte concentrations were delivered

in pg/mL. On the same day, total protein content was measured using the Pierce BCA Protein Assay Kit (Thermo; 23225) in samples diluted 10-fold in T-PER buffer and run in triplicate. Analyte concentrations were then standardized to total protein content (pg analyte/µg total protein). Analyte and total protein concentrations were determined using 4 parameter logistic regression interpolation. Due to technical limitations, the analyte IL-12 was not measured.

Statistics

All statistics were performed using Prism 7.05 (GraphPad, La Jolla, CA).

Behavioral Tests

Latency scores generated from the adhesive removal test were compared using 2-way ANOVA with repeated measures excluding baseline values. Multiple comparisons were corrected with Sidak's method. Baseline values were compared between biological sex using median values with 95% confidence intervals.

Hindlimb slip counts generated from the beam walk test were compared within biological sex using 2-way ANOVA with repeated measures excluding baseline values. Multiple comparisons were corrected with Sidak's method. Baseline values were compared between male and female mice using student's t-test.

Effect sizes generated from 2-way ANOVA comparisons were calculated as 2 times Cohen's f^2, or $2\sqrt{R^2/1-R^2}$, where R^2 = the proportion of variance explained (from Prism output) (160). This is equivalent to Cohen's *d* effect size.

Parametric methods were used after testing for normality (D'Agostino-Pearson) and homoscedasticity (Levene test).

Multiplex Electrochemiluminescent Immunoassays

Analyte levels per total protein content (pg/ug) were log-transformed (base 10) to allow for parametric analysis. To determine the temporal extent of CCI injury, data were analyzed using student's t-test within each time-point post-injury for male and female animals separately. To identify potential sex differences, data were analyzed using 2-way ANOVA between CCI-injured male and female mice, naïve values excluded, and *post-hoc* comparisons were determined using Sidak's method.

Data involving censored points (below detection levels) were evaluated using non-parametric Mann-Whitney test on ranks. Outliers were identified using the ROUT method (Q = 1%) within Prism and excluded from analysis.

RESULTS

A mild contusion TBI mouse model of sensorimotor dysfunction in the absence of neuronal and tissue loss

We have developed a mild contusion mouse model of sensorimotor injury to compare neuroinflammatory protein dynamics with well characterized behavioral and histopathological outcomes post-injury. We deliver a unilateral controlled cortical impact (CCI) to the left primary motor and somatosensory cortex of adult mice, followed by behavioral testing and brain neuroinflammatory protein quantification (Figure 4). Behavioral testing reveals sensorimotor functional deficits in the forepaws and hindpaw post-injury.

An adhesive removal test that records the time mice taken to notice and remove electrical tape from the forepaws within a familiar setting (50) reveals lateralized forepaw dysfunction (Figure 5). CCI injury produces an increase in both the latency to notice and

remove adhesive tape from the contralateral right forepaw when compared to baseline, or when compared to sham controls for the first week post-injury (2-way ANOVA with repeated measures: $F(1, 52) = 38.12$, n = 55, $p < .0001$; Figure 5a). Increased latencies to notice and remove the tape from the right forepaw return to baseline levels at 2 weeks post-injury (Figure 5a, c). In contrast, latencies for the ipsilateral left forepaw were only modestly increased and return to baseline levels by 5 days post-injury (Figure 5b, d). Baseline values were not significantly different between male and female animals (data not shown), therefore the resulting latencies were pooled between sexes.

To specifically evaluate hindlimb dysfunction resulting from our model of injury, mice were tasked to traverse a narrow, elevated wooden beam and the number of hindlimb "slips" were counted (Figure 6). Because baseline values of male animals were significantly greater than females' (t-test: $t(46,74) = 4.531$, n = 67, $p < .0001$) (see Figure 6a), we did not pool data from this task or directly compare slips between sexes. Instead, we quantified the effect of injury within each sex: 2 way-ANOVA comparisons with repeated measures revealed a significant effect of injury in male animals only ($F(1,18) = 10.11$, n = 20, $p = .0052$, effect size =0.593) which persists throughout the study duration, whereas female mice display hindlimb dysfunction within the acute period only ($F(1,18) = 2.075$, n = 20, $p = .1669$, E =0.241) (Figure 6b).

Histopathology confirms sensorimotor dysfunction is associated with sustained gliosis in the contused motor and sensory cortex. To quantify the activation of glial cells, we performed unbiased stereological estimation of anti-GFAP and anti-Iba1 immunolabeled sections throughout the impacted cortical area at 7 days and 8 weeks post-injury (PI) (Figure 7). These data demonstrate increased astrocyte and microglial

numbers compared to naïve animals, as well as a greater proportion of activated microglial cells at 7 days PI (Figure 7a).

At 8 weeks PI, increased glial numbers return to levels comparable to sham-injured animals, yet microglial activation bias (percent activated $Iba1^{+}$ cells) remains relatively high within the injured parenchyma (Figure 7a). These data suggest that the phenotypic changes associated with neurotrauma may persist despite returning to normal cell population numbers. Notably, anti-NeuN immunohistochemistry and stereological cell counts of NeuN+ labeled neurons in the impacted cortex do not reveal cortical lesions or significant neuronal loss post-injury compared to controls (t-test: $t(11) = 1.123$, $n = 13$, $p = .2854$; Figure 7c).

Lastly, we measured the integrity of the blood brain barrier (BBB) using the Evans blue dye extravasation method. Measurements at 2-days PI reveal impaired BBB integrity in mice following CCI (Figure 7d). Combined, the data confirm unilateral mild CCI to the left somatosensory and motor cortex results in an acute loss of BBB integrity, sensorimotor deficits and histopathological features consistent with CNS circuit disruption in the absence of significant neuronal or brain tissue loss.

Chemokines and cytokines with innate immune system functions are elevated by mild contusion to the motor and somatosensory cortex

To probe the neuroinflammatory protein content of the impacted cortex, we employed multiplex immunoassay array technology which quantified eighteen inflammatory cytokines and chemokines (C/Cs). Samples were taken from the impacted cortical area at 4 hours (h), 12h, 24h, 7 days, 14 days, and 8 weeks post-injury. The resulting concentration values were then standardized to the total protein content

generated from the impacted cortical tissue and compared between CCI- and sham-injured animals to determine an effect of injury, and between male and female CCI-injured animals to identify potential sex differences in the injury response.

Of the 18 analytes probed across two array kits, 9 C/Cs were found to exhibit a clear effect of injury as indicated by comparisons within sex between CCI- and sham-injured animals. These were CCL2, CCL3, CXCL1, CXCL2, CXCL10, IL-1β, IL-5, IL-6 and TNFα (Figure 8 and table 2). These 9 inflammatory proteins were further categorized by the time-point at which the effect of injury is resolved (returned to sham levels; t-test *p* values >.05). Of note, expression of 8 of the 9 injury-responsive proteins is significantly elevated at the earliest time-point measured (4 hours post-injury), the exception being IL-5. This sorting therefore designates inflammatory protein responses based on the temporal extent of their elevation over non-contused controls.

Although eight of the nine injury-responsive C/Cs have elevated levels of expression within the first 4 hours post-injury, the expression of three proteins drop to sham concentrations by 7 days post-injury. Chemokine KC/GRO (CXCL1) reached and sustained maximal levels at 4- and 12-hours post-injury and fell to sham levels by day 7 (Figure 8a). Cytokines IL-5 and IL-6 peaked at 12-hours post-injury and also resolved back to sham levels by 7 days (Figure 8a). These proteins represent inflammatory processes which persist only in the immediate acute stage of injury. A later resolution of inflammation was observed for chemokines CXCL2 (MIP-2) and CCL2 (MCP-1) at 14 days post-injury, yet both chemokines rose to maximal levels in the contused cortex immediately following injury (4 hours PI) (Figure 8b). These chemokines appear early

yet persist past the acute stage, potentially orchestrating a response different than those which resolve earlier.

A subset of injury-responsive C/Cs were found to remain elevated even at 2 weeks post-injury yet finally resolved to sham levels by 8 weeks. These long-lasting inflammatory signals include the cytokines IL-1β and TNFα, and chemokines CCL3 (MIP-1a) and CXCL10 (IP-10) (Figure 8c). In contrast to all other injury-induced C/Cs identified in our assay, CXCL10 (IP-10) proteins levels increase gradually, rather than peak early post-injury, reaching peak protein at 7 days following injury (Figure 8c). The immediate and dramatic increases in C/C levels demonstrate a robust, acute response of the innate immune system within the injured cortex. Differences in the onset, rate and peak of inflammatory protein expression post-injury are consistent with contributions from both brain-resident and infiltrating peripheral immune cells to C/C expression. In contrast, our multiplex assay did not reveal a consistent post-injury effect on the expression of inflammatory proteins IL-10, 1L-17A/F, IL-33, IL-27p28/IL-30, IL-4, IFN-γ, IL-15, IL-2 or IL-9 in the contused cortex (Figure 9 and Table 3).

Increased IL-5 expression acute post-injury is modulated by biological sex

Our multiplex CCI and sham group sizes were powered with equal male and female samples to statistically compare biological sex as an experimental variable in post-injury protein dynamics. Using 2-way ANOVA to compare protein levels between male and female CCI-injured mice, only IL-5 comparisons revealed a significant, albeit small, effect of sex ($F(1, 50) = 5.627$, n = 8, $p = .0216$; Figure 8). IL-5 protein levels reveal injury-induced increases peak in concentration at 12 hours at which point there is a significant sex-specific difference; IL-5 levels remain elevated at 24 hours post-injury,

but have returned to baseline at 7 days post-injury. These results suggest the acute, peak post-injury (12 h PI) increase IL-5 expression in the injured cortex is modulated by biological sex.

DISCUSSION

Neuroinflammatory Milieu of Mild Focal TBI

We report here the behavioral and brain inflammatory profile of adult mice delivered a single unilateral "mild" CCI injury to the primary somatosensory and motor cortical areas in both male and female animals. To evaluate cognate neurological dysfunction, we tested the animals in sensorimotor integration tasks of the forelimbs and the affected hindlimb at numerous time-points within the acute stage of injury and up to 8 weeks post-CCI. We further quantified cortical cytokine and chemokine (C/C) levels to determine the early temporal profile of inflammatory factors within male and female mice. In general, we observed significant increases in nine of the 18 analytes measured within the injured cortical parenchyma compared to non-contused control tissues, reflecting a clear effect of injury. These nine C/Cs were CCL2, CCL3, CXCL1, CXCL2, CXCL10, IL-1β, IL-5, IL-6 and TNFα. Of the nine C/C's responding to trauma, only IL-5 is not immediately activated following injury whereas the other eight reflect levels significantly greater than those produced by sham injury at 4 hours, the earliest time measured PI. Injury-responsive C/Cs are further grouped by the time at which levels return to non-traumatized levels, i.e., their temporal extent of activation. CXCL1 (KC/GRO), IL-5, and IL-6 activation is resolved within the acute phase following injury (by day 7), whereas CXCL2 (MIP-2) and CCL2 activation is resolved by day 14, and IL-1β, TNFα, CCL3 (MIP-1a), and CXCL10 (IP-10) activation is resolved at week 8. We

highlight the pre-clinical relevance of the 9 injury-induced C/Cs identified in our model of mild focal TBI.

IL-1β, IL-6, and TNFα

In agreement with numerous other models of focal brain trauma, our study demonstrates immediate activation and early peak of classic pro-inflammatory cytokines IL-1β, IL-6, and TNFα (217). These mediators are commonly identified as elevated in TBI patients and associated with poor outcomes (24; 67; 169) and secondary morbidities such as epilepsy, dementia, and PTSD (49; 129). From our model of CCI, elevated IL-6 levels were found to resolve within days after injury, yet both IL-1β and TNFα remained elevated above non-contused levels at 2 weeks PI.

IL-1β is a necessary mediator of the early phase inflammatory response to trauma (35) and is released by neuronal and glial cells upon cellular injury (81). Following experimental TBI, neutralization of IL-1β reduces tissue and behavioral pathology (25) and systemic infusion of IL-1β exacerbates these outcomes (199). Evidence of IL-1β expression was detected in human post-mortem tissue within minutes of brain injury (49), as well as within the CSF (67; 169) and serum (191) compartments.

TNFα and IL-6 are additional immediate mediators of the pro-inflammatory response and have been found to drive both negative and positive outcomes experimentally depending on timing and dosage (81; 84). TNFα plays an important role in the initiation and propagation of neuroinflammatory cascades and is currently investigated as a therapeutic target of small molecule inhibitors (11).

IL-5

IL-5 is a known cytokine of the Th2 response along with IL-4, IL-10, and IL-13, and is secreted by Th2 T-cells in response to IL-33 stimulation (124). Interestingly, neither IL-4, IL-10, nor IL-33 were measured to be significantly elevated in our study compared to non-contused controls, suggesting a novel mechanism of IL-5 release. Within the CNS, scant evidence suggests IL-5 production by astrocytes and microglia (157), however it has been shown that microglia respond to IL-5 stimulation by proliferation and synthesis of nitric oxide (108). The presence or non-detection of IL-5 within different models of TBI (31) or brain injury (174) suggests that IL-5 signaling in the brain is an underappreciated aspect of neuroinflammation and may be prominently upregulated in some but not all models of brain injury.

Interestingly, IL-5 is the only C/C measured which demonstrated a significant effect of sex: levels from CCI-injured females are consistently greater than those from males within the first 24 hours PI. Where present, sex differences in experimental TBI often implicate female sex to confer benefit on pathology and recovery (178). Our study suggests IL-5 be considered in future studies of sex-specific differences in brain injury.

CXCL1 & CXCL2

CXCL1 and CXCL2 are related ligands (amongst others) of the CXCR2 receptor, which is a known regulator of neutrophil migration to CNS injury (202). A rapid increase in CXCR2 ligands after TBI in rodent studies is associated with early robust infiltration of neutrophils into the area of brain tissue injury (19). Studies employing CXCR2 *null* mice have demonstrated massive reductions in neutrophil infiltration into injured brain tissue with a correlated decrease in lesion volume and neuronal loss, as compared to

wild-type controls (162). CXCR2 is also expressed within endothelial cells of the CNS in the presence of pro-inflammatory signals (IL-1β, TNFα) and has been shown to mediate blood brain barrier dysfunction *in vitro* (61). Interestingly, stimulation of CXCR2 expressed on neural cells (astrocytes, neurons) is found to be neuroprotective in instances of infection or induced apoptosis, suggesting that the outcome of CXCR2 stimulation is context and dose dependent (162). Our study found both measured ligands to be rapidly activated following injury (within 4 hours), yet CXCL2 remained elevated above non-contused levels longer than CXCL1. These data suggest different mechanisms govern the production of each chemokine within our model of brain injury, despite the common cognate receptor.

CCL2, CCL3 and CXCL10

CCL2 and CCL3 are β-chemokines secreted by glia and brain endothelia upon stimulation by proinflammatory cytokines and are monocyte chemoattractants (107). Interrupted signaling of either chemokine pathway generally benefits the brain by decreasing lesion volume and promoting recovery (77; 130). Both chemical signals were measured to respond immediately post-injury, yet CCL3 levels were significantly elevated above non-contused controls longer than CCL2, suggesting distinct mechanism of temporal regulation and thereby monocyte attraction and activation to the injured brain area.

CXCL10, a T-cell-attracting chemokine, measured unique kinetics as the only C/C whose levels continued to rise until at least 1 week following injury and did not resolve until after 2 weeks post-injury. CXCL10 is secreted by astrocytes to direct T-cell recruitment and is often seen in instances of multiple sclerosis (177) or infection (92).

Little is known regarding the role of CXCL10 in TBI, however a mechanistic link may exist between CXCL10-induced hyperexcitability (141) and post-traumatic epilepsy. We are surprised to see the sustained elevation of CXCL10 in the otherwise absence of evidence for T-cell secretion (i.e., IFNγ, IL-4, IL-2, IL-10).

Unexpected lack of C/C responses

Our data corroborates elevated levels of cytokines and chemokines seen in similar studies of rodent focal TBI (26; 31; 99; 150), however our results differ at very clear points. Our study detected no effect of brain injury on IFNγ or IL-10, two cytokines commonly found in experimental TBI and biofluids of TBI patients (173; 178).

One possible explanation lies in the mild-severity of our model parameters compared to more severe open-head CCI models (31; 99). Additionally, our data lack evidence of T-cell-derived cytokines even at later time-points, suggesting a minor (if present) role of T-cell-mediated pathology or recovery within our model. Following experimental neurotrauma, T-cells are generally protective. Non-specific T-cells have been shown to support neurotrophic signaling via IL-4 secretion during normal conditions in a T-cell receptor-independent manner (51) and in response to DAMPs produced from neurons (204). Paradoxically, CNS-specific T-cells produced following injury are also neuroprotective to injured axons (159). Although we are surprised T-cell-derived signals were not elevated following our model of injury, similarly mild or closed-skull models of TBI found little role of adaptive immunity by using mice genetically deficient in T-cells (210).

Based on the observed chemokine changes, it is very likely that our model of injury induces infiltration of innate peripheral immune cells as previously described in

similar TBI models (173). Neutrophils are strongly attracted by the CXCL1 and CXCL2 signals which are rapidly elevated following injury and persist above non-contused levels for over a week. Peripheral monocytes are attracted by CCL2 and CCL3, which suggests infiltration continued past 14 days post-injury. Additional peripheral immune cells (dendritic cells, natural killer cells, and CNS-adjacent T-cells) are also likely to have infiltrated the injured tissue given the loss of BBB integrity and sustained elevation of chemokine CXCL10, although our cytokine data does not support a robust adaptive response. Future studies employing cell-specific markers are required to determine the flux of infiltrating immune cells following our model of injury. These data suggest our model of low-speed CCI incites a robust innate inflammatory response within the impacted parenchyma yet avoids a similar response of the adaptive immune system. We note that elevated levels of all C/Cs return to non-contused levels by 8 weeks post-injury.

Sensorimotor Dysfunction Reflects Cortical Topography

To interrogate the functional output of our contusion injury, we observed sensorimotor tasks of both forelimb and hindlimb function. The adhesive removal test (ART) tasks mice with the removal of electrical tape applied to both forepaws. Latency to notice and to remove each piece is observed as a measure of innate forelimb function. Of the four metrics, latency to remove the adhesive from the contralateral (affected) forepaw demonstrates the greatest effect of injury and duration of deficit (day 7). Latency to notice the adhered tape on the affected forepaw is also significantly affected and may reflect reduced sensory ability of the forelimb. Mice were also tasked to traverse an elevated narrow beam wherein the number of affected hindlimb slips is recorded as a measure of hindlimb sensorimotor integration. Similar to the ART data, specific hindlimb

dysfunction is observed to fully resolve within the first week post-injury in female mice. In male animals however, hindlimb dysfunction persists throughout the duration of the study (8 weeks post-injury) and potentially longer.

Within this task, even non-injured males perform worse than females at baseline, suggesting inherent sex differences within the beam walk test. It is likely that relative body weight contributes to performance and heavier males may have required additional training to master the task. However, when animals with >10% slips at baseline were excluded from analysis, the statistical output remained the same (data not shown). Nonetheless, these data corroborate a general finding of experimental TBI in which female mice outperform their age- or weight-matched male counterparts in measures of behavioral pathology (178).

The behavioral data accurately reflect the localization of the contusion injury which fully encircles the caudal forelimb area and hindlimb area of the primary motor cortex (193). Studies involving discrete lesions to the motor cortex in rodents have shown the cortex is not necessary for learned motor tasks, yet required for learning new tasks (86). Given the long-term tissue preservation and neuronal sparing within our model, the demonstrated behavioral deficit may instead reflect "inactivation" of these corticofugal circuits (128), possibly due to inflammatory mediators within the microenvironment.

Histological findings reflect long-term changes in resident immune activation

Astrocytes and microglia are central mediators of brain inflammation and repair following injury (18; 109). Our study found that although astrocyte and microglial numbers fall to non-contused levels by 8 weeks PI, microglial morphology reflects heightened activation even at this time. Long-lasting microglial activation is a hallmark

of moderate and severe TBI's (109), and here we demonstrate this pattern of activation within our model of mild CCI.

CONCLUSION

We have characterized and exhibited a highly reproducible experimental model of mild brain contusion which relies upon low-speed impact and shallow depth of deformation within an open-head CCI injury. TBI is a heterogeneous clinical condition and no single animal model is capable of recapitulating all the pathologic features of human TBI. The goal of pre-clinical studies is to provide a spectrum of knowledge generated from multiple, distinct pre-clinical models that encompass the full range of injuries from mild to severe TBI (85; 133; 171; 172). For example, a recent large-scale proteomic study of closed head weigh drop TBI in mice reveals distinct C/C protein dynamics compared to our study with no reported increase in IL-1β, IL-5, IL-6, TNFα, CXCL1, CXCL2, CXCL10, CCL2 or CCL3 post-injury (197). Indeed, IL-6 was chronically down-regulated in this diffuse injury model highlighting the importance of generating data from multiple pre-clinical models of TBI. Here we provide inflammatory protein expression and behavioral data following focal contusion in which the impacted parenchyma is preserved and some but not all functional output is restored. We reveal widespread activation of innate but not adaptive immune modulators that, when combined with histopathology and behavioral outcomes PI, link sensorimotor dysfunction with innate immune activity in the contused motor and sensory cortex of mice.

Antibody	Structure of Immunogen	Manufacturer, Catalog number, RRID, Host species	Concentration
anti-GFAP	GFAP (full length)	Dako, Z0334, AB_2811722, rabbit polyclonal	1: 1,500 in PBS-T
anti-Iba1	Synthetic peptide of Iba1 carboxy-terminal	Wako, 019-19741, AB_839506, rabbit polyclonal	1: 1,000 in PBS-T
anti-NeuN	Recombinant fragment corresponding to human NeuN, aa 1-100 (N-terminal)	Abcam, ab104225, AB_10711153, rabbit polyclonal	1: 1,000 in PBS-T

Table 1. Antibodies used in this study.

Cytokine/Chemokine	Time PI	Female	Male
CXCL1 (KC/GRO)	4 hours	p <.001	p <.0001
	12 hours	p <.001	p <.001
	24 hours	p <.001	p <.001
CCL2 (MCP-1)	4 hours	p <.0001	p <.0001
	12 hours	p <.01	p <.0001
	24 hours	p <.0001	p <.0001
	7 days	p <.05	p <.001
	14 days	*n.s.*	p <.05
CXCL2 (MIP-2)	4 hours	p <.0001	p <.0001
	12 hours	p <.01	p <.001
	24 hours	p <.01	p <.05
	7 days	p <.05	p <.01
CCL3 (MIP-1a)	4 hours	p <.0001	p <.0001
	12 hours	p <.0001	p <.001
	24 hours	p <.01	p <.01
	7 days	p <.01	p <.001
	14 days	p <.01	p <.01
CXCL10 (IP-10)	4 hours	p <.001	p <.001
	12 hours	p <.0001	p <.05
	24 hours	p <.0001	p <.0001
	7 days	p <.001	p <.001
	14 days	p <.05	p <.05
IL-5	12 hours	p <.001	p <.001
	24 hours	p <.01	p <.0001
IL-6	4 hours	p <.0001	p <.0001
	12 hours	p <.0001	p <.001
	24 hours	p <.0001	p <.001
IL-1ß	4 hours	p <.0001	p <.001
	12 hours	p <.0001	p <.0001
	24 hours	p <.001	p <.001
	7 days	*n.s.*	p <.05
	14 days	p <.01	p <.001
TNFα	4 hours	p <.0001	p <.0001
	12 hours	p <.001	p <.001
	24 hours	p <.0001	p <.0001
	7 days	p <.05	p <.01
	14 days	p <.01	p <.01

Table 2. Statistically significant changes in C/C levels due to CCI injury.
Note: Cytokine and chemokine data presented in **Figure 8** were analyzed within each time-point using student's t-tests between CCI- and sham-injury values. Comparisons not shown were not significant (*n.s.*).

Cytokine	Time	*p* values		Cytokine	Time	*p* values	
		Female	Male			Female	Male
IFN	4h	0.31218	0.42927	IL-15	4 h	0.94457	0.55911
	12 h	0.99164	0.92182		12 h	0.45746	0.818
	24 h	0.04734*	0.76929		24 h	0.5093	0.22454
	7 d	0.60206	0.07341		7 d	0.19344	0.64072
	14 d	0.00519**	4.20E-05****		14 d	0.31293	0.13649
	8 w	0.354	0.06306		8w	0.7279	0.752
IL-2	4h	0.15672	0.22632	IL-17A/F	4h	0.36423	0.01459*
	12 h	0.8731	0.68886		12h	0.06897	0.0837
	24 h	0.71127	0.10729		24h	0.72573	0.06018
	7 d	0.95109	0.30942		7d	0.18359	0.20782
	14 d	0.00572**	0.0258*		14d	0.21751	0.11065
	8 w	0.54677	0.34685		8w	0.57582	0.34792
IL-10	4h	0.01726*	0.09529	IL-9	4h	0.97186	0.91736
	12 h	0.45454	0.5322		12h	0.02571*	0.02657*
	24 h	0.08275	0.41547		24h	0.03104*	0.06837
	7 d	0.89039	0.15403		7d	0.70311	0.59284
	14 d	0.00234**	0.00041***		14d	0.36139	0.0645
	8 w	0.53593	0.27527		8w	0.04704	0.32875
IL-4	4h	0.01188*	0.17779	IL-27p28/	4h	0.5231	0.27755
	12 h	0.75498	0.63032	IL-30	12h	0.34905	0.79996
	24 h	0.17662	0.8522		24h	0.73957	0.00599**
	7 d	0.85056	0.14711		7d	0.53428	0.49043
	14 d	0.00062***	0.00734**		14d	0.67995	0.91699
	8 w	0.27368	0.42926		8w	0.787	0.49284
IL-33	4 h	0.33518	0.57902				
	12 h	0.23424	0.31768				
	24 h	0.54564	0.46746				
	7 d	0.34902	0.25631				
	14 d	0.07407	0.09037				
	8w	0.32339	0.42628				

Table 3. Nine of 18 measured are not significantly modulated by injury. *Note:* Cytokine values were analyzed within each time-point using student's t-tests between CCI- and sham-injury values. Comparisons were predominantly not significant (*n.s.*). Significant *p* values are annotated at the 5%*, 1%**, 0.1%*** or 0.01%**** confidence level.

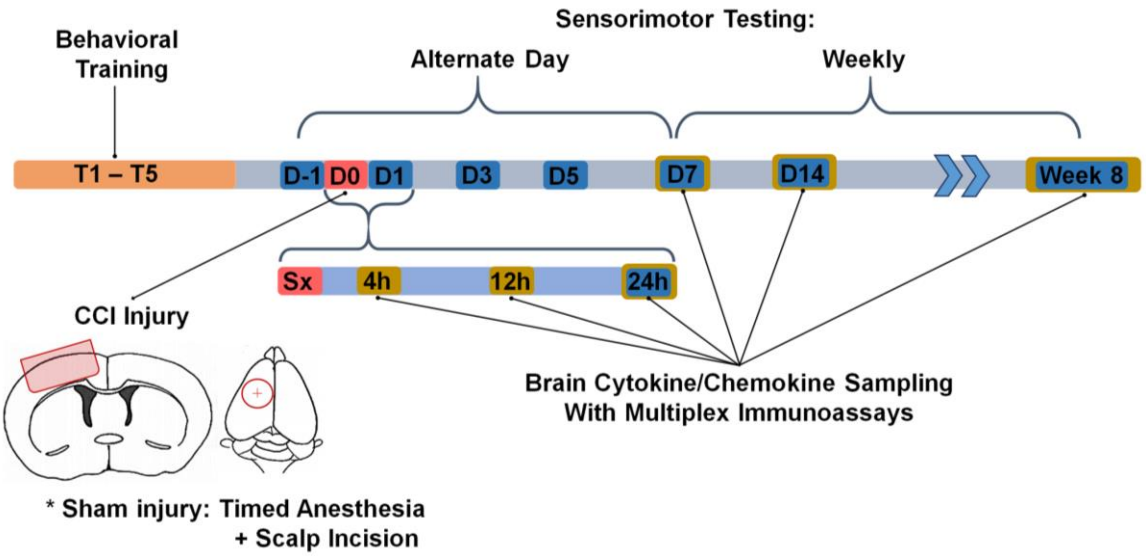

Figure 4. Mouse model of mild controlled cortical impact (CCI) injury. Traumatic contusion to the primary somatosensory and motor cortices is delivered to the exposed left forebrain. Sham injury includes timed anesthesia and scalp incision only. Sensorimotor dysfunction is tested every other day for the first week post-injury (PI) and weekly thereafter up to 8 weeks PI. The impacted cortical area was harvested at 4 hours (h), 12 h, 24 h, 7 days (D), 14 days, and 8 weeks PI and sampled for cytokine and chemokine levels using multiplex electrochemiluminescent immunoassays.

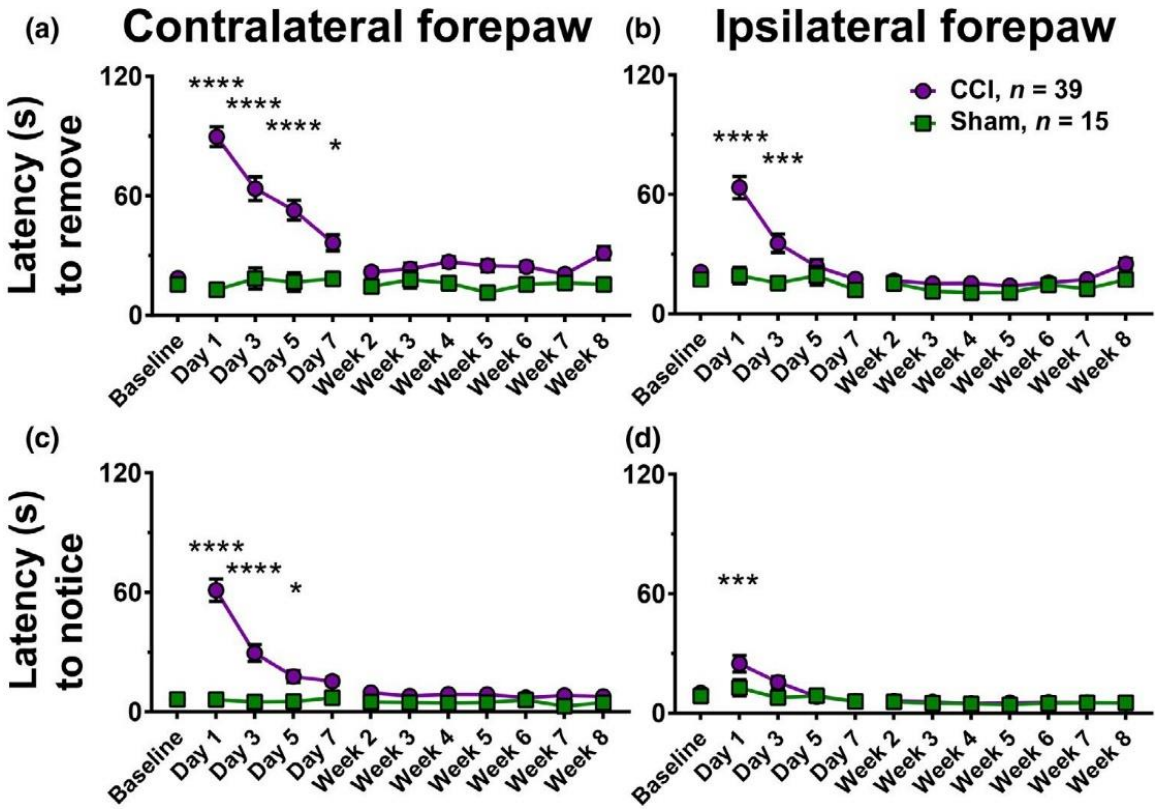

Figure 5. The adhesive removal test demonstrates sensorimotor dysfunction of forelimb use. Latencies (mean ± *SEM*) to remove **(a, b)** and notice **(c, d)** a piece of electrical tape (3 mm by 5 mm) applied to the forepaw contralateral **(a, c)** and ipsilateral **(b, d)** to the injured hemisphere in male and female mice. Two-way ANOVA with repeated measures test (excluding baseline values) evaluate the effect of injury over time for each metric: **a**: $F(1, 52) = 38.12$, $n = 55$, $p < 0.0001$, effect size, $E = 0.73$; **b**: $F(1, 52) = 17.13$, $n = 55$, $p = 0.0001$, $E = 0.42$; **c**: $F(1, 52) = 35.02$, $n = 55$, $p < 0.0001$, $E = 0.55$; **d**: $F(1, 52) = 2.153$, $n = 55$, $p = 0.1483$, $E = 0.08$. Multiple comparisons corrected with Sidak's method. ****$p < 0.0001$, ***$p < 0.001$, *$p < 0.05$.

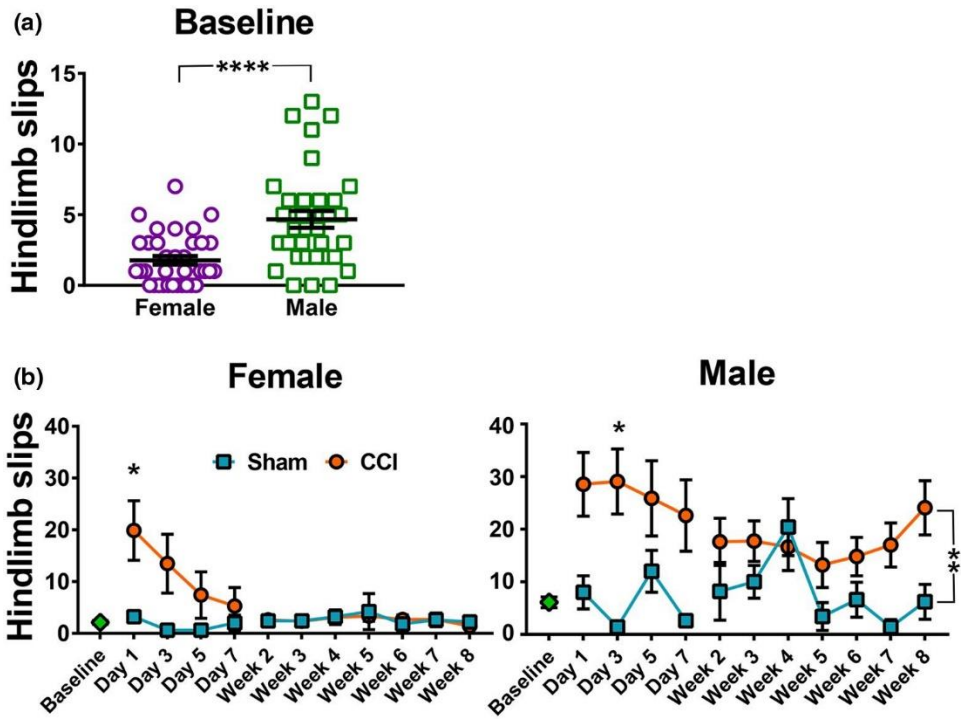

Figure 6. Beam Walk test demonstrates sustained deficits in male mice compared to a rapid recovery in female animals following CCI injury. **(a)** Baseline values demonstrate a significant sex difference in right-hindlimb slips when completing the beam walk task (unpaired *t* test with Welch's correction for unequal variances ($t(46.74) = 4.531$, $n = 67$, $p < 0.0001$)). **(b)** Hindlimb slips over time following neurotrauma reveals rapid recovery of baseline ability in female mice but sustained deficits in males. Two-way ANOVA comparison with repeated measures reveals a significant effect of injury within male animals only ($F(1, 18) = 10.11$, $n = 20$, $p = 0.0052$, effect size = 0.593). Multiple comparisons corrected with Sidak's method. ****$p < 0.0001$, *$p < 0.05$. Mean ± *SEM* are presented.

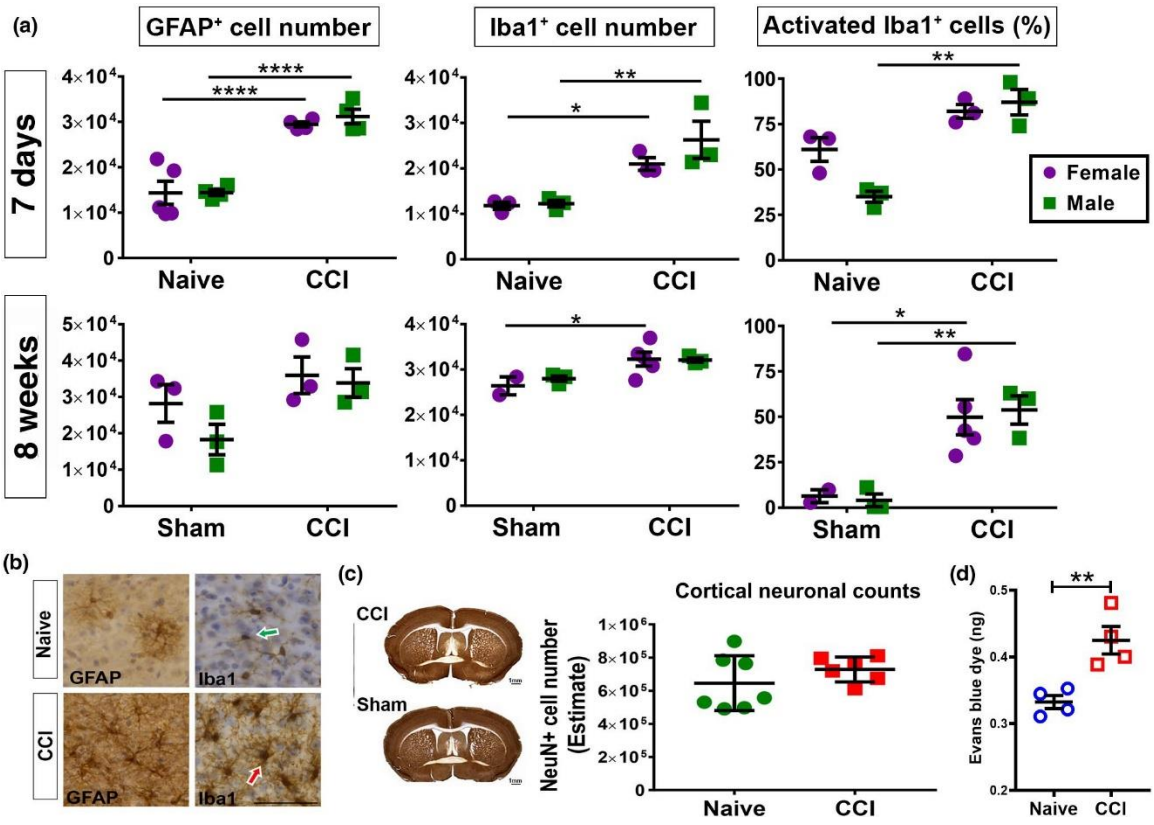

Figure 7. Histopathology confirms sustained gliosis within the contused cortex. Unbiased stereological estimation of astrocytes (GFAP+) and microglia (Iba1+) throughout the impacted cortical area. All counts were recorded from a region of interest (ROI) encompassing the impacted cortical area. The ROI was defined using a formula described in the Methods and Materials section. **(a)** Over time following CCI, GFAP, and Iba1+ cell numbers return to control levels, yet the proportion of activated, or non-"ramified," microglial cells remains elevated at 8 weeks post-injury. Error bars represent *SEM*. **(b)** Representative images of DAB-stained sections labeled with anti-GFAP and anti-Iba1 at 7 days post-injury. Iba1-probed images demonstrate typical microglial morphology encountered and identifies ramified (green arrows) and non-ramified (red arrows) cells. Tissue sections are counter-stained with hematoxylin. Scale bar = 50 µm. **(c)** Representative images of DAB-stained sections labeled with anti-NeuN at 7 days post-injury and the estimation of neurons within the impacted cortical area does not suggest significant loss of tissue or neurons at 7 days post-injury (*t* test: $t(11) = 1.123$, $n = 13$, $p = 0.2854$). Scale bar = 1 mm. **(d)** Measurements of blood–brain barrier (BBB) integrity using Evans blue dye extravasation reveal a significant loss of BBB integrity in CCI mice 2 days post-injury (*t* test: $t(6) = 4.058$, $n = 4$, $p < 0.01$).

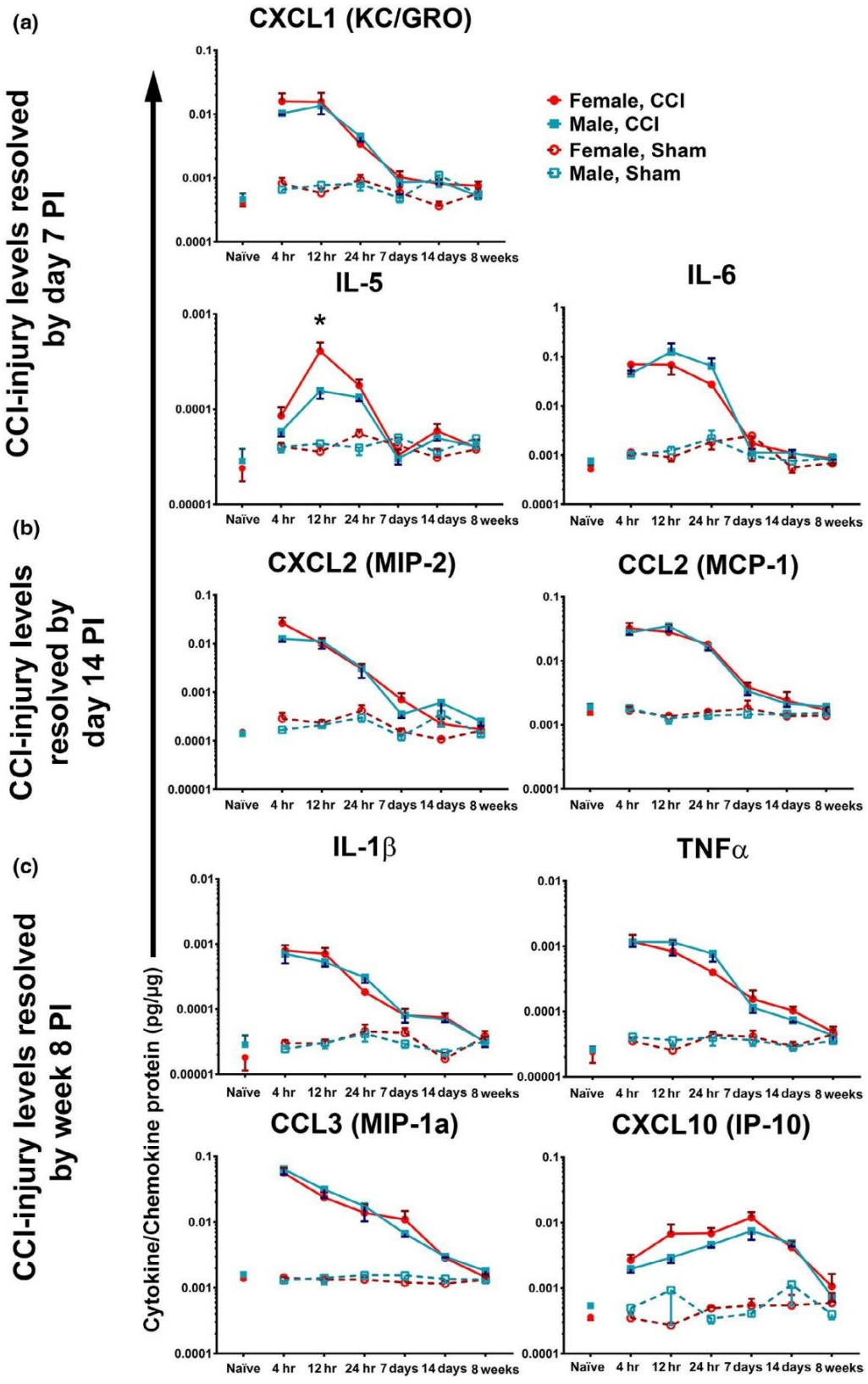

Figure 8. An immediate and robust innate immune response is initiated by CCI injury to the forebrain in C57 mice. Multiplex immunoassays quantified cytokine and

chemokine (C/C) levels within homogenized brain samples of the impacted cortical region taken at the indicated times post-injury. Nine C/C show injury-induced increases in expression that differ in dynamics. **(a)** CXCL1, IL-5 and IL-6 injury-induced increases resolve to sham concentrations by 7 days PI. **(b)** CXCL2 (MIP-2) and CCL2 (MCP-1) resolve at 14 days PI. **(c)** IL-1β, TNFα, CCL3 (MIP-1a), and CXCL10 (IP-10) activation is resolved at week 8 PI. Presented values are standardized to the sample protein content. Mean ± *SEM* are presented. Statistically significant changes in cytokine and chemokine levels due to CCI injury are presented in Table 2 (not annotated on the figures for space reasons). Annotated are sex differences between CCI-injured animals evaluated using a two-way ANOVA test, and multiple comparisons corrected with Sidak's method, $*p < 0.05$. IL-5 levels indicated a sex-specific response to trauma: $F(1, 50) = 5.627$, $n = 8$, $p = 0.0216$).

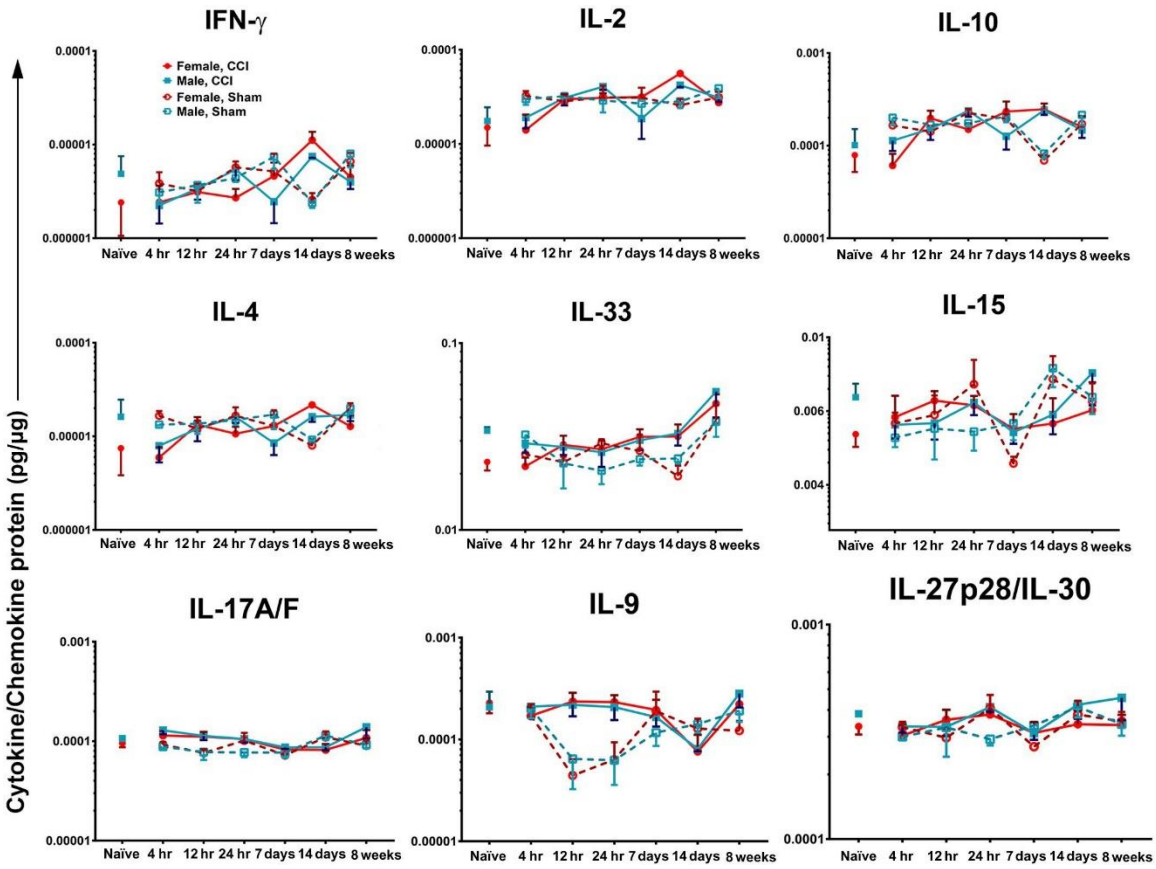

Figure 9. Inflammatory proteins associated with adaptive immune responses were not elevated following CCI injury. *p* values for each time-point using student's *t* tests between CCI- and sham-injury values are presented in **Table 3** (not annotated on the figures for space reasons). Nine cytokines do not demonstrate an effect of CCI injury despite low *p* values within a few comparisons—see **Table 3**.

CHAPTER THREE

HOST SEX AND TRANSPLANTED HUMAN INDUCED PLURIPOTENT STEM CELL PHENOTYPE INTERACT TO INFLUENCE SENSORIMOTOR RECOVERY IN A MOUSE MODEL OF CORTICAL CONTUSION INJURY

ABSTRACT

Traumatic brain injury (TBI) is a substantial cause of disability and death worldwide. Primary head trauma triggers chronic secondary injury mechanisms in the brain that are a focus of therapeutic efforts to treat TBI. Currently, there is no successful clinical strategy to repair brain injury. Cell transplantation therapies have demonstrated promise in attenuating secondary injury mechanisms of neuronal death and dysfunction in animal models of brain injury. In this study, we used a unilateral cortical contusion injury (CCI) model of sensorimotor brain injury to examine the effects of human induced pluripotent stem cell (hiPSC) transplantation on pathology in male and female adult mice. We determined transplanted hiPSC-derived neural stem cells (NSCs) and neuroblasts but not astrocytes best tolerate the injured host environment. Surviving NSC and neuroblast cells were clustered at the site of injection within the deep layers of the cortex and underlying corpus callosum. Cell grafts extended neuritic processes that crossed the midline into the contralateral corpus callosum or continued laterally within the external capsule to enter the ipsilateral entorhinal cortex. To determine the effect of transplantation on neuropathology, we performed sensorimotor behavior testing and stereological estimation of host neurons, astrocytes, and microglia within the contused

cortex. These measures did not reveal a consistent effect of transplantation on recovery post-injury. Rather the positive and negative effects of cell transplantation were dependent on the host sex, highlighting the importance of developing patient-specific approaches to treat TBI. Our study underscores the complex interactions of sex, neuroimmune responses and cell therapy in a common experimental model of TBI.

KEYWORDS

Neural stem cells, Controlled Cortical Impact, Induced pluripotent stem cells, Transplantation, Sensorimotor, Traumatic Brain Injury

HIGHLIGHTS

- An adult TBI mouse model of sensorimotor dysfunction in the absence of brain tissue loss used.
- Effects of human induced pluripotent stem cell (hiPSC) transplantation post-injury examined.
- hiPSC-derived NSCs and neuroblasts but not astrocytes tolerate transplantation.
- Cells cluster deep in the cortex and corpus callosum and extend lengthy neuritic processes.
- Cell transplantation effects on pathology are mixed and dependent on host sex.

INTRODUCTION

Traumatic brain injury (TBI) is a substantial cause of disability and death worldwide. Roughly 54-60 million or more TBI cases occur annually (46). In the USA alone, between 3.2 and 5.3 million people were living with TBI-related chronic disability

as of 2008 (22), and 2.5 - 3.5 million new TBI cases occur per year (22; 27). Typical neurologic consequences of TBI include cognitive deficits, motor deficits, psychiatric disorders, and chronic pain (134; 213). These persistent problems may negatively impact quality of life by reducing employment or limiting leisure activities (22; 182).

TBI is a chronic disease process set in motion by external forces acting upon brain tissues. The immediate consequences of injury are shearing of delicate fiber tracts and cell rupturing. Secondary injury processes, which include excitotoxicity, inflammation, necrosis and apoptosis, emerge within hours and evolve for weeks and perhaps longer following the primary insult (121). Peripheral immune cells invade the injured parenchyma and work in concert with resident microglia to promote cytotoxic inflammatory signaling (109). Numerous clinical trials have sought to prevent these secondary events and mitigate chronic health effects after TBI, but the standard of acute care for TBI remains monitoring and maintaining physiological intracranial pressure, systemic blood pressure, and caloric intake (21; 166).

Stem cell transplantation has been explored as a potential therapy to restore lost tissue and repair neural circuitry in neurotrauma. The majority of stem cell therapy studies for TBI have been conducted with mesenchymal stem cells (MSCs) harvested from bone marrow (2). However, MSCs have limited neuronal potential when compared to an alternative source of patient-specific stem cells, induced pluripotent stem cells (iPSCs) (189). iPSCs can be generated from patients for autologous transplantation or human leukocyte antigen (HLA)-matched allogenic transplantation (192), greatly expanding their clinical potential. Importantly, technical advances have greatly increased the efficiency and speed of iPSC-derivation (144; 145) and refined differentiation

protocols permit iPSCs to recapitulate specific cell phenotypes of the central nervous system (57; 106; 187; 224) for targeted cell replacement strategies. Indeed, preclinical experiments are now showing positive results from therapeutic transplantation of iPSC-derived cells into models of neurologic disorders and retinal degeneration (1; 4; 65; 95; 166; 195; 225).

In the experiments described here, we performed an open-head model of unilateral TBI with contusion to the primary somatosensory and motor cortices in mice. We used this model to examine the potential of human iPSC-derived neural cells to promote behavioral recovery after transplantation into the injured cortex. We assessed long-term viability and host tissue integration of transplanted neural stem cells or isogenic immature neurons. Transplantation influence on recovery from TBI was assessed using a behavioral test of sensorimotor integration. Finally, we performed systematic quantification of neuronal and glial cell markers to indicate whether transplanted human neural cells were associated with neuroprotective benefits and/or glial activation in the host mouse brain.

RESULTS

Contusion Neurotrauma to the Somatosensory and Motor Cortices Produces Robust Sensorimotor Deficits and Gliosis

In order to test the effects of human iPSC-derived (iPS) cell engraftment on TBI pathology, we developed an adult mouse model of unilateral contusion injury to the primary somatosensory and motor cortices. A low-speed (1.5 m/s), 1 mm deep controlled cortical impact (CCI) was delivered to the exposed surface of the left forebrain. Our mild CCI preserved cortical tissue within the contused hemisphere (Figure 10A), yet produced

acute disruption of the blood-brain barrier (BBB; Figure 10B) and sustained astrocyte and microglial activation (Figure 10C); acute, transient BBB disruption is a clinical hallmark of TBI in patients suffering chronic behavioral and cognitive deficits in cases of mild or undetected structural brain damage (73; 123; 170). Behavioral testing of CCI mice revealed deficits in motor coordination acutely and forepaw sensorimotor integration chronically (Figure 10D), consistent with sustained injury-induced functional deficits in mice. Lastly, as engrafted mice would be given daily injections of the immunosuppressant Cyclosporin A (a known neuroprotectant) to limit host rejection of engrafted cells, we also compared neuronal survival in mice with or without CsA treatment. The data reveal no neuroprotective effect of CsA (10 mg/Kg, daily) on neuronal survival at 7 days post-injury in our CCI mice (see Supplemental Figure 1). Taken together, these characterization data support a clinically-relevant TBI model and intervention for the investigation of iPS cell therapy.

Engrafted human iPSC-derived Cells Survive and Differentiate within the Host White-Matter Following Transplantation into the Contused Cortex

To test the effects of cell therapy, CCI and sham craniectomy mice were given a single intraparenchymal injection of 1 x 10^5 cells into the contused cortex 1 day post-injury. We delivered neural stem cells (NSCs), immature neurons (referred to as neuroblasts, or Nb), or astrocytes (Astro) derived from the same human iPSC line. Mice were tested repeatedly for sensorimotor function and sacrificed for histopathological analysis at 7 days or 8 weeks post-engraftment (Figure 11). Engrafted iPS cells were identified within the host brain using anti-human nuclear antigen (hNA) immunohistochemistry (IHC). For graft screening, we inspected animals without

cavitation through the cortical lamina (91% of cell-engrafted brains). We found that NSC and Nb grafts were detected in similar frequencies (50%-60% of engrafted animals, Supplemental Figure 2) whereas engrafted astrocytes were detected in notably fewer animals by 7 days post-transplantation (<30%). Within NSC- and Nb-transplanted animals, detection rates were similar between 1 and 8 weeks, suggesting that graft elimination occurs within the acute phase following our transplantation protocol. Within each cell type at either time-point, there is no significant difference in proportions between sham and CCI-injured animals (Fischer's exact test, all p values >.05, Supplemental Figure 2), suggesting that this contusion injury model does not exacerbate graft elimination compared to craniectomy-only sham injury.

We used unbiased stereological methods to estimate the total number of immunoreactive cells (Figure 12A) and the volume of the grafts (Figure 12B) from brain sections with detectable hNA+ cell populations. At both 7 day and 8 week time-points, engrafted Nbs survived in the greatest quantities (45% and 22% of starting cell number) compared to either NCSs (32% and 12%) or astrocytes (5% at 7 days only). 2-way ANOVA comparisons between NSC and Nb cell numbers did not reveal any significant differences in mean cell number at 7 days or 8 weeks. At 8 weeks, however, cell number estimates of surviving Nbs varied to a greater extent than NSCs, within each injury cohort as well as a pooled comparison (F test for unequal variance: $F_{8,5} = 11.04$, $p = .0171$). Engrafted cells were found to remain clustered near the injection site along the corpus callosum and external capsule (Figure 12C-D). Whole NSC and Nb grafts were immunoreactive for markers of neural lineage *in vivo* (Figure 13). At 7 days post-transplantation, hNA^+ grafts co-label with the immature neural lineage marker

doublecortin (Dcx). By 8 weeks, Dcx expression persisted within grafts in addition to the mature neuronal marker NeuN (Figure 13B). These data demonstrate that human iPS NSC and Nb grafts survive in the injured mouse brain parenchyma, and are able to develop over time into a mixture of cells expressing immature and mature neuronal markers.

At 8 weeks post-transplantation, immunolabeling with Dcx and the human cytoplasmic marker STEM 121 revealed neuritic processes along the white-matter tracts distal to the graft core (Figure 14). Processes were visualized spreading along the corpus callosum across the midline (Figure 14A) to the contralateral hemisphere (Figure 14B) and along the ipsilateral external capsule into the grey-matter of the entorhinal cortex (Figure 14C). These data demonstrate an active process of growth consistent with integration into host tissue by the transplanted iPS cells of either NSC or Nb identity.

Additional histology experiments revealed iPS grafts associate with host T-cells and glia within the parenchyma. Acutely following transplantation at 7 days, $CD3^+$ cells (peripheral T-cells) were seen adjacent to graft cores (Figure 15A). The presence of T-cells may indicate a host versus graft process of rejection, despite pharmacological immunosuppression. By 8 weeks post-transplantation, graft cores were encapsulated within $GFAP^+$ cell bodies and processes, suggestive of glial scar formation (Figure 15B). Furthermore, STEM121-labeled neuritic processes extending from the external capsule into entorhinal cortex coincided with numerous GFAP-labeled cells as well (Figure 15C). Neighboring tissue sections through iPS transplants show close coincidence of immunoreactivity for hNA, GFAP, and the microglial marker Iba1 extending contralaterally through corpus callosum and ipsilaterally down the external capsule

(Supplemental. Figure 3). Together, these data suggest that host adaptive immunity may be influencing xenotransplant survival and integration success despite daily sub-cutaneous administration of the immunosuppressant Cyclosporin A.

Sex-dependent Modulation of the Recovery of Sensorimotor Function by human iPS Cell Transplantation

To determine whether iPS cell transplantation alleviates long-term neurofunctional deficits, we used the adhesive removal test of forelimb sensorimotor performance until 2 months post-transplantation of Nbs and NSCs (Figure 16). Briefly, adhesive strips were applied to each forelimb and the latency to remove the adhesives was recorded. This test reveals long-term functional deficits in the forepaw contralateral to the cortical site of injury but not the ipsilateral forepaw (Figure 10D). Contrary to expectation, analysis revealed a significant adverse effect of Nb transplantation in sham-injured males but not female animals, and not in CCI-injured animals of either sex (Figure 16A).

Because the data demonstrated the greatest difference in latency at 1 week post-injury, we formatted these observations into a population-based Kaplan-Meier curve to determine the relative rate of task completion (hazard ratio) between vehicle- versus cell-injected groups (Figures 16C-D). Results of the log-rank tests (Mantel-Cox) to compare the two curves revealed that sham-injured male animals transplanted with Nbs complete the ART at 0.21 times the rate as those given the vehicle control (Figure 16C). These results demonstrate more severe neurofunctional deficits in male mice than female mice engrafted with Nbs (but not NSCs), suggesting an interaction between host sex and transplanted cell type.

Cell Engraftment Post-injury Exacerbates Neuronal Loss in the Contused Cortex

In view of the unexpected adverse effect of engraftment on sensorimotor function, we quantified host neuronal numbers in mice at 8 weeks post-transplantation. We used an unbiased stereological counting approach with immunohistochemistry to the neuronal marker NeuN to determine the effect of cell transplantation on host neuron loss post-TBI. The impacted cortical area was traced in serial coronal sections (Figure 17A) and counted with the optical fractionator probe within the Stereo Investigator software. Two-way ANOVA comparisons revealed a significant effect of engraftment with transplantation of Nbs resulting in fewer $NeuN^+$ counts within the sham-injured, but not CCI-injured cohorts, when compared to vehicle-injected controls (Figure 17B). These data indicate iPS-derived Nbs, but not NSCs, impair neuronal recovery in an injury-dependent manner.

Cell Engraftment Post-injury Modulates Gliosis in the Contused Cortex in a Sex-dependent Manner

Astrogliosis

To assess the effects of cell transplantation on injury-induced astrogliosis, we used a similar stereological approach to quantify GFAP+ astrocyte numbers in the impacted cortex at 8 weeks post-transplantation (Figure 18). Two-way ANOVA comparisons revealed CCI significantly increased astrogliosis in female but not male mice at this time point but did not reveal a main effect of transplantation on astrogliosis in either female or male mice (Figure 18A). Our analysis did reveal a simple effect within injury groups: transplanting NSCs reduced astroglial cell counts in sham-injured male mice (Figure 18A). Overall, these data do not reveal a consistent effect of cell

engraftment on astrogliosis. Rather the data suggests astroglial effects are injury severity- and sex-dependent.

Microglial Reactivity

We next used Iba1 immunohistochemistry and stereology to quantify microglia cell numbers and their ramified or non-ramified (reactive) morphology within the impacted cortex of host mice (Figure 19). At 8 weeks post-transplantation, estimates of cortical $Iba1^{+}$ cell numbers were statistically similar amongst all groups within either sex (Figure 19A). This is consistent with no effect of injury or transplantation on the presence of microglia. Morphologic analysis at 8 weeks post-transplantation revealed a significant effect of transplantation in male but not female mice (p =.0009): engraftment of iPS NSCs increased the proportion of activated microglia in both sham- and CCI-injured animals (Figure 19B). Similar to the astroglia data, these findings do not reveal a consistent effect of cell engraftment on microgliosis but do suggest sex-specific differences in microglia activation.

DISCUSSION

This study was designed to examine the potential therapeutic benefit of transplanted human iPSC-derived neural cells on neuropathology and functional recovery in a mouse model of cortical contusion injury. We assessed the viability and therapeutic potential of implanted cells to determine which neural cell phenotype (NSC or isogenic progeny neuroblasts or astrocytes) may best tolerate the injured host environment and provide clinically-relevant beneficial outcomes.

We determined engraftment success as both the proportion of animals with detectable transplanted cells as well as the number of surviving cells within graft-positive

brains. Host-graft incompatibility is often mitigated via administration of pharmacological immunosuppression agents or the use of immunodeficient host animals (5). We have found a daily regimen of the calcineurin inhibitor Cyclosporin A (10 mg/kg) was sufficient to allow for detection of NSCs and Nbs in 50-60% of xenotransplanted animals by 7 days. Despite these results, host immune responses can be seen at acute and chronic time points. T lymphocytes are detected within and around the graft by 7 days, suggestive of a host *versus* graft response. Glial cells remain associated with graft core and extensions at 8 weeks, possibly indicating a continued attempt to promote or hinder tissue integration (Figure 15A).

By 8 weeks, cell number estimates of detectable NSC grafts are found within a smaller range than at 7 days or compared to Nb grafts, indicating phenotype-specific mechanisms of graft survival. Qualitative immunohistochemistry has revealed that although both NSC and Nb grafts express the neuron-specific marker NeuN by 8 weeks, only Nb grafts do so at 7 days and therefore commit to the neuronal fate within the acutely injured parenchyma. Other groups have found xenotransplanted human NSCs may remain in an undifferentiated state (175) or express predominantly neuronal markers (53; 105) or astroglial markers (211). The advantage of Nbs for graft success may indicate that pre-transplantation commitment to the neuronal fate confers some resilience against host rejection or cell death. Conversely, we have found that transplanted cells previously cultured toward the astroglial fate were discovered in minute quantities at 7 days (Figure 11, Supplemental Figure 2) suggesting rapid and robust death of implanted cells. Haus et al. (2016) demonstrated that the *in vitro* passage number of human NSCs prior to transplantation influences long-term graft survival as well as differentiation

potential (neuronal *versus* glial fate) (66). Together, these data implicate *in vitro* culture conditions as determinants of *in vivo* viability and fate.

We have found that transplantation influenced sensorimotor recovery in sham (craniectomy)-injured animals only and that these effects are sex-dependent. Transplantation of iPS-Nbs worsens forelimb task performance in sham mice with a greater effect in male animals (Figure 16C). These data suggest that graft-mediated effects on functional recovery are dependent on injury-induced micro-environmental cues and are modulated by sex. Female sex steroid hormones have been well described as neuroprotective within a variety of preclinical models of brain and neuronal injury (89). However, rodent TBI studies report mixed results whether females display superior locomotive outcomes (60; 178). These inconsistencies within the preclinical TBI literature regarding sex-specific differences may indicate these effects are restricted spatially or temporally, and may be subject to sex-interacting variables not otherwise controlled (127). Our data demonstrate superior functional recovery in female animals compared to their male counterparts as well as sex-specific effects of transplanted cells on long-term glial reactivity.

Preservation of neurons and their network function is a major goal of preclinical therapeutic efforts (2). Our data suggests that transplantation of Nb exacerbates cortical neuronal loss early following brain injury. Compared to vehicle-injected controls, neuronal loss in Nb-transplanted brains is greater in sham-injured animals versus the CCI groups. These data correspond with the pattern of transplant influence on behavioral recovery and suggest that worsened sensorimotor function post-CCI may be directly related to enhanced neuronal loss within the impacted somatosensory and motor cortices.

Our paradigm of brain injury is unique in that sensorimotor deficits are not due to cavitation (gross tissue loss) of the contused cortex or underlying structures.

Posttraumatic neuroinflammation is acknowledged as a prominent pathophysiological syndrome underlying poor outcomes (121) and chronic neurodegeneration (109). Central to the inflammatory response are activated glial cells (principally microglia and astrocytes) which respond to trauma by acting as brain-resident immune cells (through the release of cytokines, chemokines, and complement factors, among others) and eschewing functionally vital homeostatic and brain-maintenance mechanisms.

Recent studies have implicated inflammatory cells, especially microglia, to underlie sex differences post-TBI (20). One study comparing weight-matched male and female mice discovered a more rapid and robust microglia/macrophage phenotype in male mice within the acute-phase post TBI (201). Doran et al. extended these findings in age-matched animals and demonstrated greater phagocytic and pro-inflammatory activity in male-generated microglia than those from females (38). Interestingly, our study found that transplantation of NSCs produces sex-dependent changes in glial activation such that male animals display significantly greater proportions of activated microglia and that this effect is robust in contused and non-contused brains as well. Interestingly, we did not see this effect in vehicle-injected animals. Our study is one of few (203) to report host sex differences in the effects of cell transplantation-based therapy following TBI and demonstrates the necessity of examining a variety of pathological measures in both sexes for preclinical neurotrauma research (151). Additionally, cell transplantation studies in particular must also contend with the chromosomal sex of the transplanted cell and how

that may influence interaction with the host parenchyma (17). Our chosen source of cellular material (IPS-NSCs) and its isogenic derivatives are chromosomally male cells (222).

Cell transplantation parameters such as timing, location, and dose of delivery are crucial determinants of regenerative outcomes. For instance, Péron and colleagues determined that transplantation at 7 days post-TBI significantly enhanced graft viability, integration, and benefit on host cortical physiology than immediately following injury (140), likely owing to reduced inflammation at this time (10). This study highlights the need to systematically optimize cell transplantation parameters. Additionally, preclinical studies of human cell transplantation require immunosuppression to counter host rejection. Although genetically immunocompromised mice have successfully been used as human cell transplantation hosts, pharmacological immunosuppression in otherwise immunocompetent animals represent a more clinically relevant paradigm of allogenic transplantation. Although this study controlled for the effect of Cyclosporin A on pathophysiological outcomes by delivering the drug to all groups, we cannot rule out a broad neuroprotective effect due to daily administration. Cyclosporin A can act as a neuroprotectant via anti-inflammatory and anti-apoptotic mechanisms. Cyclosporin A complexes with cyclophilin A to inhibit calcineurin function and repress the activation of pro-inflammatory mediators (198). Cyclosporin A also blocks the mitochondrial permeability transition pore to inhibit cytochrome c release and the initiation of apoptosome activity (179).

CONCLUSION

In summary, the current study demonstrates successful xenotransplantation of human iPSC-derived NSCs and isogenic neural cell progenies into the contused mouse brain. We demonstrated long-term survival, neuronal maturation, and extensive neuritic processes which traverse through host white-matter tracts despite the presence of graft-associated peripheral immune cells. Additionally, engrafted NSCs and Nbs show continued maturation toward the neuronal fate *in vivo*. We employed a model of contusion TBI to the primary motor and somatosensory cortices that produced sustained neurofunctional deficits within its cognate behavioral domain (sensorimotor), yet spared gross tissue loss and cortical neurodegeneration. Using this paradigm, transplantation of iPS-NSCs confers little-to-no benefit on functional recovery and transplantation of Nbs worsens sensorimotor deficits and exacerbates neuronal loss following TBI. Importantly, we reveal transplantation effects are host sex-dependent underscoring the importance of including biological sex as a variable in pre-clinical xenograft studies to determine the tolerance and efficacy of human stem cells for transplantation.

METHODS AND MATERIALS

Animals

Male and female C57Bl/6J mice were obtained from The Jackson Laboratory (Bar Harbor, ME; Cat. No. 0664) and allowed to acclimate after arrival for 3-10 days before intervention, such that mice were 10-11 weeks-old at the time of surgery. Animals were group-housed (5 same-sex mice per cage) and remained with the same cage-mates for the duration of the study. Male and female cages were housed in the same room in a standard

12:12 h light: dark cycle. Food and water were available *ad libitum*. Surgical procedures and behavioral testing were performed during the light phase of the diurnal cycle. Animal housing facilities were accredited by the Association for the Advancement and Accreditation of Laboratory Animal Care and all animal procedures described were approved by the institutional animal care and use committee at the Uniformed Services University of the Health Sciences (Bethesda, MD).

Study Design

This study employed a 2X2 factorial design comparing CCI or sham injury crossed with cell or vehicle transplantation for each sex. Preliminary experiments for 7-day histology planned for 10 animals for each group to determine the proportion of graft survival and yield sufficient numbers of engrafted brains. Secondary experiments to validate and further investigate histopathology at 7-days called for additional mice for NSC- and Nb-transplanted groups. For longitudinal behavioral testing, we planned for 15 animals per group per sex as a minimal sample size to detect medium-sized behavioral effects (assumed .5 standard deviations and within-subjects correlation of .1) to yield 120 animals total.

Cell Culture

Neural stem cells (NSC) derived from the human induced pluripotent stem cell (hiPSC) line NCRM-1 (43; 222) were generated through collaboration with the NIH, Sigma-Aldrich and XCell Sciences from CD 34^{+} human cord blood cells by episomal plasmid reprogramming (https://www.nimhgenetics.org/stem_cells/crm_lines.php).

Differentiation to neuronal and astroglial fates as well as maintenance of all cell types were followed as previously described by our laboratory (106).

Surgeries

Craniectomy and Controlled Cortical Impact (CCI)

Mice were anesthetized in a clear induction chamber with 3% isoflurane (Forane, Baxter Healthcare Corporation, Deerfield IL). After cessation of corneal and pedal reflexes, the scalp fur was clipped. Mice were then placed into a stereotaxic device with an incisor bar and atraumatic ear bars; anesthesia (1.5-2% isoflurane) was maintained via a flow-through nose cone. The scalp was sterilized with betadine then 70% ethanol, and anti-microbial ophthalmic ointment was applied to the orbits. A midline incision was performed and fascia cleared to expose the left side of the skull. A 5 mm craniectomy centered at 2.0 mm left of Bregma (Anterior-Posterior = 0 mm) was outlined then cut using a high-speed rotary tool with a 0.6 mm burr drill bit. Cortical impact was performed with the Impact One™ device (Leica Microsystems, Buffalo Grove, IL) using a 3mm diameter probe at a 15-degree angle relative to the sagittal plane. Impact velocity was set at 1.5 m/s, displacement depth was 1 mm, and dwell time was 100 ms. Sham surgeries were performed as craniectomy and probe positioning but without cortical impact. After CCI or sham injury, the incision site was sutured with simple interrupted stiches (silk, 5-0) without replacement of bone flap. Immediately following cessation of anesthesia, all animals received a single subcutaneous injection of the immunosuppressant Cyclosporin A (10 mg/Kg in DMSO) into the neck scruff. Mice were allowed to recover in a pre-warmed cage with softened chow until fully alert and ambulatory. All mice received acetaminophen in their drinking water (Children's Mapap,

Livonia, MI; 1 mg/ml) from the time period of acclimation to the surgical suite until approximately 24 h after the final surgery. Cyclosporin A injections were administered daily as described above until sacrifice.

Cell Transplantation

Transplantation was performed on the day after CCI or sham surgery. Cultured cells were enzymatically dissociated and re-suspended in basal culture medium without additives (DMEM; Cat. #A1443001) at $5x10^4$ cells/microliter. NSCs were transplanted between passages 8-12, astrocytes were transplanted between day 35-50 of astroglial differentiation, and neuroblasts were transplanted at day 4 of neuronal differentiation. Cell suspensions were maintained in 37° C cell culture incubators prior to and in between same-day transplantations. Mice were anesthetized with isoflurane as mentioned above. After successful induction, the incision site was reopened. Cell suspension was quickly loaded into a glass gastight syringe (Hamilton, Model 1701-RN) attached to a pulled-glass pipette needle (World Precision Instruments, Sarasota, FL). The syringe was loaded into to a syringe pump attached to a stereotaxic frame. The injection site was located at 2 mm left and 1 mm posterior to Bregma. The needle point was lowered 1.4 mm ventral from the dura mater surface. 2 microliters of cell suspension were injected at a rate of 0.2 microliters per minute. An additional 5 minute pause after injection allowed graft suspension to equilibrate in host tissue and mitigated backflow upon needle withdrawal. The incision site was sutured closed and animals returned to their home cages.

Rotarod Behavior Testing

Testing was conducted following the protocol of Tucker and colleagues (196). Mice were acclimated to a rotating rod apparatus (Ugo-Basile) for 3 days prior to baseline testing. The apparatus was programmed to accelerate rotation from 4 RPM to 60 RPM over the course of 3 minutes. The first training session consisted of placing animals on the rod for 1 minute to acclimate to 4 RPM rotation before initiating acceleration. Subsequent training was performed with accelerating rotation only. Latency to fall from the rod or to cling to the beam for 3 consecutive rotations was recorded. Mice that did not meet these failure criteria and completed an entire trial were given a score of 180 sec. Three such trials were performed for each mouse on each testing day. The three latency times per testing day were averaged to yield a single score for each mouse. Testing was performed on postoperative days 1, 3, 5, 7, 10, and 14.

Adhesive Removal Behavior Testing

Animal experiments were initiated when animals were 10-11 weeks old. Experiments were conducted during the light phase of animals' waking cycle. Similar experiments were conducted during light phase with minimal impact on behavior (196). Sensorimotor integration behaviors were tested at baseline on the day before surgeries, and then on postoperative days as described below. Mice were allowed to rest for a minimum of 30 min between transportation to the testing facility and beginning behavior testing. Testing was conducted according to a detailed protocol by Bouet and colleagues (16). Briefly, adhesive electrical tape (3M) was cut into 3mm x 5mm strips. Each mouse was held immobilized while tape strips were applied to the ventral "palm" of each forepaw. The mouse was placed in an elevated transparent chamber and observed during

a 2 min trial. Latencies to notice the tape and to remove the tape of each paw was recorded. Notice events were indicated by shaking the paw or bringing the paw to the mouth. Mice were acclimated to this procedure for 5 days prior to recording baseline testing data. Two trials were performed per testing day for each mouse. The latencies to notice and to remove the tape were averaged. Testing was performed on postoperative days 1, 3, 5, 7, and weekly thereafter until 8 weeks post-injury.

Tissue Preparation, Histology, and Immunostaining

Transcardial Perfusion

Mice were deeply anesthetized with inhaled 4% isoflurane in O_2 vehicle gas. When mechanical stimuli failed to produce paw withdrawal or eye blink reflexes, thoracotomy was performed to expose the heart. A probe was introduced into the left ventricle to flow 0.1 M sodium phosphate-buffered saline solution (PBS; pH 7.4) from a peristaltic pump, and the right atrium was cut to permit exsanguination. When perfused PBS ran clear, the pump solution was changed to 4% paraformaldehyde in PBS (PFA). Mice were perfused until either 25 ml PFA was used or the extremities were sufficiently rigid. Tissues were further post-fixed overnight in PFA at 4° C.

Histologic Sectioning

PFA-fixed brains were embedded in 4% agarose gel and mounted on a vibratome. Brains were cut into 50 µm sections, and serial sections were collected from anterior to posterior starting just prior to the anterior commissure. Sections were stored in PBS with 0.04% NaN_3 in 96-well plates.

Diaminobenzidine (DAB) Immunohistochemistry

Tissue sections were rinsed with deionized water (diH_2O), then treated with antigen retrieval buffer (10 mM Sodium Citrate, 0.05% Tween 20; pH 6.0) at 60° C for 30 min. Tissues were rinsed again with diH_2O, then treated with 0.3% hydrogen peroxide in diH_2O for 10 min. Tissues were rinsed in diH_2O, PBS, and PBS with 0.4% Triton X-100 (PBS-T). Tissues were incubated overnight at 4° C with primary antibody in MOM Diluent. Primary antibodies were: mouse anti-Human nuclear antigen antibody (anti-hNA, Millipore; 1:500); rabbit anti-NeuN antibody (Abcam; 1:1000; Cat. #ab104225); rabbit polyclonal anti-GFAP antibody (DAKO; 1:1500); rabbit polyclonal anti-Iba1 antibody (Wako; 1:1000; #019-19741). For anti-hNA only, tissues were treated with the Vector Labs Mouse-on Mouse (MOM) kit to reduce non-specific staining. Following anti-hNA incubation tissues were rinsed with PBS-T then incubated at room temperature for 1-2 hr with donkey anti-mouse HRP-conjugated secondary antibody (Jackson Immunoresearch; 1:250). For all other primary antibodies, tissue sections were rinsed with PBS, then processed using Vectastain® ABC kit (Vector Laboratories; PK-4001) according to the manufacturer's instructions: tissues were incubated at room temperature for 1 hr with anti-rabbit biotinylated secondary antibody, rinsed with PBS, then incubated with ABC reagent for 1 hr. All tissues were rinsed again with PBS-T, then PBS, and immunoreactivity was revealed using Vector Labs DAB Kit. Anti-hNA immunostained tissue sections were mounted directly on poly-L-lysine coated slides and coverslipped for microscopy using Mowiol® embedding medium (Millipore-Sigma). All other immunostained sections were counter-stained in Mayer's Hematoxylin Solution (Millipore-Sigma; MHS1) for 3 minutes, then in 1% sodium-bicarbonate for 3 minutes.

Counter-stained sections were then mounted on poly-L-lysine coated slides and coverslipped for microscopy using Mowiol®.

Fluorescence Immunohistochemistry

Tissue sections were permeabilized by repeated rinsing with PBS-T (0.04%) at room temperature, followed by rinsing with saline, then treating with antigen retrieval buffer (10 mM Sodium Citrate, 0.05% Tween 20; pH 6.0) at 80° C for 30 min. Tissues were rinsed in saline, then PBS-T. Tissues were incubated in 10% NGS blocking solution made with PBS-T (0.4%). Tissues were incubated for no less than 48 hours at 4° C in 5% NGS blocking solution with combinations of the following primary antibodies: rabbit anti-GFAP (1:500; DAKO, S3020), rabbit anti-Iba1 (1:500; WakoChem, 019-19741), mouse anti-STEM121 (1:500; StemCell Technologies, AB-121-U-050), rat anti-CD3 (1:1000; R&D Systems, MAB4841), guinea pig anti-doublecortin (1:1000; MilliporeSigma, AB2253), mouse anti-human nuclear antigen (hNA, 1:300; MilliporeSigma, MAB1281), rabbit anti-human nestin (1:300; MilliporeSigma, ABD69). Tissue sections were secondary antibodies conjugated to Alexa fluorophores 488, 555, or 647 (Invitrogen). Sections were rinsed with PBS and were mounted on poly-L-lysine coated slides and coverslipped for microscopy using Mowiol® embedding medium (Millipore-Sigma).

Blood-Brain Barrier Integrity

Evans Blue dye was injected and measured *ex vivo* as previously published (79). Two days following CCI or sham surgery, injured and naïve animals received a single injection of 4% Evans Blue dye (2.5 mL/kg; MilliporeSigma) via the lateral tail-vein under isoflurane anaesthesia. Animals were transcardially perfused with 20-30 mL

heparinized (10U/mL) saline and de-brained. Freshly harvested hemispheres were homogenized in 50% Trichloroacetic acid (TCA; MilliporeSigma) at 3 times the tissue mass (w/v) using the BeadBug Microtube Homogenizer (Benchmark Scientific). Extravasated dye within the supernatant was quantified using a plate reader with emission equal to 612 nm.

Microscopy

Stereologic Analysis

Sections containing DAB-stained cells were analyzed using Stereo Investigator software (MicroBrightfield, Williston, VT) on a PC connected to a Zeiss AxioImager M2 upright (model number) microscope with a XYZ-motorized stage and visualized with Zeiss Axiocam MRc color camera. All parameters were defined during pilot experiments to produce a stereologically reliable sampling density (coefficient of error, m=0, <0.1) for all target probes. The lateral extent of the counting volume for the estimation of anti-NeuN, anti-GFAP or anti-Iba1 immunolabeled cells was determined using the equation $y = \sqrt{x^2} - 1.52 + 2$, where x is the anterior-posterior (AP) Bregma coordinate of the section. The counting volume encompasses the cortical area directly impacted by the CCI device. Regions of interest were outlined while magnified with a 2.5x objective. Unbiased stereological cell counts were conducted by researchers blinded to the identity of the experimental groups.

Human Nuclear Antigen Estimation

Tissue sections 50 µm thick were taken from a range encompassing 1.5 mm centered on the point of cell injection. Every third section in the range was selected for hNA immunostaining (100 µm interval), for a total of 11 sections. DAB-stained grafts

were outlined, and a counting grid of 100x100 µm/region was overlaid. A stereologic counting frame of 25x25 µm was used to sample graft regions in a random systematic manner. Mounted section thickness was defined as 25 µm. hNA-positive nuclei were counted under 40x magnification (numerical aperture = 0.4). Immunopositive nuclei where counted at the Z depth of the widest circumference. Average number of counted cells per animal = 716 (7 day), 282 (8 week); range = 62-2034 (7 day), 1-1398 (8 week). The serial section manager was used to estimate total number of engrafted cells within the quantified region.

NeuN Estimation

Sets of every tenth section (500 µm interval), were taken from the brain impact region spanning AP +1.5 mm to AP -1.5 mm relative to Bregma, for a total of 6 sections. The sampling grid was set at 450x450 µm, the counting frame 30x30 µm, and the counting height 20 µm was set to the middle of the mounted section thickness (measured at 23.86 µm, 1.23 (mean, SD)). The impacted cortex and ipsilateral striatum were counted under 40x magnification (numerical aperture = 0.4). Immunopositive nuclei where counted at the Z depth of the widest circumference. Average number of counted cells per animal = 261, range = 151-500.

Astrocyte and Microglia Estimation

Sets of every third section (150 µm interval), were taken from the brain impact region spanning AP +0.3 mm to AP -0.4 mm relative to Bregma, for a total of 5 sections. The sampling grid was set at 400x400 µm, the counting frame 50x50 µm, and the counting height 10 µm was set to the middle of the mounted section thickness (measured at 16.23 µm, 3.07 (mean, SD)). The impacted cortex was counted under 63x oil

immersion magnification (numerical aperture = 0.9). Immunopositive Iba1$^+$ cells where counted at the Z depth of the widest circumference. Iba1$^+$ cell were simultaneously classified based on morphology as "ramified" (small cell body, numerous and thin processes) or "non-ramified" to denote activation status (109). Astrocytes were identified by using GFAP$^+$ processes to find the corresponding hematoxylin-stained nuclei, and were counted at the widest nuclear circumference. Average number of GFAP$^+$ counted cells per animal = 153, range = 52-326. Average number of Iba1$^+$ counted cells per animal = 150, range = 101-255.

Confocal Microscopy

Fluorescence images were captured using a Zeiss LSM 700 microscope system in the Uniformed Services University Biomedical Instrumentation Core laboratory. Tissues were scanned in Z-stacks of 1 µm-thick images. Flattened images were exported from stacks using the maximum intensity projection function in Zeiss ZEN software.

Statistics

All statistics were performed using Prism 7.05 (GraphPad, La Jolla, CA).

iPS-cell Graft Quantification

Frequencies of detecting extant engrafted cells were compared using Fischer's exact test between cell types within injury levels and time-points, then within cell types between acute and chronic time points and finally between sham and CCI conditions. Mean graft cell number and volume estimates were compared using 2-way ANOVA within each time-point. Estimates of iPS-astro grafts were not included in these analyses.

To formally test variability of mean graft cell numbers, we used the F test of unequal variance.

Host Neuropathology and Gliosis

NeuN+, GFAP+, and total Iba1+ cell number estimates were analyzed using 2-way ANOVA for main effects of transplantation and injury within each time-point. *Post-hoc* comparisons to vehicle analyzed as simple effects within injury and corrected using Dunnett's method. To compare activation status of identified microglia, the proportion of "non-ramified" $Iba1^{+}$ cells (non-ramified Iba1+ cell number/ total Iba1+ cell number) was first processed by log-ratio transformation (logit(*proportion*)) then analyzed using 2-way ANOVA with Dunnett's *post-hoc* method (176).

Behavioral tests

Latency scores generated from the ART and Rotarod tasks were compared using 2-way ANOVA with repeated measures within each injury level. *Post-hoc* comparisons to vehicle analyzed as simple effects within each time-point and corrected using the Sidak-Holm method. ART data from time-point day-7 was formatted into a Kaplan-Meier plot to compare the relative rate of task completion. Curves were directly compared using the Mantel-Cox test and the log-rank hazard ratio as reported (80).

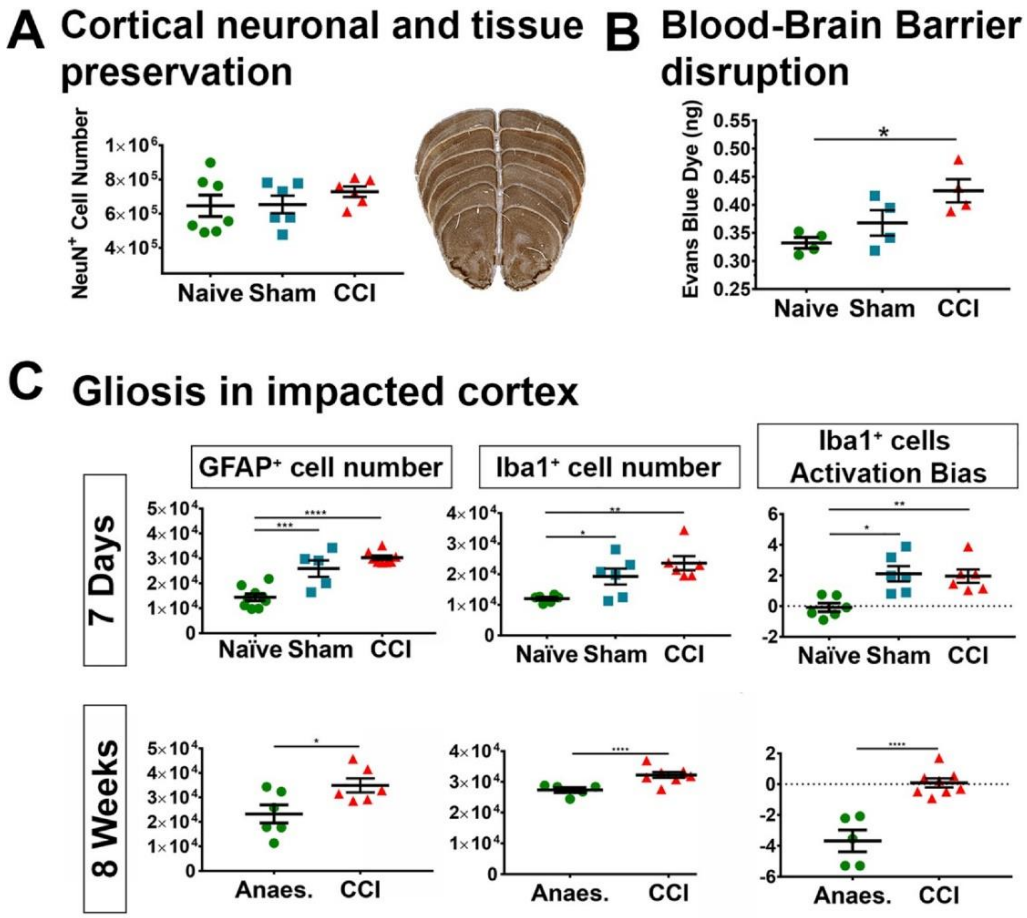
A Cortical neuronal and tissue preservation
NeuN+ Cell Number
1×10^6
8×10^5
6×10^5
4×10^5
Naive Sham CCI
B Blood-Brain Barrier disruption
Evans Blue Dye (ng)
0.55
0.50
0.45
0.40
0.35
0.30
0.25
*
Naive Sham CCI
C Gliosis in impacted cortex
GFAP+ cell number
Iba1+ cell number
Iba1+ cells Activation Bias
7 Days
5×10^4
4×10^4
3×10^4
2×10^4
1×10^4
0
Naïve Sham CCI
6
4
2
0
-2
8 Weeks
Anaes. CCI
D Sensorimotor Neurofunctional Deficits
Rotorod Test
Latency (s) to fall
150
120
90
60
Naïve Sham CCI
N = 10-12
Base 1 3 5 7 10 14
Days Post-Injury (DPI)
Adhesive Removal Test
Contralateral Forepaw
Ipsilateral Forepaw
Latency (s) to remove adhesive
120
90
60
30
0
Naïve
Sham
CCI
N = 12
Base 1 3 5 7 10 14 21 28 35 42
Days Post-Injury (DPI)

Figure 10. Contusion neurotrauma to the mouse somatosensory and motor cortices produces hallmarks of clinical TBI with minimal neuronal pathology. **(A)** Neuronal preservation of the ipsilateral cortex at 7 days post-injury is confirmed using unbiased stereological estimation of Neuronal Nuclei+ (NeuN+)-immunopositive cells. Series of coronal sections taken from the contused brain demonstrates gross tissue preservation. **(B)** Blood- brain barrier (BBB) disruption at 3 days post- injury indicated by Evans Blue dye extravasation into the impacted hemisphere. **(C)** Robust astrocyte and microglia reactivity within the impacted cortex at 7 days and 8 weeks post-injury indicated by increased cell number and microglial phenotype bias. **(D)** Behavioral deficits of sensorimotor function at acute and chronic time-points following TBI assessed through the Rotarod and Adhesive removal tests. Groups: CCI receive anesthesia, scalp incision, craniectomy and controlled cortical impact; sham receive anesthesia, scalp incision, craniectomy; Anaes receive anesthesia, scalp incision only. * = CCI versus Naïve, + = CCI versus Sham; * < 0.05, ** < 0.01, *** < 0.001, **** < 0.0001.

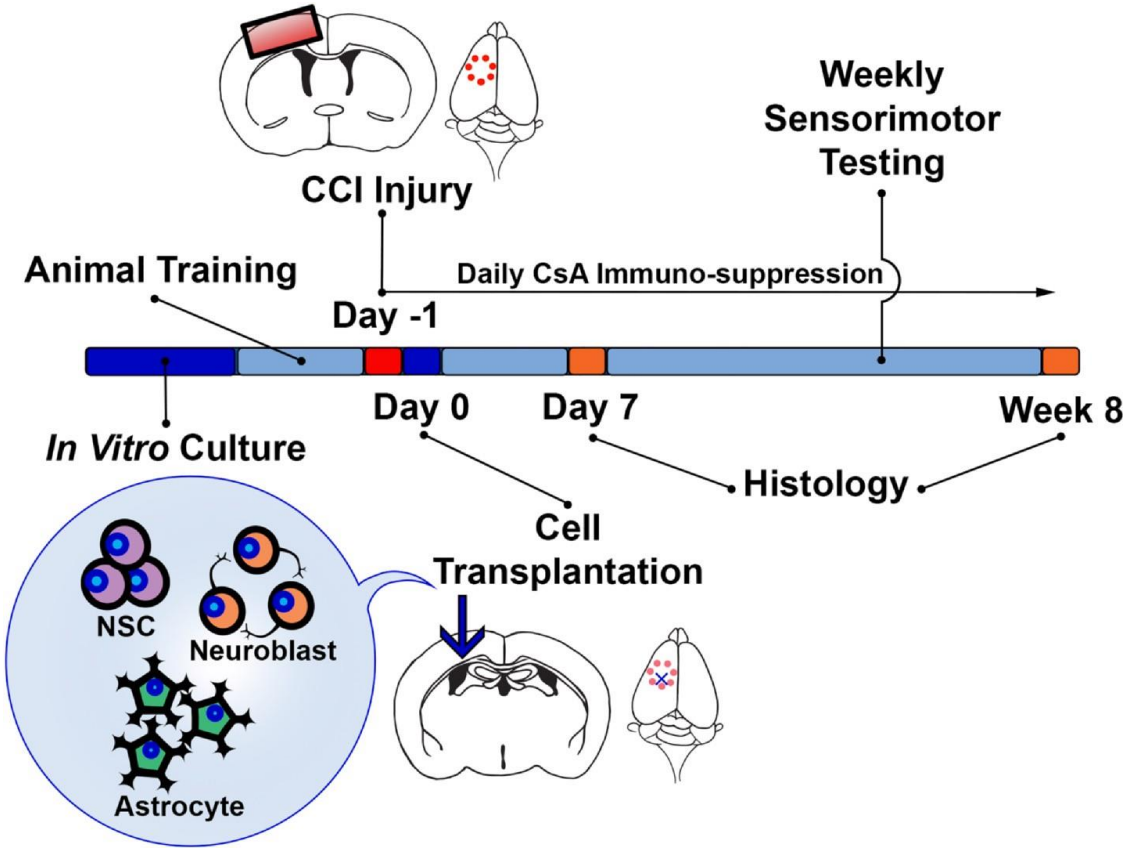

Figure 11. Mouse model of traumatic brain injury followed by cellular transplantation paradigm. Traumatic contusion to the somatosensory and motor cortices is delivered to the exposed left forebrain by controlled cortical impact (CCI) and is following 1 day later with a single microinjection of 1 x 10^5 suspended hiPSC-derived neural cells into the deep layers of the impacted cortex. Mice are testing for sensorimotor function repeatedly and sacrificed for histopathological analysis at 7 days and 8 weeks post-transplantation.

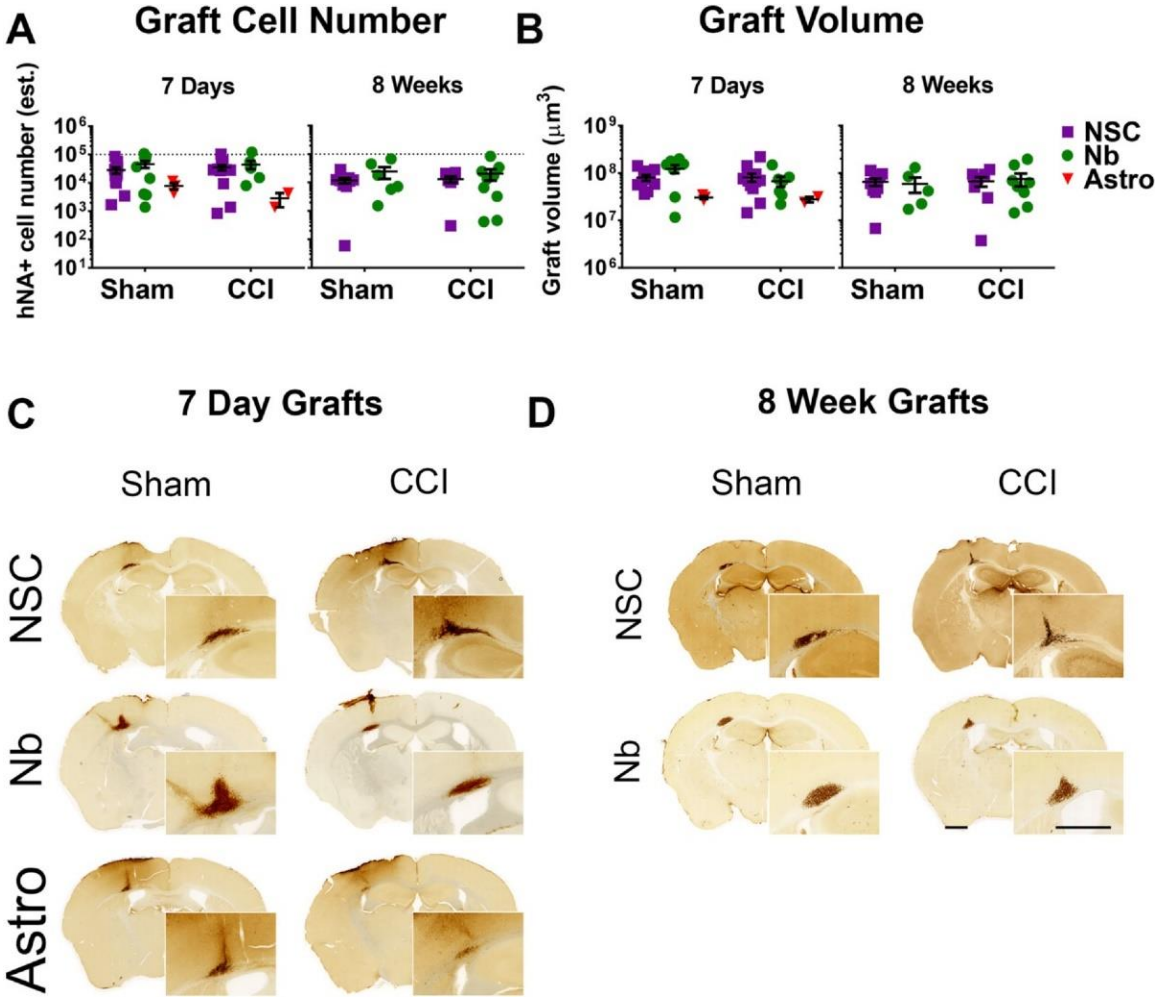

Figure 12. hiPSC-derived graft detection and quantification at 7 days and 8 weeks post-transplantation using hNA-directed immunohistochemistry. **(A, B)** Graft cell number and graft volume were quantified using stereological estimation probes. Dotted line represents 10^5 cells injected. **(C, D)** Representative micrographs of brightfield hNA^+ IHC across all treatment groups and time-points. Note clustering of hNA^+ cells in white matter tracts. Scale bars = 1 mm.

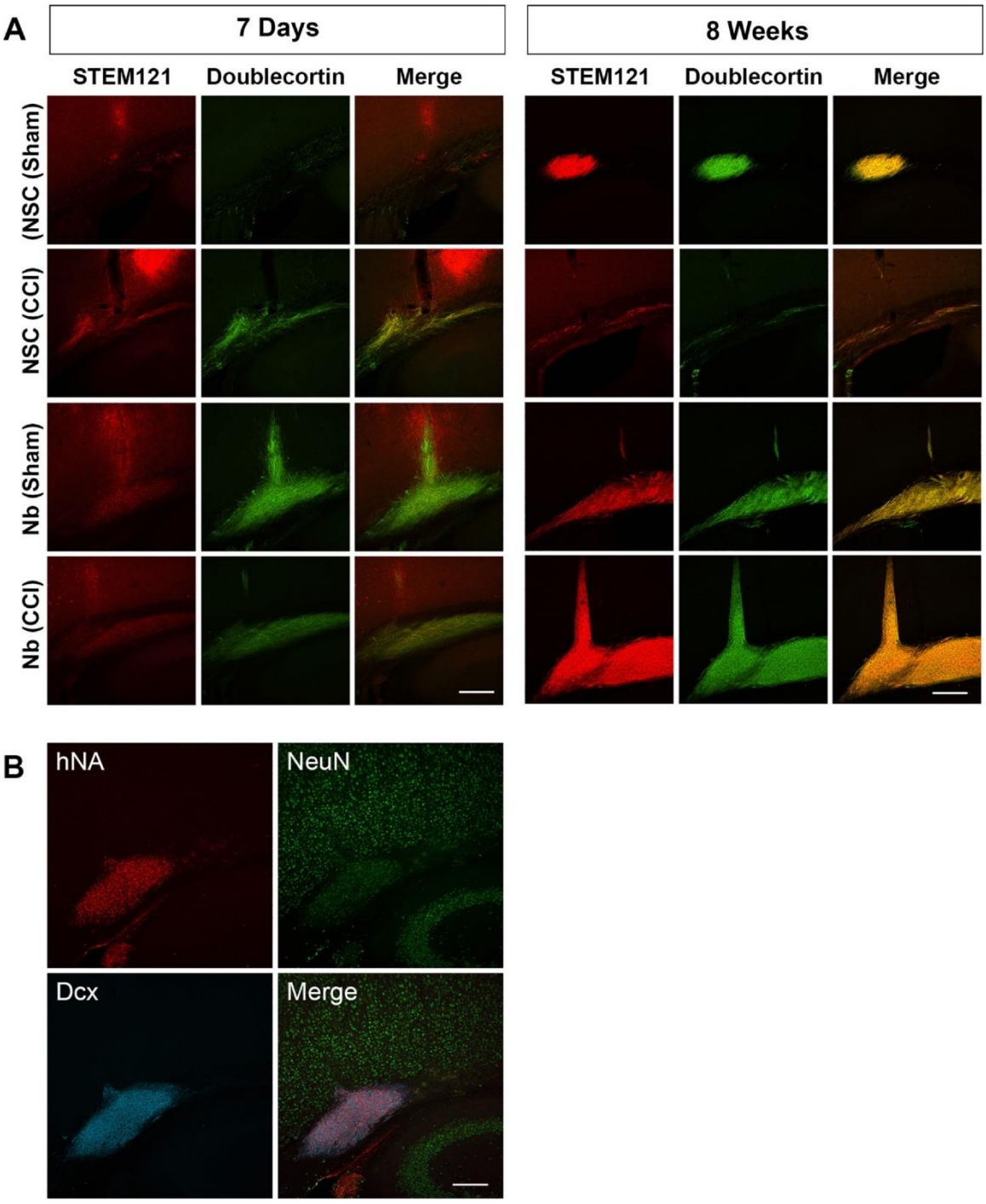

Figure 13. hiPSC-derived neural cell transplants remain clustered near the graft core up to 8 weeks post-transplantation. (**A**) Engrafted cells continue to express the immature neural cell marker doublecortin (Dcx) at 7 days and 8 weeks. (**B**) Fluorescent microscopy demonstrates human nuclear antigen (hNA)-labelled grafts as a mixture of cells expressing immature and mature markers of neuronal fate in an Nb-engrafted brain at 8 weeks. Scale bars = 200 µm.

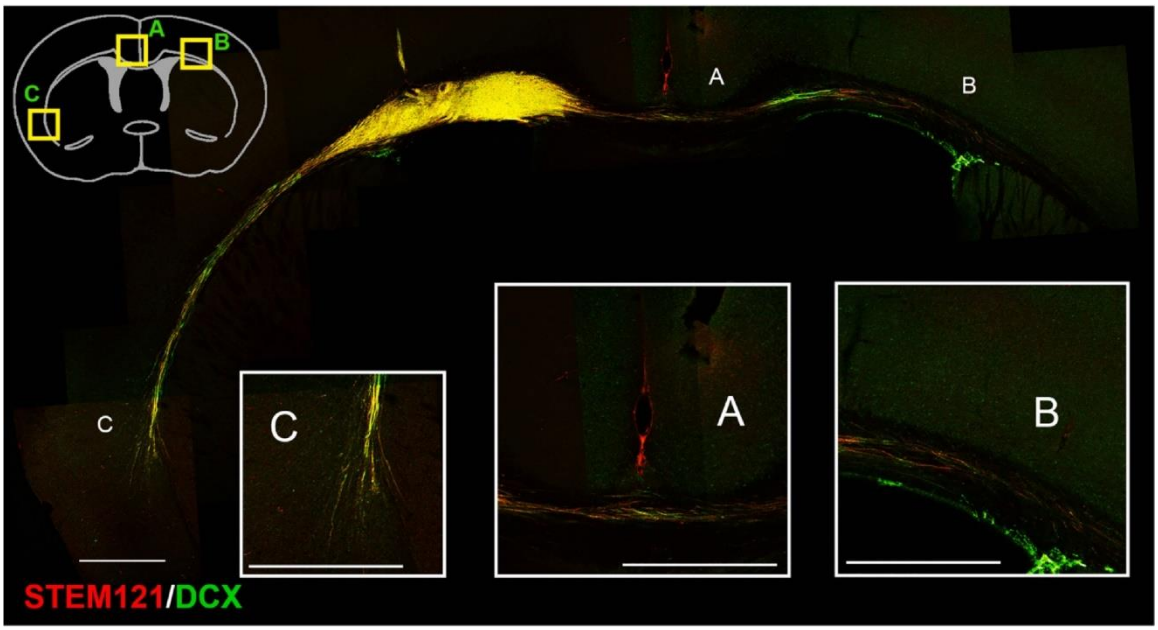

Figure 14. hiPSC-derived neural cell transplants send extensive processes and maintain an immature phenotype by 8 weeks post-transplantation. **(A, B)** Processes spread past the midline along the corpus callosum into the contralateral white-matter tracts.
(C) Processes of both graft cell types emanate from the white-matter into the entorhinal gray-matter and co-localize with immature neural cell marker doublecortin (Dcx). Scale bars = 200 µm.

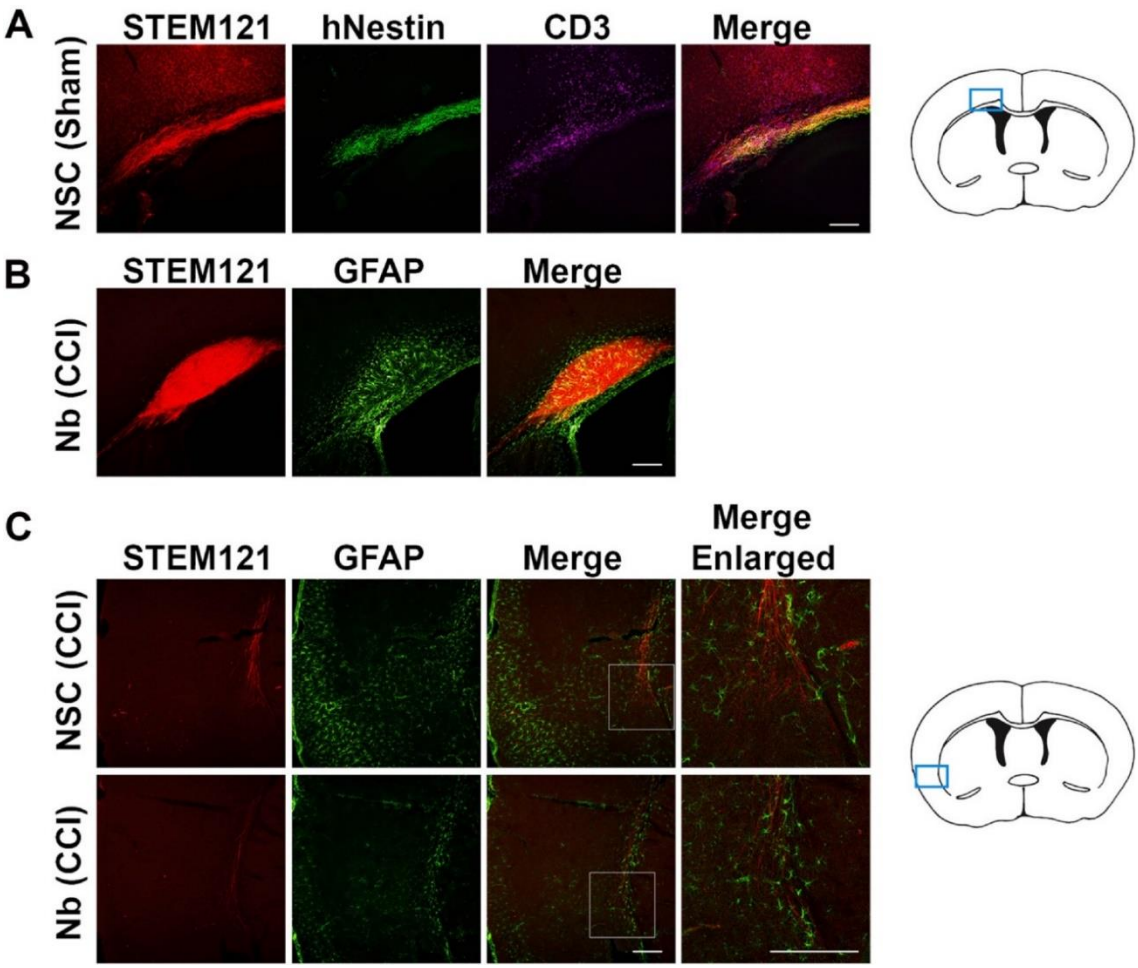

Figure 15. hiPSC-derived neural cell grafts associate with T-cells and host astroglial cells. (**A**) Human cytoplasmic marker STEM 121 is seen in association with $CD3^{+}$ T-cells at 7 days. (**B**) Astroglial encapsulation of the graft core is evident up to 8 weeks post-transplantation. (**C)** Graft processes distal to the injection spot are also seen in interaction with host astroglial cells. Scale bar = 200 µm.

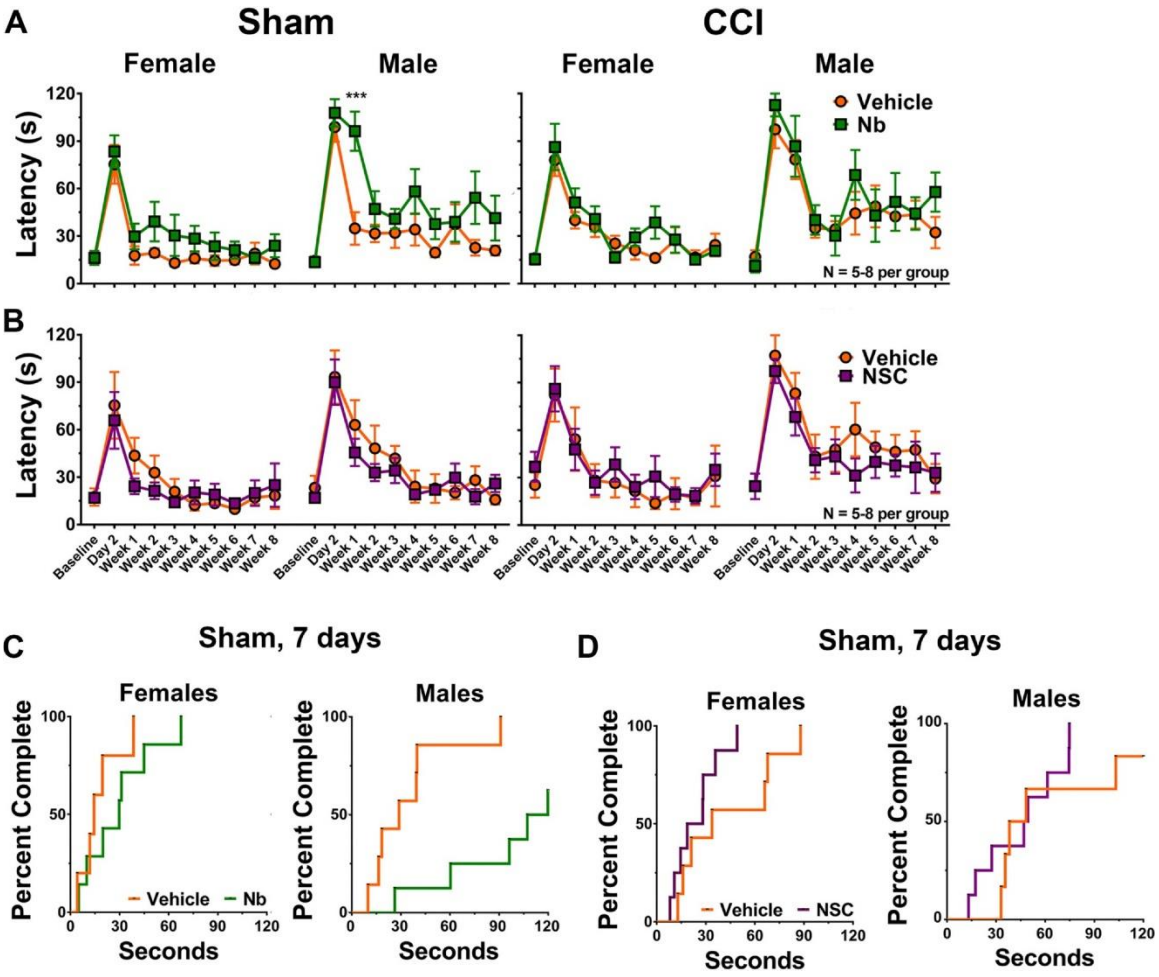

Figure 16. Longitudinal recovery of forelimb sensorimotor function following transplantation of hiPSC-Neuroblasts and -NSCs. **(A)** Transplantation of Nbs significantly lengthens the latency to remove the adhesive from the affected forelimb in sham-, but not CCI-injured male animals (2-way ANOVA, effect of graft, $F_{1,13} = 5.003$, $p = .0435$). **(B)** In contrast, no significant contribution to latency outcomes are observed following transplantation of NSCs in either injury treatment or between sexes. **(C-D)** Cumulative incidence plots of ART performance in sham-injured animals at 7 days post-injection. **(C)** Following Nb transplantation, male animals complete the task slower than vehicle-injected controls at ~one-fifth the rate (Log-Rank Test: Hazard ratio = 0.21, $p = .0016$). **(D)** Differences in the rate of task completion in male and female mice transplanted with NSCs is not significant (HR = 2.088, $p > .1$). Transplantation effects within injury and within sex were analyzed by repeated measures 2-way ANOVA, and Sidak's *post-hoc* analysis was performed for multiple comparisons, ***$p < 0.001$. Mean ± *SEM*.

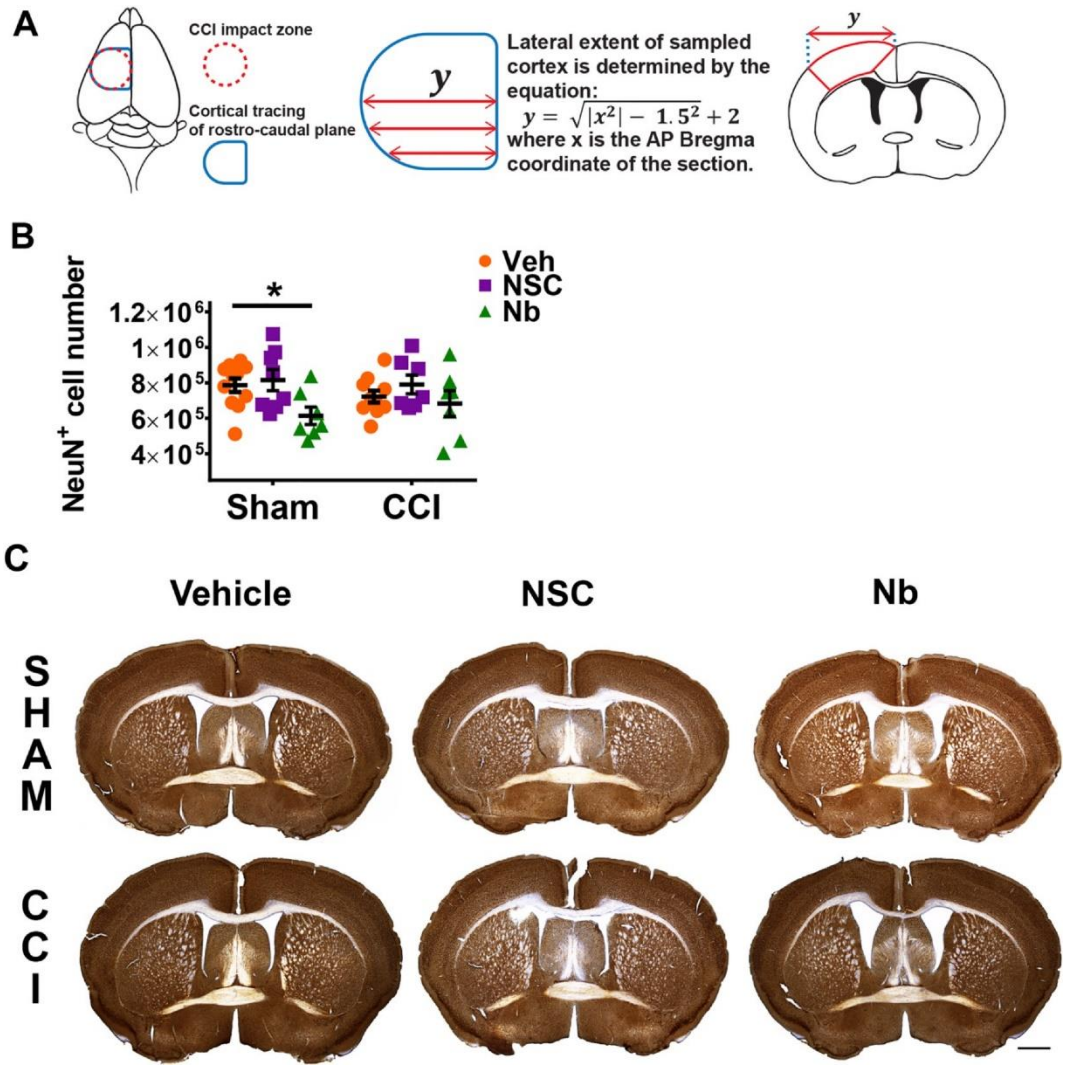

Figure 17. Reduced host neuronal survival with Nb transplantation. Host neuronal survival was quantified using immunohistochemistry and an unbiased stereological counting method. (**A**) Tracing method used to identify CCI impact area on serial coronal sections for stereological estimation. (**B**) Estimates of $NeuN^+$ cell number within the ipsilateral cortex at 8 weeks post-transplantation. Cell counts from both sexes reveal a significant effect of transplantation (2-way ANOVA, effect of graft, $F_{2,44} = 4.393$, $p = .0182$). *Post-hoc* comparisons to vehicle analyzed as simple effects within injury and corrected using the Dunnett method. *<0.05. **C**, Representative images of NeuN immunoreactivity at 8 weeks post-transplantation in coronal sections including the anterior commissure. Scale bar = 1 mm.

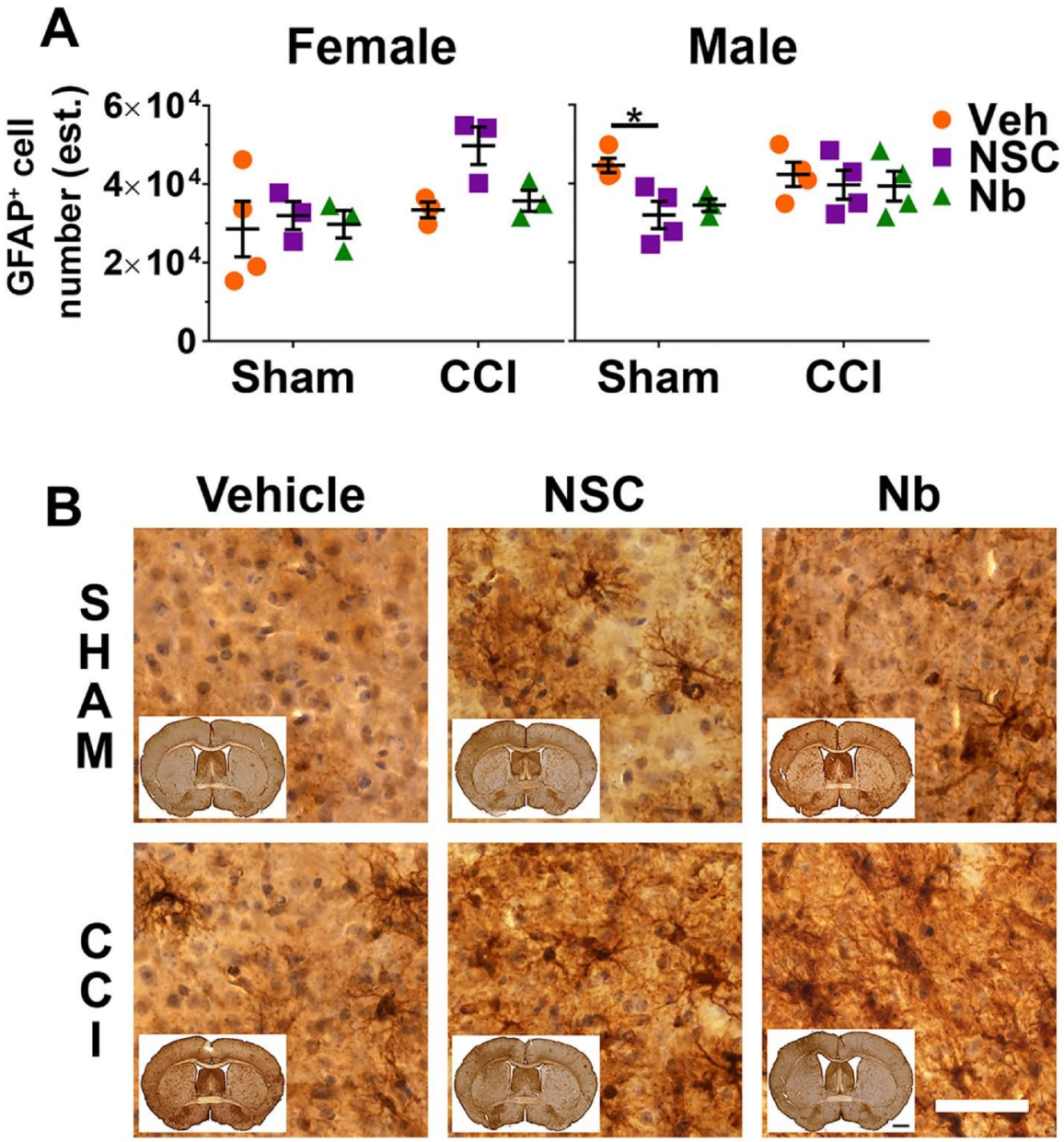

Figure 18. Host astrogliosis was quantified at 8 weeks post-transplantation using immunohistochemistry against GFAP and stereology. **(A)** Effect of injury in female but not male mice. 2-way ANOVA, effect of injury in females, $F_{1,13} = 5.799$, $p = .0316$. *Post-hoc* comparisons to vehicle analyzed as simple effects within injury and corrected using the Dunnett method. *<0.05. **(B)** Representative images of relative GFAP immunoreactivity within the impacted cortex at 8 weeks post-transplantation. Tissue sections are counterstained with hematoxylin. Scale bar = 50 µm. Inset Scale bar = 1 mm.

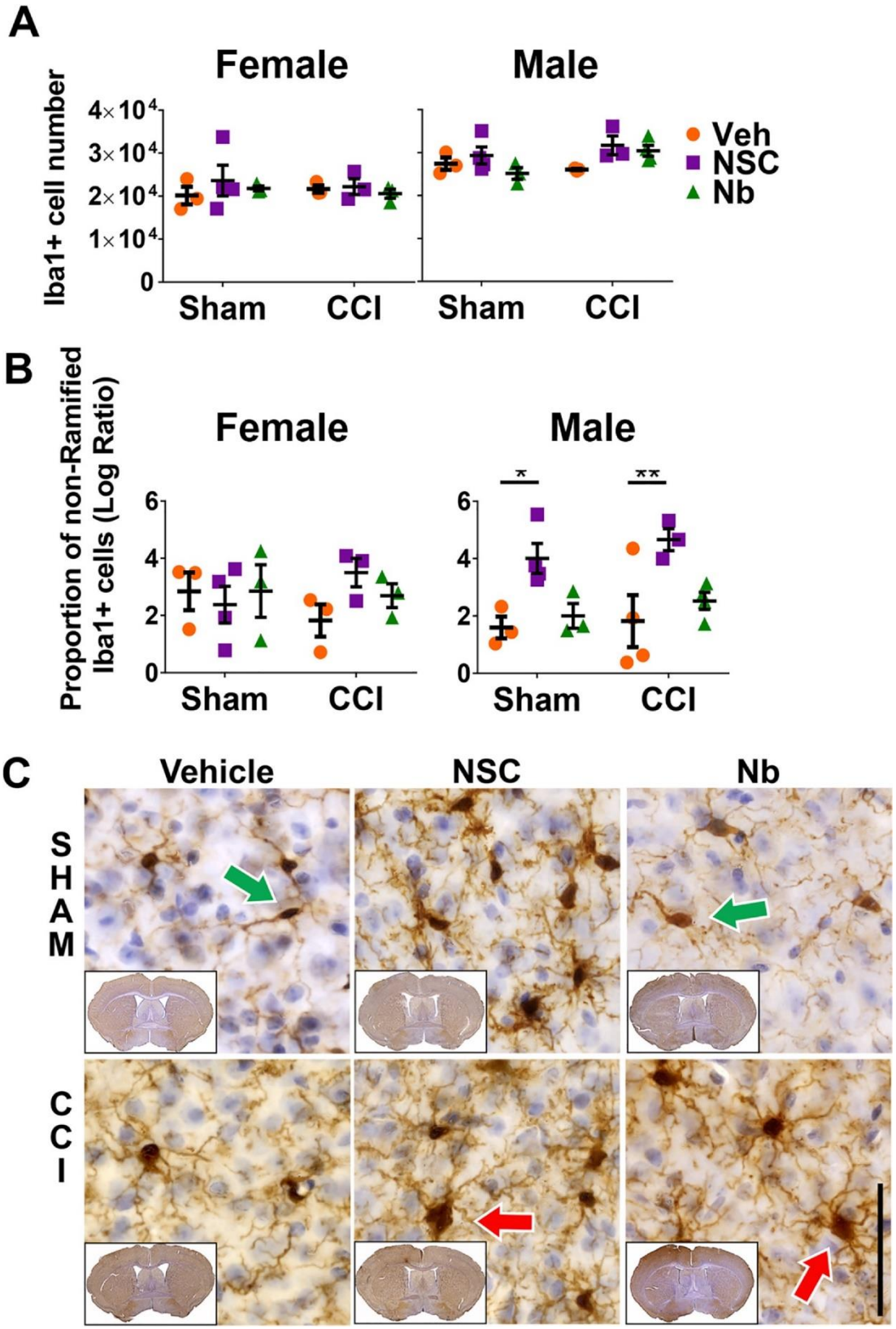

Figure 19. Host microglial reactivity was quantified at 8 weeks post-transplantation using immunohistochemistry against Iba1 and stereology. **(A)** Cortical Iba1^{+} cell counts

do not differ amongst groups within either sex. **(B)** However the proportion of non-ramified cells within males reveals a significant effect of NSC engraftment (2-way ANOVA, effect of graft, $F_{2,15} = 11.53$, $p = .0009$). *Post-hoc* comparisons to vehicle analyzed as simple effects within injury and corrected using the Dunnett method. *<0.05, **<0.01. The increased ratio non-ramified to ramified microglia is consistent with increased microglia activation with NSC transplantation in sham and CCI male mice. **(C)** Representative images of relative Iba1 immunoreactivity within the impacted cortex at 8 weeks post-transplantation. High magnification images (40x) demonstrate typical microglial morphology encountered and identifies ramified (green arrows) and non-ramified (red arrows) cells. Tissue sections are counterstained with hematoxylin. Scale bar = 50 μm.

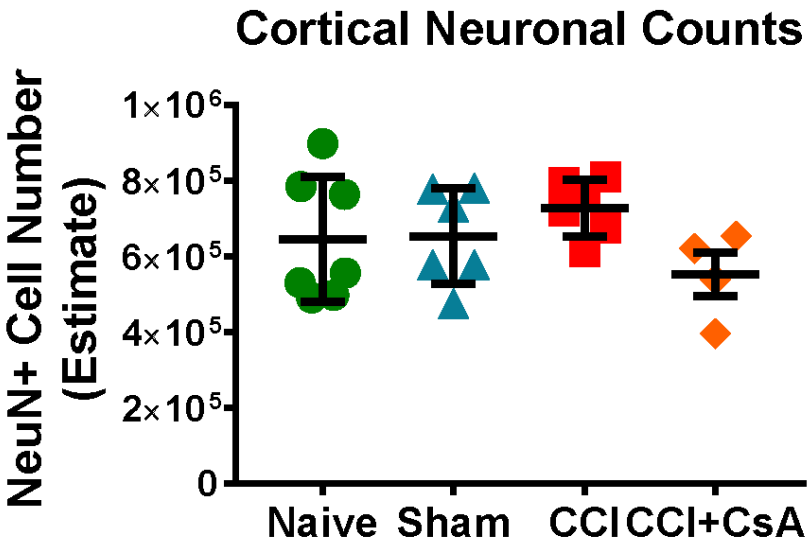

Supplemental Figure 1. Post-injury Cyclosporin A (CsA) administration is not neuroprotective following our model of controlled cortical impact (CCI). CsA was administered immediately post-CCI and then daily until end-point. Mice were sacrificed for immunohistochemistry at 7 days post-injury. Unbiased stereological estimation of Neuronal Nuclei (NeuN)-immunopositive cells confirms daily CsA administration following our model of CCI injury is not neuroprotective. One-way ANOVA: $F_{3, 19}$ = 1.518, p =.2421.

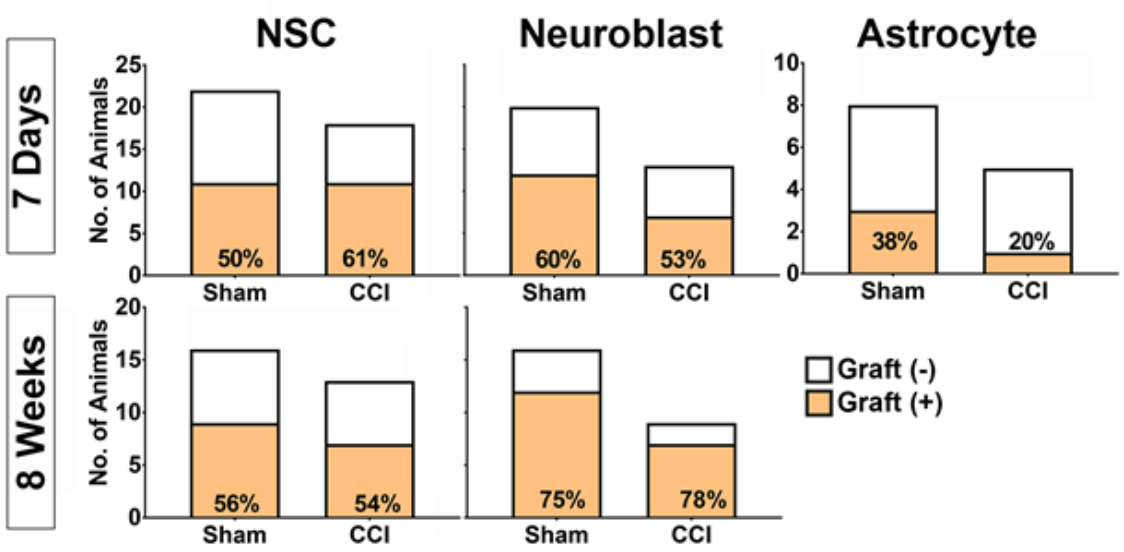

Supplemental Figure 2. hiPSC-derived neural cell graft detection at 7 days and 8 weeks post-transplantation. Graphs display the number of implanted animals with detectable hNA^{+} immunoreactivity. Coronal brain sections are screened every 150 µm rostro-caudally. For each cell type at either time-point, there is no significant difference in proportions between sham and CCI-injured animals (Fischer's exact test, all $p > .05$).

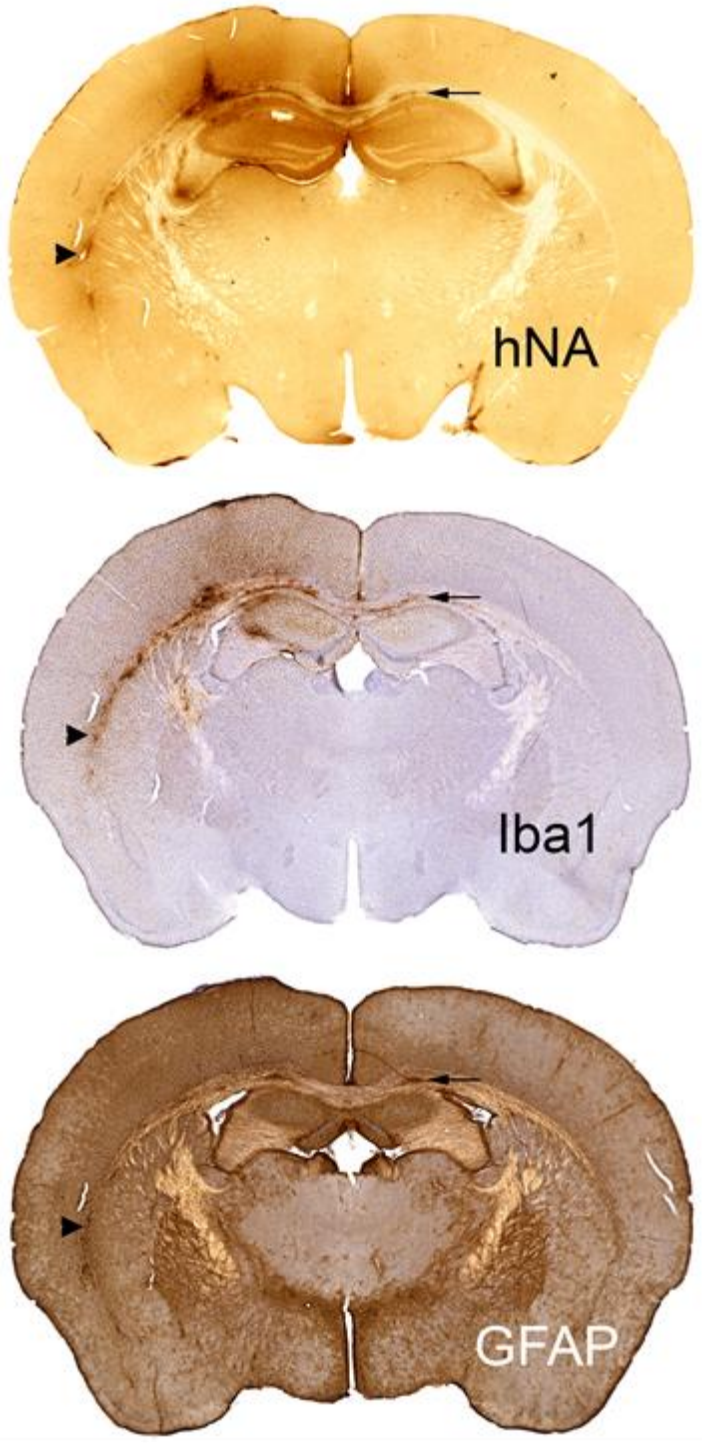

Supplemental Figure 3. Transplanted human cells coincide with activated host neuroimmune cells. Neighboring brain sections from a representative transplant at 8-weeks survival time. Immunoreactivity for hNA, Iba1, and GFAP localize to similar histologic features at the graft core, contralateral corpus callosum (arrows), and ipsilateral external capsule (arrowheads).

CHAPTER FOUR

DISCUSSION

We have characterized and exhibited a mouse model of mild contusion TBI that results in robust innate neuroinflammation and cognate behavioral dysfunction, yet preserves cortical tissue long after the traumatic event. By using mild injury parameters within an open-skull model, the injury results in categorically mild tissue pathology (Figures 7 and 10). The low-velocity contusion (1.5 m/s) and shallow depth (1 mm) of the CCI avoids tissue loss in the cortex and underlying structures yet instigates a period of cortical inflammation characterized by robust astrocyte and microglial activation (gliosis), loss of blood-brain barrier (BBB) integrity, and elevated levels of proinflammatory cytokines and chemokines. Additionally, by targeting the primary somatosensory and motor cortices, we are able to track cognate sensorimotor function up to 8 weeks post-injury (PI) in behavioral measures of complex limb function and ambulation. The robust and lasting behavioral and neuroinflammatory pathology produced by the mild injury parameters despite a lack of gross tissue or neuronal loss (Figure 10a) provides an excellent model to interrogate pathophysiological and neuroinflammatory correlates of TBI-induced sensorimotor dysfunction.

BEHAVIORAL PATHOLOGIC FEATURES OF OUR MODEL

A major goal of experimental TBI research is the adequate representation of human TBI features within animal models. We have developed a mouse model of contusion TBI to the left primary somatosensory and motor cortices which produces

sensorimotor deficits cognate to the injured cortex. CCI impact centered at 2 mm left of Bregma is positioned to impact cortical areas corresponding to forelimb, hindlimb, and head motion (193)(Figure 3A). Behavioral tasks administered following CCI demonstrated deficits in motor coordination acutely PI and lateralized forepaw and hindpaw sensorimotor integration chronically.

When challenged with nuisance adhesives placed on both forepaws during the adhesive removal test (ART), CCI-injured mice demonstrate impairments to notice and remove the adhesives from either paw, yet are especially impaired on the side contralateral to injury reflecting the unilateral nature of the brain injury (Figure 5). When tasked to traverse an elevated narrow beam wherein the number of affected (right) hindlimb "slips" are recorded, CCI-injured mice demonstrate a clear impairment compared to non-injured controls (Figure 6), although even injured mice were able to reach the beam's end. In both behavioral tests, observed limb functions generally recover by day 7 PI and are nearly indistinguishable from those of control animals by day 14, with an important exception: hindlimb dysfunction in male mice persists throughout the duration of the study (8 weeks PI) and potentially longer.

These behavioral data nicely reflect the localization of the contusion injury on the cortical areas previously determined to provoke forelimb, hindlimb, neck, and jaw movements (193). Specifically, our injury site fully encircles the caudal forelimb area (CFA; centered about 0.25, -1.5 mm Bregma) and the hindlimb area (HA; immediately caudal to the CFA), as well as partially includes the rostral forelimb area (RFA) and the anterior-lateral motor area (ALM) (Figure 3). Studies have demonstrated the differential contribution of these areas to various trained and spontaneous movements (71; 128).

Hira et al. (2015) behaviorally defined and cortically mapped ethologically relevant movements that were also observed within the ART: when bringing the forepaw to the mouth while the mouth simultaneously opened (forepaw-to-mouth movement), or when raising the pronated forepaw followed by moving outward with rhythmic shaking as if rejecting something at the face (termed "defensive-like" movement) (72). These movements were mapped to the ALM and RFA, respectively, and therefore are only partially encompassed within the impacted area. Non-impacted foci of these areas may therefore contribute to the restoration of ART performance at 2 weeks PI. Furthermore, musculature of the jaw and neck may also assist in completion of the ART task and are similarly attributable to areas of the cortex only partially impacted by our CCI site parameters.

DiGiovanna et al. (2016) probed the hindlimb motor cortex across a number of locomotive behavioral paradigms and found that the degree of volitional engagement (i.e., initiation and gait adjustments) correlate with increased cortical activation parameters (34), whereas basic aboveground locomotion has been known to be largely controlled subcortically (183). Given the inherent naivety of encaged laboratory mice to the Beam Walk (BW) test, we suspect cortical contribution of the task to reflect the degree of training achieved. We suspect rapid recovery of performance on the BW test by female mice to reflect mastery of the task prior to injury, whereas the inherent variable performance of male mice may instead reflect imperfect training due to greater mass. Indeed, age-matched male mice are more massive than females during the training period as well as increase body mass more rapidly during the PI recovery period, potentially increasing the demand for cortical facilitation during the BW test to maintain balance.

Going forward, it will be important to characterize the contribution of physiological sex differences like body mass on neurobehavioral paradigms as we perfect preclinical modeling systems.

Our model of tissue-sparing cortical trauma aims to recapitulate sensorimotor and balance impairments in human mild TBI (mTBI). About a third of mTBI patients experience incomplete recoveries, or may report decreased balance confidence despite a clinically-determined complete recovery (44; 120). Current clinical tests to assess motor and cognitive function are not sensitive enough to uncover subtle sensorimotor impairments, especially long-after the initial insult (119). Sergio et al. (2020) argue instead for multi-domain tasks which rely on skilled cognitive-motor integration to reveal impairments often overlooked by single-domain assessments of either motor or cognitive function, potentially owing to faulty communication between brain networks (163).

Rao et al. (2020) used an immersive virtual environment able to capture lower limb motion, accelerations, kinematic, and electromyography features to discern between mTBI and control patients who scored similarly within a battery of standard cognitive and motor tests. They found that perturbations of the treadmill base and/or the visual field held a high degree of discrimination, and that discrimination is improved during dynamic movement (as opposed to standing still) and mismatched perturbations (as opposed to congruent base and visual challenges)(146). This study highlights persistent underlying pathology in mTBI patients who otherwise test normally within clinical settings. Such balance and sensorimotor impairments increase the risk of falls (and therefore risk of additional or repeat TBI) as well as limit activities of daily living, thereby intruding upon quality of life (62; 147). Additionally, accurate assessment of recovery—or lack

thereof—is central to operational decisions regarding return-to-risk status (e.g., return-to-play for athletes or return-to-duty for service members) as well as benefits appropriation for veterans (120; 135; 163). Recovery and adequate assessment of sensorimotor faculties is therefore a top priority in the treatment of neurotrauma and within pre-clinical modeling. Animal models like ours provide a framework which may guide future studies that address sensorimotor pathology in brain injury.

NEUROINFLAMMATORY PATHOLOGIC FEATURES OF OUR MODEL

To determine the effect of our injury model parameters on resident glial cells, we first quantified astrocyte and microglia activation (termed gliosis) using an unbiased stereological counting approach of histologically-stained tissues at 7 days and 8 weeks PI. Our data demonstrate increased astrocyte and microglial numbers compared to naïve animals, as well as a greater proportion of activated microglial cells at 7 days PI (Figure 7a). At 8 weeks PI, increased glial numbers return to levels comparable to sham-injured animals, yet microglial activation bias (percent activated Iba1+ cells) remains relatively high within the injured parenchyma (Figure 7a). These data demonstrate that the cellular activation changes associated with neurotrauma may persist despite returning to normal cell population numbers.

As the resident immune cells of the CNS, astrocytes and microglia can determine the magnitude and duration of neuroinflammation by contributing both pro-inflammatory and anti-inflammatory C/C's as well as neurotrophic or neurotoxic factors. Furthermore, glial cells can act to dampen the extent of injury by creating a physical barrier (astroglial scar) between damaged and penumbral parenchyma as well as by phagocytosis of debris, yet both processes are subject to deleterious maladaptation if left unchecked. The

capability of both astrocytes and microglia to act in benefit or detriment of the injured brain has focused much attention to understanding and manipulating these neural cell populations.

A current challenge of glial biology is the accurate characterization of phenotypic changes associated with reactive gliosis. The classic dichotomy of monocyte polarization applied to microglia (M1/M2) and later astroglia (A1/A2) has been, and continues to be, revised to appreciate the wide spectrum of cellular activity across different brain regions as well as between individual cells of a regional population. Importantly, it has been shown that these cells are able to simultaneously express markers of both phenotypes and are not dedicated to either polar state (131). Our studies used general markers of activated astrocytes or microglia to identify these cell types rather than labels specific to their phenotypic state or function, potentially underappreciating the acute and long-lasting changes to the neuroinflammatory state. The long list of failed attempts to improve TBI outcomes using broad-acting inflammation-targeting agents, as well as astrocyte- or microglia-specific agents, demonstrates the need for a nuanced approach to immunomodulation with respect to dual-acting cellular players. The use of multiple phenotype-specific markers (rather than markers of general reactivity) and functional assessments of glial cell activity following brain injury remains a crucial focus of pre-clinical TBI experimentation.

Soluble Inflammatory Mediators

To better probe the state of neuroinflammation resulting from our model of injury over time, we quantified the amount of various cytokines and chemokines (C/C) within the impacted cortical parenchyma at multiple time-points between 4 hours and 8 weeks

PI. In agreement with other studies using similar injury models and proteomic experimental procedures, our data revealed a clear effect of injury in nine of eighteen C/Cs (Figure 8), yet we also found that some commonly elevated factors were not responsive to the CCI (Figure 9). Specifically, we note evidence of an immediate innate immune response without strong evidence of a robust adaptive or T-cell-mediated response, potentially due to the mild severity of our model compared to more severe open-head percussion models.

For example, T-cell-derived cytokines IFN, IL-2, IL-10, and IL-4 are not elevated above naïve levels at any time-point PI, yet all four factors significantly differ from sham controls at 14 days PI. These data are in contrast to more severe models of percussion or penetrating injury as these cytokines are often measured to respond immediately (4-24 hours) and resolve prior to 2 weeks PI (31; 99; 184; 190). Flow cytometry studies further verify T-cell infiltration early (1-3 days) following moderate or severe contusion injury in mouse models (82; 97). Histological studies on human brain tissue taken during neurosurgery or postmortem following severe TBI corroborate the finding that T-cells appear within lesioned or perilesional tissue no earlier than 4 days post-injury and are regularly detected thereafter (39; 73). These data suggest T-cell activity is expected within the first week following moderate or severe TBI which contrasts the findings from our mild model of injury.

Furthermore, we found the T-cell-attracting chemokine CXCL10 (IP-10) is immediately elevated and continues to rise prior to 2 weeks PI, further suggesting an absent or insufficient T-cell response until that time-point. Taken together, the data suggest T-cell infiltration or activity is limited or delayed—relative to other CCI

models—as a result of the mild injury parameters despite the invasive craniotomy. We therefore hypothesize that the possibly reduced or delayed T-cell response observed within our model may be due to a temporally unique pathophysiological composition of sub-pathologies related to primary versus secondary damage of the cerebral microvasculature (e.g., ischemia, BBB integrity)(155). Of course, we cannot rule out the possibility that our model of injury incites an effective or robust T-cell response between 2 weeks and 8 weeks PI, however additional experiments within this window are needed.

An important challenge to the interpretation of our data revolves around the biological complexity of neuroinflammation subsequent to trauma. Neuroinflammatory cascades are characterized by collinearity and overlap amongst a multitude of soluble inflammatory mediators, many having displayed dual roles in injury and recovery processes. Therefore, univariate statistical approaches of a select few mediators does not assess the interrelationships inherent within inflammatory processes and prevents conclusive inferences on causality when applied to pathophysiological outcomes (194). Studies employing multivariate projection methods such as principal component analysis (PCA) and cluster-based approaches are able to condense variability within multiplex data and thus highlight patterns more accurately reflective of underlying biological processes. For instance, Helmy et al. (2012) was able to discern clusters of TBI patients based on cytokine data reflective of the post-injury temporal phase and tissue collection site (i.e., brain interstitium versus blood)(69). Similarly, Kumar et al. (2016) demonstrated that PCA and cluster-based derivative analysis of C/Cs measured 0-3 days post-injury was able to discern between demographic (age, sex) and clinical variables (CT findings, length of stay in acute care, 6-month disability rating)(98). By condensing

the glut of C/C data generated by biofluid sampling, investigators have been able to further develop models with greater promise of clinical prognostic utility for patients (70; 200).

TARGETING BRAIN INJURY WITH CELL TRANSPLANTATION

As a central tenet of neurotrauma-induced neurodegeneration and potential recovery, neuroinflammation remains a common target in the development of therapeutics to mitigate brain damage and dysfunction. Although initially developed as a strategy to replace lost neurons within the context of focal neurodegeneration, stem cell (SC) or neural stem cell (NSC) engraftment strategies into the injured CNS have been demonstrated to limit pathological processes and accelerate functional recovery(195). These benefits are often attributed to the ability of engrafted cells to secrete a variety of immunomodulatory and neurotrophic factors (15). Indeed, clinical trials of SC-based therapies are currently underway for the treatment of stroke, spinal cord injury, and TBI (219; 228). Preclinical studies, however, have demonstrated extreme heterogeneity in outcomes dependent on: pharmacological parameters, transplant phenotype and composition, and host variables. For example, Péron et al. (2017) demonstrated improvements in graft and host outcomes following a delayed versus immediate transplantation following brain injury (140). Tajiri et al. (2014) demonstrated reduced or no benefit of SC treatment in brain-injured aged animals compared to young adults (188). Together, these studies underscore the necessity of optimizing treatment parameters and methods to provide therapy within the context of the inherent variability of brain injury outcomes.

Our model of cortical contusion neurotrauma—which results in cognate behavioral deficits and robust neuroinflammation yet avoids cortical cavitation—serves here as a model to test and optimize SC-based strategies.

Transplant Phenotype and Composition

Although MSCs have historically been the preferred cellular source of transplant material, advancements in SC biology and technology have also been incorporated into cell-based strategies. Induced pluripotent SC (iPSC) derivation and subsequent differentiation protocols have provided mechanisms for widespread use of totipotent material with virtually limitless phenotypic potential. Our study of post-TBI transplantation employed the use of a human iPSC (hiPSC) line generated for the purpose of a standardized population of cells available to preclinical researchers that was further differentiated toward a stable neural stem cell (NSC) phenotype (43; 222). As a multipotent progenitor, NSCs are capable of self-duplication and differentiation toward neuronal, astroglial, and oligodendroglial fates (222). Preclinical studies have demonstrated benefit to the injured brain by transplanted NSCs and their fated progenies, however, the optimal phenotype and *in vitro* culture conditions of transplanted cells remain to be determined.

Our study employed an established method of *in vitro* culture conditions to derive neuronal- and astroglial-fated cells from human NSCs (hNSCs) for transplantation purposes. These cell populations (NSCs, neuroblasts, and astrocytes) maintained phenotypic markers of identity corroborated through immunohistochemical, transcriptomic, and physiological data (106). Furthermore, all three populations were isogenic, having been derived from a single population of stem cells. Together, these

properties provided an excellent opportunity to determine the phenotypic contribution of *in vitro* cell culture and differentiation conditions on post-TBI transplantation outcomes.

Our study demonstrated that transplanted NSCs and neuron-fated cells (neuroblasts; Nbs) were able to persist within the injured parenchyma up to 8 weeks post-injury and were found to migrate as well as sprout neuritic processes (Figure 14). Additionally, both cell types displayed markers of neuronal fate at later time points (Figure 13). Transplanted astrocytes however were discovered in a smaller proportion of engrafted brains and in minute quantities (Figure 12 and Sup. Figure 2). These data suggest that the neuronal fate is robust, tolerated, and encouraged within the injured parenchyma whereas hiPSC-derived astrocytes are not suitable for engraftment. The disappearance of engrafted astrocytes may be due to intrinsic cell-mediated processes (e.g., apoptosis) or immune-vs-graft actions taken by local or infiltrating immune cells (Figure 15A and Sup. Figure 3) in response to the astrocyte phenotype. We suspect these cells may have assumed a pro-inflammatory phenotype. For example, Liddelow et al. (104) demonstrated *in vitro* polarization of astrocytes toward neurotoxic (A1) or beneficial (A2) states using brain inflammatory signals, providing a potential blueprint for optimizing the astrocyte phenotype for transplantation strategies. Additional studies may elucidate the functional phenotype of hiPSC-astrocytes derived following our *in vitro* culture conditions and whether pre-transplantation conditioning can improve survival and integration within the host brain.

Our transplanted NSCs and Nbs populations persist predominantly clustered around the site of injection but also appear to migrate along white-matter tracts, extend neuritic processes, and maintain expression of immature neural cells (Figures 12-14).

Additionally, transplanted NSCs appear fated to differentiate toward the neuronal lineage, but were not observed to express the astrocyte marker GFAP. However, other studies employing hNSCs of embryonic or induced origin transplanted into the rodent brain have found heterogeneous populations of differentiated cells inclusive of the astroglial fate. Haus et al. (2016) demonstrates *in vivo* expression of neuronal, astroglial, and oligodendroglial markers within engrafted hNSCs and determined the relative proportion of each to depend on the *in vitro* passage number of the transplanted cells (66). *In vivo* persistence and fate of transplanted cells, as well as their subsequent effect on neuropathology, are therefore dependent on numerous microenvironmental cues and cell-intrinsic qualities. Poor retention of implanted hiPSC-derived astrocytes and unobserved differentiation to this fate suggest our injury model and transplantation paradigm provide an inhospitable environment for this cell type. For example, it is possible our *in vitro* astrocyte differentiation protocol induces the expression of more MHC class I antigens than isogenic NSCs or Nbs. Sequencing studies of neural cells pre-transplantation may better identify means to experimentally mitigate host rejection. Alternatively, MHC I proteins may serve as an attractive target of transgenic ablation for improved transplant survival.

Transplant Effects on Neuropathology Following Brain Injury

Brain injury is well known to initiate enhanced neurogenesis and neural progenitor migration which aid in mitigating neural damage (37). Therefore, transplanted exogenous NSC's are thought to supplement endogenous populations in this endeavor post-injury as well as supplant lost neural cells. Within the context of experimental rodent stroke, enhanced neurogenesis and dispersal within the penumbral tissue is well

characterized following ischemia (74). Within experimental brain trauma, however, the activity of either endogenous or transplanted NSCs varies significantly depending on the model of injury used and other host variables including age and sex(23).

NSC transplantation and SC-based strategies are generally beneficial within instances of experimental TBI, SCI, stroke, and non-injury neurodegeneration (14; 181; 219). Although pleiotropic in action, cell-based therapies are thought to benefit the injured brain by acting as generators of neurotrophic and anti-inflammatory products—termed the "bystander" effect, i.e., by mitigating toxic neuroinflammation and promoting restoration of brain homeostatic and restorative processes(15). Systemic transfusion of SCs or SC-derived material (e.g., exosomes or conditioned *in vitro* culture-derived media) ameliorates brain pathology comparable to intra-parenchymal administration, providing further evidence for the action of transplanted cells to serve as paracrine secretory effectors(188; 220). In addition to the brain parenchyma, systemically infused cells and cellular products are capable of directly interacting with peripheral immune tissues to influence humoral immunity and therefore mitigate neuroinflammation.

Notwithstanding the bystander effect, some groups have demonstrated the ability of transplanted cells to functionally integrate within the host tissue. In animal models of discrete nucleus degeneration such as Parkinson's disease, cells engrafted into the lesioned striatum were found to assume the functional role of lost nigrostriatal neurons, thereby facilitating behavioral recovery (180). Within the context of (traumatic) brain injury, widespread cellular loss can be more difficult to target as the diffuse nature of injury may complicate such signals necessary for neuron progenitor integration and circuit formation. Certain populations of neural progenitor cells may be better suited for

this environment. For example, oligodendrocyte progenitor cells (OPCs) transplanted following rodent models of TBI have demonstrated successful parenchymal integration, remyelination, and restoration of functional recovery (221), potentially owing to the natural tendency of oligodendrocyte turnover within the adult uninjured brain. Given the predominance of hiNSCs to mature toward a neuronal fate *in vivo* and the inherent difficulty of neuroblasts to integrate into the adult brain, engraftment strategies employing *in vitro* differentiation protocols prior to transplantation are warranted to optimize engraftment integration to target specific pathophysiological processes or endophenotypes.

Having determined greater engraftment success of isogenic NSCs and neuroblasts over astrocytes following our model of TBI, we employed the adhesive removal test (ART) of sensorimotor integration as well as histologic quantitation of cortical neurons and activated glia to determine the effect of transplantation on functional recovery and neural pathology. Weekly behavioral observations up to 8 weeks PI demonstrated that cell type, host sex, and severity of brain injury interacted to influence the behavioral outcome such that transplantation only affected the performance of animals delivered the sham (craniectomy) injury rather than the cortical contusion (CCI) (Figure 16). Within sham-injured animals, transplantation effects are cell type-specific compared to vehicle injection such that Nb engraftment worsens performance yet NSC engraftment has no significant effect. Furthermore, host sex influences these behavioral effects such that engrafted females display superior performance compared to engrafted male mice in both cell type contexts.

Although the precise mechanisms of engrafted cells to influence behavioral outcome is unclear, we found that the quantity of cortical neurons within the impacted area reflect the cell-type and injury severity interaction. Specifically, Nb transplantation induces neuronal loss compared to vehicle injection or NSC transplantation (Figure 8B), potentially reflective of the mechanisms underlying the corresponding behavioral impairments. Studies have demonstrated that functional impairment following TBI is strongly associated with white-matter impairment(68). It is possible that our engrafted cells—which cluster and migrate along white-matter tracts—impact behavioral metrics by their interaction with axons or white-matter glia. Additional experiments on axonal pathology following transplantation are needed to test this hypothesis.

Previous studies have demonstrated the injurious effect of craniectomy without contusion. Specifically, cranial drilling and disruption of underlying meningeal tissue incites robust neuroinflammation as well as behavioral deficits characteristic of CCI injury (99; 149). The overlap of neuropathology between sham- and CCI-injury within our study provides further evidence that cranial surgery alone models traumatic injury and can be exploited in preclinical studies to provide insight on mechanisms of pathophysiology and therapeutic treatments (149).

Our metrics of glial activation at 8 weeks PI are also influenced by interactions of host sex, injury level, and cell type; however these changes do not reflect the behavioral output. For example, transplantation of either cell type reduced astroglial activation ($GFAP^+$ cell number) in sham-injured male mice but not CCI-injured male mice or sham-injured female mice (Figure 18). Additionally, engraftment had no effect on cortical microglia ($Iba1^+$) cell number, yet robustly enhanced microglial activation in male mice

regardless of transplant cell type (Figure 19). These data extend the acknowledgement that simple markers of glial activation cannot adequately assess the neuroinflammatory state related to neuropathology and that functional cellular metrics of the microenvironment instead are necessary to uncover the pathophysiological basis of dysfunction following brain injury and therapeutic treatments. Transcriptional quantitation, especially cell-specific methods, may serve to better assess the functional state of glia within the engrafted brain.

Furthermore, our study demonstrates the effects of NSC-derived cell transplantation on neuropathology and sensorimotor function following TBI to be strongly influenced by host sex. By incorporating sex as a biological variable, our data suggests differential interactions of host sex on the therapeutic efficacy of iPSC-derived neural cell transplantation on outcomes following brain injury. As an increasingly promising strategy for brain repair, cell-based therapies must contend with the defining role of sex in neurological pathology.

SEX DIFFERENCES WITHIN BRAIN INJURY

Within both studies elaborated above, we determined biological sex to be an important influencing variable for behavioral and inflammatory outcomes following our paradigm of brain injury, especially within the context of cell-based therapy. Sex differences in human and experimental brain injury are poorly understood and remain controversial, yet there is growing interest and recognition of sex as a biological variable across basic, preclinical, and translational research domains(9), especially within the neurosciences(113; 216) and with respect to brain injury(117; 151).

Within human TBI, gender and sociocultural factors (e.g., vulnerabilities, attitudes, expectations) present additional covariables that complicate investigations into the epidemiology and pathophysiology of sex-based differences on outcome (55; 127). Meta analyses and reviews have additionally shown that injury severity, patient sample size, and measured outcomes (i.e., quality of life, cognition, psychiatric, neurologic, survival) differentially interact to delineate the presence, magnitude, and direction of sex-based differences within TBI patients (60). Animal studies similarly present wide variability in regard to sex differences(151). However, there exist an overarching trend in both human and animal studies wherein sex and TBI severity interact such that women or female animals fare better than their matched counterparts and this effect is greater with increased injury severity (60). As sex is differentiated at the chromosomal level to influence systems-level physiology, identifying the root causes of sex-based differences on outcomes remains a complex yet important area of TBI research.

Sex Differences in Behavioral Outcomes

An important consideration in the interpretation of sex-based differences relies on the outcome metric and appropriate matching between subjects (e.g., age- versus weight-matched animals). Our studies employed the adhesive removal test (ART) of sensorimotor function to circumvent sexual dimorphism in age-matched mice, namely greater mass and size of male mice. Completion of the ART is weight-independent and relies on the intrinsic grooming behavior of rodents rather than learned or conditioned skills (158). We further adapted our testing protocol to observe mice within a clear Plexiglas cylinder rather than their home cage as to minimize extraneous cues. Baseline testing revealed no differences in ART performance within any study cohort between

male and female mice (Figure 20a). Interestingly, however, robust sex differences are uncovered following our paradigm of post-injury transplantation but not following CCI alone (Figure 20). We further observed this effect within control groups delivered either a craniectomy and/or the vehicle injection. These data strongly suggest that injury severity and model characteristics are able to precipitate sex differences in behavioral outcome.

A few key features of our transplant paradigm may foster the expression of sex differences. Firstly, transplantation involves a secondary surgical event at day 1 post-injury. The pulled glass borosilicate pipette-tip used for transplant delivery produces a penetrating injury to the brain synergistic to and more severe than the CCI or craniectomy injury alone. Mounting evidence has demonstrated the injured brain is particularly vulnerable to secondary trauma due to initiated neural-immune interactions (75). Furthermore, the direct shearing of neural and vascular parenchyma likely heightened infiltration of peripheral immune cells and systemic constituents. The increased injury severity and therefore enhanced inflammatory potential of the intraparenchymal injection are potential drivers for the demonstrated sex differences in behavioral outcome given the wealth of data on sex differences in neuroinflammatory processes (discussed below).

Additionally, animals within the transplantation paradigm cohorts were subjected to a second, prolonged exposure to isoflurane anesthesia at 1 day PI as well as daily subcutaneous administration of the immunosuppressant Cyclosporin A (CsA). Post-TBI treatment with isoflurane or other anesthetics are known to improve neurological outcomes in rodents (8), although our data does not corroborate this effect (Supplemental Figure 1). The choice of intraoperative anesthesia delivered during TBI has been found to interact with sex such that isoflurane produced sex differences in mortality and cognitive

outcomes in favor of female rats, but the inhalation anesthetic halothane did not (137). Additionally, isoflurane-treated females outperformed halothane-treated females in recovery of spontaneous exploratory behavior post-injury. Lastly, pre-conditioning animals with isoflurane prior to brain injury provided neuroprotection to young-adult and middle-aged male mice yet exacerbated ischemic injury in young females only (91). These data suggest isoflurane acts upon sexual dimorphic processes that influence damage and recovery following brain injury.

CsA has been investigated as a neuroprotectant following neurotrauma with mixed results (36). Although long-used clinically as an immunosuppressant, CsA also acts to stabilize the mitochondrion during cellular stress thereby halting apoptotic processes and release of injurious free-radicals (179). Sexual dimorphism in mitochondrial function as well as its role in the generation of sex steroid hormones is currently hypothesized as an underlying cellular mechanism of sex differences following brain injury (60). Further pharmacologic manipulation by CsA post-injury may therefore exacerbate mitochondria-related sex differences effecting cell survival and function. Additionally, as a potent immunosuppressant, CsA broadly attenuates systemic adaptive immunity potentially driving sex differences in neuroinflammation and therefore TBI outcomes, namely the superior performance observed within the ART.

Our study also employed the Beam Walk (BW) task as a measure of sensorimotor impairment. Unlike the ART, the BW task is directly influenced by the weight and size of the animal and therefore cannot circumvent the inherent sexual dimorphism in age-matched mice. Indeed, pre-injury baseline observations highlight more hindlimb slips (or "foot faults") in males than females (Figure 6). Albeit not directly comparable between

sexes, it is worth noting that hindlimb slips of CCI-injured male mice never return to pre-injury performance and that sham-injured (anesthesia + scalp incision only) male mice exhibit wide variability throughout the duration of the study. This pattern of performance is in stark contrast to the rapid recovery and mastery of the task by female mice. Although we suspect the inherent variability of male mice may be due to imperfect training pre-injury, studies employing weight-matched mice of varying mass are necessary to better elucidate the specific interactions between weight and sex on the BW test and whether neuromotor strategies of ambulation are inherently sexually dimorphic. These data stress the importance of appropriate functional outcome metrics and matched subjects in the interpretation of sex differences in animal studies, as well as the potential shortcoming of studies employing only one sex.

The behavioral outcomes employed here therefore seem to demonstrate two non-mutually exclusive categories of sex differences(118): the BW test indicates sexual dimorphism (evidenced by significantly different pre-injury performance) and the ART reflects sexual divergence in which the expression of sex differences precipitates following some challenge (i.e., brain injury and cell transplant paradigm), suggestive of sexually dimorphic underlying mechanisms that normally converge to the same outcomes in healthy conditions.

Uncovering the pathophysiological processes between inherent sexual dimorphisms and the expression of brain injury outcomes is therefore necessary for preclinical and translational researchers to adequately address treatment of TBI.

Sex Differences in Neuroinflammation

As immunity and neuroinflammation have been centrally indicated in TBI outcomes, sex differences in peripheral and neural immunity are a natural target in identifying the pathological basis of neurological damage and recovery following brain trauma. Sex differences in immunity and subsequent expression of auto-immune disorders, response to infection, and development of non-reproductive cancers are well established in human and animal models alike (93).

Using advanced flow-cytometry techniques, Doran et al. (2019) demonstrated sex differences in baseline microglial function such that female microglia had decreased phagocytic activity and reactive oxygen species (ROS) levels, yet greater levels of pro-inflammatory cytokines TNFα and IL-1β (38). This study uncovered greater numbers of infiltrating myeloid cells (neutrophils and monocytes) in moderate-severe injured male brains than females' at 1 day PI, followed by increased numbers of microglia at 3 days and 7 days PI. Using histological methods, Villapol et al. (2017) similarly demonstrated greater gliosis and microglial/macrophage-driven inflammation in male brains acutely following TBI (201). These studies indicate the neuroinflammatory response to brain trauma is directed by sex-based differences in peripheral and local (brain) innate immunity.

We measured astrocyte and microglia activation within the impacted cortex using stereological counting of immunohistochemically-stained sections. Using morphology to indicate microglial activation, our data suggest naive male mice possess a smaller proportion of activated microglia than female mice (Figure 7a). Following our model of CCI injury, we measured no sex difference in cell number or activation bias at 7 days or 8

weeks, reflecting convergence of microglial-regulating processes at these times. Interestingly, we found that transplantation of NSCs but not Nbs lead to a significantly greater proportion of activated microglia in male but not female mice as far as 8 weeks PI, regardless of injury status (Figure 19b). The observed patterns of sex differences in gliosis do not correlate or match our measures of behavioral output. Taken together, our data support the hypothesis that biologic sex mediates cell-intrinsic differences of which expression further depends on injury and intervention paradigm.

To further characterize potential sex differences in neuroinflammation following our model of CCI, we quantified protein levels of cytokines and chemokines (C/C) that have been determined to significantly affect neuropathology, hold clinical relevance, or for which sex differences have been previously observed. Given the wide spectrum of TBI models, host variables, and expression quantitation methods, studies have yet to identify sex differences in immunoproteins independent of experimental characteristics (178). We employed multiplexed high-precision immunoassays to simultaneously measure cortical homogenate samples collected using a randomized block complete factorial study design to address technical and nuisance variable biases. Furthermore, we sampled the injured brain at numerous time-points within the acute period PI to detect early differences in signals which may converge later. Only one of 18 measured C/Cs indicated a sex difference between male and female levels: IL-5 (Figure 8). Interestingly, IL-5 has not previously been identified to hold any sex-based relevance to experimental or clinical brain injury, although studies designed for such comparison are rare (178). Furthermore, only scant evidence suggests a significant role of IL-5 in brain trauma (31; 174). Animal studies employing monoclonal antibodies against IL-5 represent an

attractive experimental paradigm to better interrogate the role of this cytokine in trauma-induced brain injury.

In contrast to elegant studies that have clearly demonstrated sex differences in neuroinflammation following TBI, our study failed to corroborate robust sexual dimorphism within the sampled inflammatory milieu. The majority of preclinical TBI studies, however, result in gross tissue pathology more severe than our model produces (60). The relatively mild nature of our injury pathology may avoid sub-pathologies or endophenotypes which precipitate sex differences in C/C protein levels. Additional variations of model features may serve as under-recognized drivers of sex differences. For example, the length of time under anesthesia during experimental brain injury influences sex differences, varies independently of injury severity, and is rarely reported.

Preclinical studies that have identified sex differences in C/C expression have relied on *in-situ* or intracellular mRNA quantitation (38; 201). The opportunity of intracellular regulatory processes to act upon translation or protein manufacture and secretion, however, may normalize differences in transcription—especially temporal differences. Processes which constrain underlying sex differences can therefore result in sexual convergence even at the protein level (118).

Lastly, inclusion of sex as a biological variable is often considered in *post-hoc* inference rather than *a priori*, thereby limiting the power of inferential capability (125). As sex is rarely considered a primary variable of interest, experimental design and statistical analysis is often not powered for direct comparisons between male- and female-derived metrics, nor are sex-based biases or interactions considered. For example, Spani et al. (2018) identified direct sex differences in C/C protein levels measured over

the span of numerous single-sex experimental paradigms (178). Studies which do simultaneously test both male and female animals rarely if ever report efforts to minimize interactions despite well-known activational effects of sex-specific odor cues (e.g., urine, pheromones). Our study is unique in its design to include sex as an independent variable within a complete factorial design to measure C/C protein levels with care to avoid inter-sex interactions.

CONCLUSION

We have characterized a mouse model of controlled cortical impact (CCI) contusion TBI which incites robust neuroinflammation and cognate behavioral deficits. Although widely used in favor of fine control over biomechanical parameters, the CCI model of brain injury has often been employed to drive severe damage to the brain and loss of cortical structure. By applying a shallow depth of percussion and low-speed impact, our model avoids gross tissue loss and permits investigation into the cellular and molecular pathophysiology of the contused cortex.

Focal contusion trauma to the forebrain left of Bregma disrupts function of the primary motor and somatosensory cortices. The caudal forelimb area (CFA), rostral forelimb area (RFA), hindlimb area (HA), and anterior-lateral motor area (ALM) have been shown to control discrete and rhythmic ethologically relevant movements involving the forelimb, the jaw, the head & neck, and the hindlimb such as forepaw-to-mouth movements, defensive-like movements, and gait-adjusted ambulation. We show that our model of brain injury produces deficits in performance of sensorimotor integration tasks inclusive of these movements and cognate to the impacted cortical area.

We further used immunohistochemical and immunosorbent assays to demonstrate robust innate neuroinflammation within the impacted cortical area. Astrocyte and microglia cell numbers are acutely elevated post-injury (PI) yet are comparable with sham-injury levels by 8 weeks PI. In contrast, microglial morphologic activation remains elevated at this chronic time-point. High-sensitivity multiplex immunoassays of cytokines and chemokines (C/C) reveal the extent of neuroinflammation is limited to innate rather than adaptive immune processes; only nine of eighteen measured C/Cs demonstrate an effect of injury. Sampling at multiple time-points within the acute phase PI further reveals immediate increases in C/C levels, and graded resolution of activity over time such that three C/Cs return to control levels by 7 days PI, two by 14 days PI, and the remaining four by 8 weeks PI.

We used our model of mild TBI pathology and cognate behavioral deficits to test neural stem cell (NSC)-based transplantation paradigms derived from human induced pluripotent stem cells (hiPSCs) as a strategy for neurorestorative therapy. We demonstrate survival, adaptation, and integration of transplanted isogenic NSCs and neuronal-fated neuroblasts (Nbs), but not astrocytes. We further demonstrate that the effects of hiPSC-derived neural cells on gliosis and sensorimotor recovery depend on the interaction of injury severity, cell phenotype, and host sex. Engrafted Nbs hinder behavioral recovery whereas NSCs non-significantly benefit performance. Importantly, host sex interacts with these effects of transplantation such that female mice exhibit superior recovery compared to their male counterparts regardless of transplant cell phenotype. Transplantation also impacts glial histologic outcomes dependent on injury

severity, cell phenotype, and host sex, yet these data generally do not correlate or reflect the effects on behavioral recovery.

Importantly, we have demonstrated the significant interaction of sex as a biologic variable with model injury paradigm. We note that our paradigm of brain injury followed by neural cell transplantation precipitates robust sex differences in corroboration with established findings, yet our model of CCI injury alone fails to recapitulate these data. We discuss experimental features which may underlie this distinction in light of established sex differences in immunity.

Taken together, this work serves to address: (1) the call to represent diverse and heterogeneous mechanisms and outcomes in TBI by using reproducible small animal models, (2) the need to systematically optimize stem cell (SC)-based strategies for neuro-restorative therapy following brain injury, and (3) the urgent requirement to adequately address sex as an independent biologic variable in preclinical neuroscience. Neurotrauma, brain injury, and neurodegeneration remain significant sources of death and disability globally. Regenerative brain medicine is the key to alleviate these devastations.

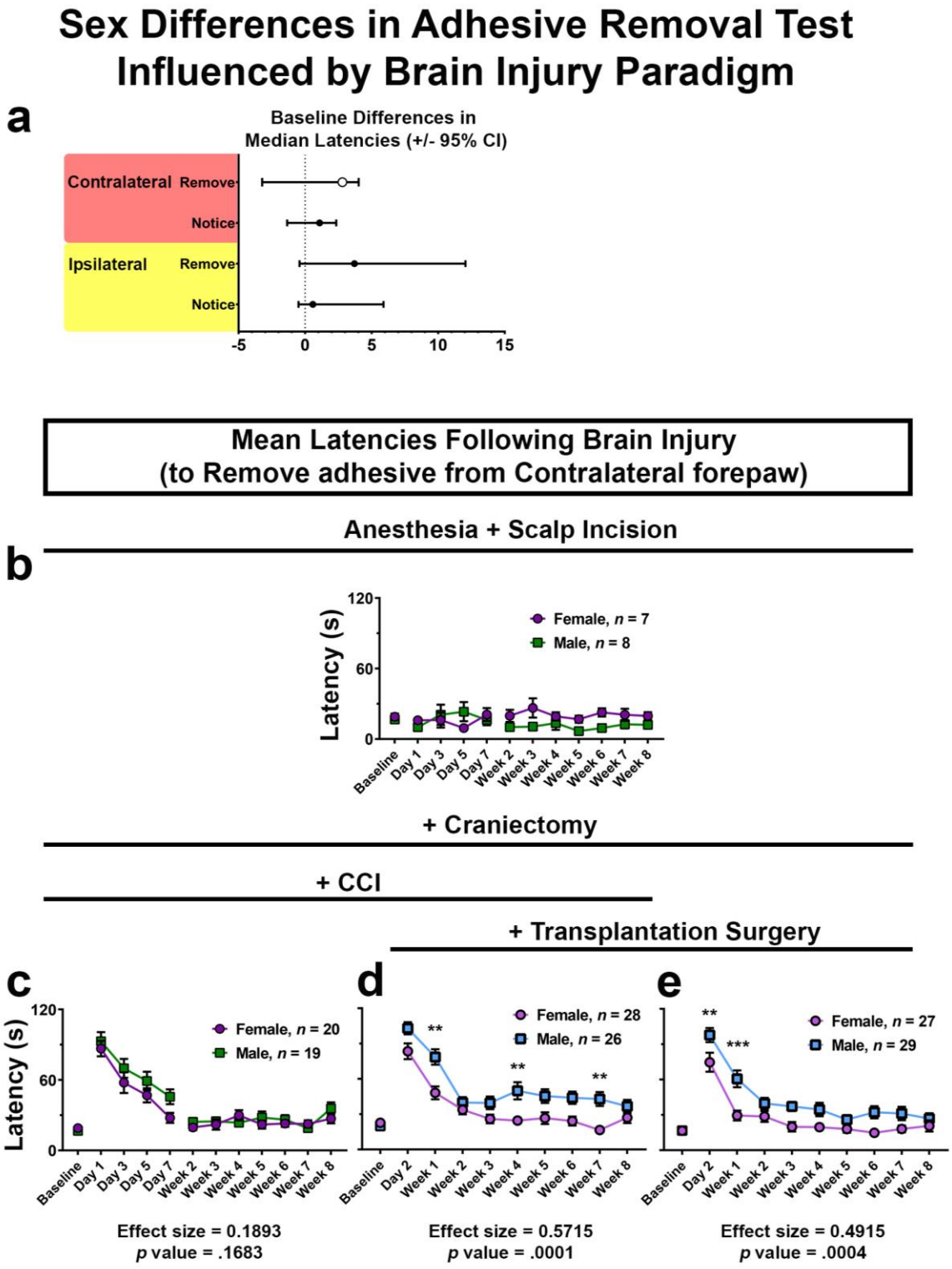

Figure 20. Sex differences in adhesive removal test (ART) performance is influenced by brain injury model and experimental paradigm. **(a)** Baseline differences in median latency to remove or notice the nuisance adhesive attached to the forepaw ipsi- or contra-lateral to the side of injury between male and female mice. **(b-e)** Sex-based comparisons

of the mean latency to remove the adhesive from the affected forepaw. Mice were subject to **(b)** no brain injury, **(c)** CCI injury only, **(d)** CCI injury followed by intraparenchymal transplantation surgery, and **(e)** craniectomy followed by transplantation surgery without CCI. See Chapters 2 and 3 for experimental details for graphs **b** & **c** and **d** & **e**, respectively. Data analyzed using 2-way ANOVA with repeated measures excluding baseline values; Effect size and *p*-values reflect the effect of sex. **(b)** Significant sex X time interaction effect: $F(10, 130) = 1.949$, $p = 0.0442$. **(c)** Effect of sex: $F(1, 37) = 1.975$; **(d)** Effect of sex: $F(1, 52) = 16.85$; **(e)** Effect of sex: $F(1, 54) = 14.35$. Multiple comparisons corrected with Sidak's method. ***$p < 0.001$, **$p < 0.01$.

REFERENCES

1. Acharya MM, Martirosian V, Christie LA, Riparip L, Strnadel J, et al. 2015. Defining the optimal window for cranial transplantation of human induced pluripotent stem cell-derived cells to ameliorate radiation-induced cognitive impairment. *Stem cells translational medicine* 4:74-83
2. Aertker BM, Bedi S, Cox CS, Jr. 2016. Strategies for CNS repair following TBI. *Exp Neurol* 275 Pt 3:411-26
3. Alam A, Thelin EP, Tajsic T, Khan DZ, Khellaf A, et al. 2020. Cellular infiltration in traumatic brain injury. *J Neuroinflammation* 17:328
4. All AH, Gharibani P, Gupta S, Bazley FA, Pashai N, et al. 2015. Early intervention for spinal cord injury with human induced pluripotent stem cells oligodendrocyte progenitors. *PLoS One* 10:e0116933
5. Anderson AJ, Haus DL, Hooshmand MJ, Perez H, Sontag CJ, Cummings BJ. 2011. Achieving stable human stem cell engraftment and survival in the CNS: is the future of regenerative medicine immunodeficient? *Regen Med* 6:367-406
6. Anderson MA, Burda JE, Ren Y, Ao Y, O'Shea TM, et al. 2016. Astrocyte scar formation aids central nervous system axon regeneration. *Nature* 532:195-200
7. Arbour C, Bouferguene Y, Beauregard R, Lavigne G, Herrero Babiloni A. 2020. Update on the prevalence of persistent post-traumatic headache in adult civilian traumatic brain injury: protocol for a systematic review and meta-analysis. *BMJ Open* 10:e032706
8. Archer DP, McCann SK, Walker AM, Premji ZA, Rogan KJ, et al. 2018. Neuroprotection by anaesthetics in rodent models of traumatic brain injury: a systematic review and network meta-analysis. *Br J Anaesth* 121:1272-81
9. Arnegard ME, Whitten LA, Hunter C, Clayton JA. 2020. Sex as a Biological Variable: A 5-Year Progress Report and Call to Action. *J Womens Health (Larchmt)* 29:858-64
10. Ballout N, Rochelle T, Brot S, Bonnet ML, Francheteau M, et al. 2019. Characterization of Inflammation in Delayed Cortical Transplantation. *Front Mol Neurosci* 12:160
11. Batsaikhan B, Wang JY, Scerba MT, Tweedie D, Greig NH, et al. 2019. Post-Injury Neuroprotective Effects of the Thalidomide Analog 3,6'-Dithiothalidomide on Traumatic Brain Injury. *Int J Mol Sci* 20
12. Bazarian JJ, Blyth B, Mookerjee S, He H, McDermott MP. 2010. Sex differences in outcome after mild traumatic brain injury. *J Neurotrauma* 27:527-39
13. Bergold PJ. 2016. Treatment of traumatic brain injury with anti-inflammatory drugs. *Exp Neurol* 275 Pt 3:367-80
14. Boese AC, Le QE, Pham D, Hamblin MH, Lee JP. 2018. Neural stem cell therapy for subacute and chronic ischemic stroke. *Stem cell research & therapy* 9:154
15. Bonsack B, Heyck M, Kingsbury C, Cozene B, Sadanandan N, et al. 2020. Fast-tracking regenerative medicine for traumatic brain injury. *Neural Regen Res* 15:1179-90
16. Bouet V, Boulouard M, Toutain J, Divoux D, Bernaudin M, et al. 2009. The adhesive removal test: a sensitive method to assess sensorimotor deficits in mice. *Nat Protoc* 4:1560-4
17. Bramble MS, Vashist N, Vilain E. 2019. Sex steroid hormone modulation of neural stem cells: a critical review. *Biol Sex Differ* 10:28
18. Burda JE, Bernstein AM, Sofroniew MV. 2016. Astrocyte roles in traumatic brain injury. *Exp Neurol* 275 Pt 3:305-15

19. Bye N, Habgood MD, Callaway JK, Malakooti N, Potter A, et al. 2007. Transient neuroprotection by minocycline following traumatic brain injury is associated with attenuated microglial activation but no changes in cell apoptosis or neutrophil infiltration. *Exp Neurol* 204:220-33
20. Caplan HW, Cox CS, Bedi SS. 2017. Do microglia play a role in sex differences in TBI? *J Neurosci Res* 95:509-17
21. Carney N, Totten AM, O'Reilly C, Ullman JS, Hawryluk GW, et al. 2017. Guidelines for the Management of Severe Traumatic Brain Injury, Fourth Edition. *Neurosurgery* 80:6-15
22. Centers for Disease Control and Prevention. 2015. *Report to Congress on Traumatic Brain Injury in the United States: Epidemiology and Rehabilitation*.National Center for Injury Prevention and Control; Division of Unintentional Injury Prevention. Atlanta, GA.
23. Chang EH, Adorjan I, Mundim MV, Sun B, Dizon ML, Szele FG. 2016. Traumatic Brain Injury Activation of the Adult Subventricular Zone Neurogenic Niche. *Front Neurosci* 10:332
24. Chiaretti A, Genovese O, Aloe L, Antonelli A, Piastra M, et al. 2005. Interleukin 1beta and interleukin 6 relationship with paediatric head trauma severity and outcome. *Childs Nerv Syst* 21:185-93; discussion 94
25. Clausen F, Hanell A, Israelsson C, Hedin J, Ebendal T, et al. 2011. Neutralization of interleukin-1beta reduces cerebral edema and tissue loss and improves late cognitive outcome following traumatic brain injury in mice. *Eur J Neurosci* 34:110-23
26. Cole JT, Yarnell A, Kean WS, Gold E, Lewis B, et al. 2011. Craniotomy: true sham for traumatic brain injury, or a sham of a sham? *J Neurotrauma* 28:359-69
27. Coronado VG, McGuire LC, Sarmiento K, Bell J, Lionbarger MR, et al. 2012. Trends in Traumatic Brain Injury in the U.S. and the public health response: 1995-2009. *J Safety Res* 43:299-307
28. Corso P, Finkelstein E, Miller T, Fiebelkorn I, Zaloshnja E. 2006. Incidence and lifetime costs of injuries in the United States. *Inj Prev* 12:212-8
29. Cunningham TL, Cartagena CM, Lu XC, Konopko M, Dave JR, et al. 2014. Correlations between blood-brain barrier disruption and neuroinflammation in an experimental model of penetrating ballistic-like brain injury. *J Neurotrauma* 31:505-14
30. Daglas M, Draxler DF, Ho H, McCutcheon F, Galle A, et al. 2019. Activated CD8(+) T Cells Cause Long-Term Neurological Impairment after Traumatic Brain Injury in Mice. *Cell Rep* 29:1178-91 e6
31. Dalgard CL, Cole JT, Kean WS, Lucky JJ, Sukumar G, et al. 2012. The cytokine temporal profile in rat cortex after controlled cortical impact. *Front Mol Neurosci* 5:6
32. Dewan MC, Rattani A, Gupta S, Baticulon RE, Hung YC, et al. 2018. Estimating the global incidence of traumatic brain injury. *J Neurosurg*:1-18
33. Diaz-Arrastia R, Kochanek PM, Bergold P, Kenney K, Marx CE, et al. 2014. Pharmacotherapy of traumatic brain injury: state of the science and the road forward: report of the Department of Defense Neurotrauma Pharmacology Workgroup. *J Neurotrauma* 31:135-58
34. DiGiovanna J, Dominici N, Friedli L, Rigosa J, Duis S, et al. 2016. Engagement of the Rat Hindlimb Motor Cortex across Natural Locomotor Behaviors. *J Neurosci* 36:10440-55
35. Dinarello CA. 2018. Overview of the IL-1 family in innate inflammation and acquired immunity. *Immunol Rev* 281:8-27
36. Dixon CE, Bramlett HM, Dietrich WD, Shear DA, Yan HQ, et al. 2016. Cyclosporine Treatment in Traumatic Brain Injury: Operation Brain Trauma Therapy. *J Neurotrauma* 33:553-66

37. Dixon KJ, Theus MH, Nelersa CM, Mier J, Travieso LG, et al. 2015. Endogenous neural stem/progenitor cells stabilize the cortical microenvironment after traumatic brain injury. *J Neurotrauma* 32:753-64
38. Doran SJ, Ritzel RM, Glaser EP, Henry RJ, Faden AI, Loane DJ. 2019. Sex Differences in Acute Neuroinflammation after Experimental Traumatic Brain Injury Are Mediated by Infiltrating Myeloid Cells. *J Neurotrauma* 36:1040-53
39. Dressler J, Hanisch U, Kuhlisch E, Geiger KD. 2007. Neuronal and glial apoptosis in human traumatic brain injury. *Int J Legal Med* 121:365-75
40. Duffy SS, Keating BA, Perera CJ, Moalem-Taylor G. 2018. The role of regulatory T cells in nervous system pathologies. *J Neurosci Res* 96:951-68
41. Dunnett SB, Bjorklund A. 2017. Mechanisms and use of neural transplants for brain repair. *Prog Brain Res* 230:1-51
42. Edwards P, Arango M, Balica L, Cottingham R, El-Sayed H, et al. 2005. Final results of MRC CRASH, a randomised placebo-controlled trial of intravenous corticosteroid in adults with head injury-outcomes at 6 months. *Lancet* 365:1957-9
43. Efthymiou A, Shaltouki A, Steiner JP, Jha B, Heman-Ackah SM, et al. 2014. Functional screening assays with neurons generated from pluripotent stem cell-derived neural stem cells. *J Biomol Screen* 19:32-43
44. Eman Abdulle A, van der Naalt J. 2020. The role of mood, post-traumatic stress, post-concussive symptoms and coping on outcome after MTBI in elderly patients. *Int Rev Psychiatry* 32:3-11
45. Faul M, Coronado V. 2015. Epidemiology of traumatic brain injury. *Handb Clin Neurol* 127:3-13
46. Feigin VL, Theadom A, Barker-Collo S, Starkey NJ, McPherson K, et al. 2013. Incidence of traumatic brain injury in New Zealand: a population-based study. *Lancet Neurol* 12:53-64
47. Fox GB, Fan L, Levasseur RA, Faden AI. 1998. Sustained sensory/motor and cognitive deficits with neuronal apoptosis following controlled cortical impact brain injury in the mouse. *J Neurotrauma* 15:599-614
48. Frattalone AR, Ling GS. 2013. Moderate and severe traumatic brain injury: pathophysiology and management. *Neurosurg Clin N Am* 24:309-19
49. Frugier T, Morganti-Kossmann MC, O'Reilly D, McLean CA. 2010. In situ detection of inflammatory mediators in post mortem human brain tissue after traumatic injury. *J Neurotrauma* 27:497-507
50. Furmanski O, Nieves MD, Doughty ML. 2019. Controlled Cortical Impact Model of Mouse Brain Injury with Therapeutic Transplantation of Human Induced Pluripotent Stem Cell-Derived Neural Cells. *J Vis Exp*
51. Gadani SP, Cronk JC, Norris GT, Kipnis J. 2012. IL-4 in the brain: a cytokine to remember. *J Immunol* 189:4213-9
52. Gan ZS, Stein SC, Swanson R, Guan S, Garcia L, et al. 2019. Blood Biomarkers for Traumatic Brain Injury: A Quantitative Assessment of Diagnostic and Prognostic Accuracy. *Front Neurol* 10:446
53. Gao J, Prough DS, McAdoo DJ, Grady JJ, Parsley MO, et al. 2006. Transplantation of primed human fetal neural stem cells improves cognitive function in rats after traumatic brain injury. *Exp Neurol* 201:281-92
54. Gennai S, Monsel A, Hao Q, Liu J, Gudapati V, et al. 2015. Cell-based therapy for traumatic brain injury. *Br J Anaesth* 115:203-12

55. Giordano KR, Rojas-Valencia LM, Bhargava V, Lifshitz J. 2020. Beyond Binary: Influence of Sex and Gender on Outcome after Traumatic Brain Injury. *J Neurotrauma* 37:2454-9
56. Goldstein EZ, Church JS, Hesp ZC, Popovich PG, McTigue DM. 2016. A silver lining of neuroinflammation: Beneficial effects on myelination. *Exp Neurol* 283:550-9
57. Gorris R, Fischer J, Erwes KL, Kesavan J, Peterson DA, et al. 2015. Pluripotent stem cell-derived radial glia-like cells as stable intermediate for efficient generation of human oligodendrocytes. *Glia* 63:2152-67
58. Grabert K, Michoel T, Karavolos MH, Clohisey S, Baillie JK, et al. 2016. Microglial brain region-dependent diversity and selective regional sensitivities to aging. *Nat Neurosci* 19:504-16
59. Graham JE, Radice-Neumann DM, Reistetter TA, Hammond FM, Dijkers M, Granger CV. 2010. Influence of sex and age on inpatient rehabilitation outcomes among older adults with traumatic brain injury. *Arch Phys Med Rehabil* 91:43-50
60. Gupte R, Brooks W, Vukas R, Pierce J, Harris J. 2019. Sex Differences in Traumatic Brain Injury: What We Know and What We Should Know. *J Neurotrauma* 36:3063-91
61. Haarmann A, Schuhmann MK, Silwedel C, Monoranu CM, Stoll G, Buttmann M. 2019. Human Brain Endothelial CXCR2 is Inflammation-Inducible and Mediates CXCL5- and CXCL8-Triggered Paraendothelial Barrier Breakdown. *Int J Mol Sci* 20
62. Hammond FM, Perkins SM, Corrigan JD, Nakase-Richardson R, Brown AW, et al. 2021. Functional Change from Five to Fifteen Years after Traumatic Brain Injury. *J Neurotrauma* 38:858-69
63. Hammond TR, Dufort C, Dissing-Olesen L, Giera S, Young A, et al. 2019. Single-Cell RNA Sequencing of Microglia throughout the Mouse Lifespan and in the Injured Brain Reveals Complex Cell-State Changes. *Immunity* 50:253-71 e6
64. Hara M, Kobayakawa K, Ohkawa Y, Kumamaru H, Yokota K, et al. 2017. Interaction of reactive astrocytes with type I collagen induces astrocytic scar formation through the integrin-N-cadherin pathway after spinal cord injury. *Nat Med* 23:818-28
65. Hargus G, Cooper O, Deleidi M, Levy A, Lee K, et al. 2010. Differentiated Parkinson patient-derived induced pluripotent stem cells grow in the adult rodent brain and reduce motor asymmetry in Parkinsonian rats. *Proceedings of the National Academy of Sciences of the United States of America* 107:15921-6
66. Haus DL, Lopez-Velazquez L, Gold EM, Cunningham KM, Perez H, et al. 2016. Transplantation of human neural stem cells restores cognition in an immunodeficient rodent model of traumatic brain injury. *Exp Neurol* 281:1-16
67. Hayakata T, Shiozaki T, Tasaki O, Ikegawa H, Inoue Y, et al. 2004. Changes in CSF S100B and cytokine concentrations in early-phase severe traumatic brain injury. *Shock* 22:102-7
68. Hayes JP, Bigler ED, Verfaellie M. 2016. Traumatic Brain Injury as a Disorder of Brain Connectivity. *J Int Neuropsychol Soc* 22:120-37
69. Helmy A, Antoniades CA, Guilfoyle MR, Carpenter KL, Hutchinson PJ. 2012. Principal component analysis of the cytokine and chemokine response to human traumatic brain injury. *PLoS One* 7:e39677
70. Hinson HE, Li P, Myers L, Agarwal C, Pollock J, McWeeney S. 2021. Incorporating Immunoproteins in the Development of Classification Models of Progression of Intracranial Hemorrhage After Traumatic Brain Injury. *J Head Trauma Rehabil*
71. Hira R, Ohkubo F, Tanaka YR, Masamizu Y, Augustine GJ, et al. 2013. In vivo optogenetic tracing of functional corticocortical connections between motor forelimb areas. *Front Neural Circuits* 7:55

72. Hira R, Terada S, Kondo M, Matsuzaki M. 2015. Distinct Functional Modules for Discrete and Rhythmic Forelimb Movements in the Mouse Motor Cortex. *J Neurosci* 35:13311-22
73. Holmin S, Soderlund J, Biberfeld P, Mathiesen T. 1998. Intracerebral inflammation after human brain contusion. *Neurosurgery* 42:291-8; discussion 8-9
74. Huang L, Zhang L. 2019. Neural stem cell therapies and hypoxic-ischemic brain injury. *Prog Neurobiol* 173:1-17
75. Hunter LE, Branch CA, Lipton ML. 2019. The neurobiological effects of repetitive head impacts in collision sports. *Neurobiology of disease* 123:122-6
76. Iljazi A, Ashina H, Al-Khazali HM, Lipton RB, Ashina M, et al. 2020. Post-Traumatic Stress Disorder After Traumatic Brain Injury-A Systematic Review and Meta-Analysis. *Neurol Sci*
77. Israelsson C, Kylberg A, Bengtsson H, Hillered L, Ebendal T. 2014. Interacting chemokine signals regulate dendritic cells in acute brain injury. *PLoS One* 9:e104754
78. Iverson GL, Gardner AJ, Terry DP, Ponsford JL, Sills AK, et al. 2017. Predictors of clinical recovery from concussion: a systematic review. *Br J Sports Med* 51:941-8
79. Jaffer H, Adjei IM, Labhasetwar V. 2013. Optical imaging to map blood-brain barrier leakage. *Sci Rep* 3:3117
80. Jahn-Eimermacher A, Lasarzik I, Raber J. 2011. Statistical analysis of latency outcomes in behavioral experiments. *Behav Brain Res* 221:271-5
81. Jassam YN, Izzy S, Whalen M, McGavern DB, El Khoury J. 2017. Neuroimmunology of Traumatic Brain Injury: Time for a Paradigm Shift. *Neuron* 95:1246-65
82. Jin X, Ishii H, Bai Z, Itokazu T, Yamashita T. 2012. Temporal changes in cell marker expression and cellular infiltration in a controlled cortical impact model in adult male C57BL/6 mice. *PLoS One* 7:e41892
83. Johnson VE, Meaney DF, Cullen DK, Smith DH. 2015. Animal models of traumatic brain injury. *Handb Clin Neurol* 127:115-28
84. Jung YJ, Tweedie D, Scerba MT, Greig NH. 2019. Neuroinflammation as a Factor of Neurodegenerative Disease: Thalidomide Analogs as Treatments. *Front Cell Dev Biol* 7:313
85. Katz PS, Molina PE. 2018. A Lateral Fluid Percussion Injury Model for Studying Traumatic Brain Injury in Rats. *Methods Mol Biol* 1717:27-36
86. Kawai R, Markman T, Poddar R, Ko R, Fantana AL, et al. 2015. Motor cortex is required for learning but not for executing a motor skill. *Neuron* 86:800-12
87. Kelso ML, Gendelman HE. 2014. Bridge between neuroimmunity and traumatic brain injury. *Curr Pharm Des* 20:4284-98
88. Kenney K, Amyot F, Haber M, Pronger A, Bogoslovsky T, et al. 2016. Cerebral Vascular Injury in Traumatic Brain Injury. *Exp Neurol* 275 Pt 3:353-66
89. Khaksari M, Soltani Z, Shahrokhi N. 2018. Effects of Female Sex Steroids Administration on Pathophysiologic Mechanisms in Traumatic Brain Injury. *Transl Stroke Res* 9:393-416
90. Kirkcaldie MTK. 2012. Chapter 4 - Neocortex. In *The Mouse Nervous System*, ed. C Watson, G Paxinos, L Puelles:52-111. San Diego: Academic Press. Number of 52-111 pp.
91. Kitano H, Young JM, Cheng J, Wang L, Hurn PD, Murphy SJ. 2007. Gender-specific response to isoflurane preconditioning in focal cerebral ischemia. *J Cereb Blood Flow Metab* 27:1377-86
92. Klein RS, Lin E, Zhang B, Luster AD, Tollett J, et al. 2005. Neuronal CXCL10 directs CD8+ T-cell recruitment and control of West Nile virus encephalitis. *J Virol* 79:11457-66
93. Klein SL, Flanagan KL. 2016. Sex differences in immune responses. *Nat Rev Immunol* 16:626-38

94. Kokiko-Cochran ON, Godbout JP. 2018. The Inflammatory Continuum of Traumatic Brain Injury and Alzheimer's Disease. *Front Immunol* 9:672
95. Kondo T, Funayama M, Tsukita K, Hotta A, Yasuda A, et al. 2014. Focal transplantation of human iPSC-derived glial-rich neural progenitors improves lifespan of ALS mice. *Stem Cell Reports* 3:242-9
96. Kornev VA, Grebenik EA, Solovieva AB, Dmitriev RI, Timashev PS. 2018. Hydrogel-assisted neuroregeneration approaches towards brain injury therapy: A state-of-the-art review. *Comput Struct Biotechnol J* 16:488-502
97. Kramer TJ, Hack N, Bruhl TJ, Menzel L, Hummel R, et al. 2019. Depletion of regulatory T cells increases T cell brain infiltration, reactive astrogliosis, and interferon-gamma gene expression in acute experimental traumatic brain injury. *J Neuroinflammation* 16:163
98. Kumar RG, Rubin JE, Berger RP, Kochanek PM, Wagner AK. 2016. Principal components derived from CSF inflammatory profiles predict outcome in survivors after severe traumatic brain injury. *Brain Behav Immun* 53:183-93
99. Lagraoui M, Latoche JR, Cartwright NG, Sukumar G, Dalgard CL, Schaefer BC. 2012. Controlled cortical impact and craniotomy induce strikingly similar profiles of inflammatory gene expression, but with distinct kinetics. *Front Neurol* 3:155
100. Lee H, Wintermark M, Gean AD, Ghajar J, Manley GT, Mukherjee P. 2008. Focal lesions in acute mild traumatic brain injury and neurocognitive outcome: CT versus 3T MRI. *J Neurotrauma* 25:1049-56
101. Lewis CT, Savarraj JPJ, McGuire MF, Hergenroeder GW, Alex Choi H, Kitagawa RS. 2019. Elevated inflammation and decreased platelet activity is associated with poor outcomes after traumatic brain injury. *J Clin Neurosci* 70:37-41
102. Liao GP, Harting MT, Hetz RA, Walker PA, Shah SK, et al. 2015. Autologous bone marrow mononuclear cells reduce therapeutic intensity for severe traumatic brain injury in children. *Pediatr Crit Care Med* 16:245-55
103. Liddelow SA, Barres BA. 2017. Reactive Astrocytes: Production, Function, and Therapeutic Potential. *Immunity* 46:957-67
104. Liddelow SA, Guttenplan KA, Clarke LE, Bennett FC, Bohlen CJ, et al. 2017. Neurotoxic reactive astrocytes are induced by activated microglia. *Nature* 541:481-7
105. Lin GQ, He XF, Liang FY, Guo Y, Sunnassee G, et al. 2018. Transplanted human neural precursor cells integrate into the host neural circuit and ameliorate neurological deficits in a mouse model of traumatic brain injury. *Neurosci Lett* 674:11-7
106. Lischka FW, Efthymiou A, Zhou Q, Nieves MD, McCormack NM, et al. 2018. Neonatal mouse cortical but not isogenic human astrocyte feeder layers enhance the functional maturation of induced pluripotent stem cell-derived neurons in culture. *Glia* 66:725-48
107. Liu KK, Dorovini-Zis K. 2012. Differential regulation of CD4+ T cell adhesion to cerebral microvascular endothelium by the beta-chemokines CCL2 and CCL3. *Int J Mol Sci* 13:16119-40
108. Liva SM, de Vellis J. 2001. IL-5 induces proliferation and activation of microglia via an unknown receptor. *Neurochem Res* 26:629-37
109. Loane DJ, Kumar A. 2016. Microglia in the TBI brain: The good, the bad, and the dysregulated. *Exp Neurol* 275 Pt 3:316-27
110. Loane DJ, Kumar A, Stoica BA, Cabatbat R, Faden AI. 2014. Progressive neurodegeneration after experimental brain trauma: association with chronic microglial activation. *J Neuropathol Exp Neurol* 73:14-29
111. Lyu J, Jiang X, Leak RK, Shi Y, Hu X, Chen J. 2021. Microglial Responses to Brain Injury and Disease: Functional Diversity and New Opportunities. *Transl Stroke Res* 12:474-95

112. Ma X, Aravind A, Pfister BJ, Chandra N, Haorah J. 2019. Animal Models of Traumatic Brain Injury and Assessment of Injury Severity. *Mol Neurobiol* 56:5332-45
113. Mamlouk GM, Dorris DM, Barrett LR, Meitzen J. 2020. Sex bias and omission in neuroscience research is influenced by research model and journal, but not reported NIH funding. *Front Neuroendocrinol* 57:100835
114. Manners JL, Forsten RD, Kotwal RS, Elbin RJ, Collins MW, Kontos AP. 2016. Role of Pre-Morbid Factors and Exposure to Blast Mild Traumatic Brain Injury on Post-Traumatic Stress in United States Military Personnel. *J Neurotrauma* 33:1796-801
115. Marehbian J, Muehlschlegel S, Edlow BL, Hinson HE, Hwang DY. 2017. Medical Management of the Severe Traumatic Brain Injury Patient. *Neurocrit Care* 27:430-46
116. Margulies S, Anderson G, Atif F, Badaut J, Clark R, et al. 2016. Combination Therapies for Traumatic Brain Injury: Retrospective Considerations. *J Neurotrauma* 33:101-12
117. McCabe JT, Tucker LB. 2020. Sex as a Biological Variable in Preclinical Modeling of Blast-Related Traumatic Brain Injury. *Front Neurol* 11:541050
118. McCarthy MM, Arnold AP, Ball GF, Blaustein JD, De Vries GJ. 2012. Sex differences in the brain: the not so inconvenient truth. *J Neurosci* 32:2241-7
119. McCrea M, Iverson GL, McAllister TW, Hammeke TA, Powell MR, et al. 2009. An integrated review of recovery after mild traumatic brain injury (MTBI): implications for clinical management. *Clin Neuropsychol* 23:1368-90
120. McCrea M, Pliskin N, Barth J, Cox D, Fink J, et al. 2008. Official position of the military TBI task force on the role of neuropsychology and rehabilitation psychology in the evaluation, management, and research of military veterans with traumatic brain injury. *Clin Neuropsychol* 22:10-26
121. McGinn MJ, Povlishock JT. 2016. Pathophysiology of Traumatic Brain Injury. *Neurosurg Clin N Am* 27:397-407
122. McInnes K, Friesen CL, MacKenzie DE, Westwood DA, Boe SG. 2019. Correction: Mild Traumatic Brain Injury (mTBI) and chronic cognitive impairment: A scoping review. *PLoS One* 14:e0218423
123. McKee AC, Daneshvar DH. 2015. The neuropathology of traumatic brain injury. *Handb Clin Neurol* 127:45-66
124. Miller AM. 2011. Role of IL-33 in inflammation and disease. *J Inflamm (Lond)* 8:22
125. Miller LR, Marks C, Becker JB, Hurn PD, Chen WJ, et al. 2017. Considering sex as a biological variable in preclinical research. *FASEB J* 31:29-34
126. Mohamadpour M, Whitney K, Bergold PJ. 2019. The Importance of Therapeutic Time Window in the Treatment of Traumatic Brain Injury. *Front Neurosci* 13:07
127. Mollayeva T, Mollayeva S, Colantonio A. 2018. Traumatic brain injury: sex, gender and intersecting vulnerabilities. *Nat Rev Neurol* 14:711-22
128. Morandell K, Huber D. 2017. The role of forelimb motor cortex areas in goal directed action in mice. *Sci Rep* 7:15759
129. Morganti-Kossmann MC, Semple BD, Hellewell SC, Bye N, Ziebell JM. 2019. The complexity of neuroinflammation consequent to traumatic brain injury: from research evidence to potential treatments. *Acta Neuropathol* 137:731-55
130. Morganti JM, Jopson TD, Liu S, Riparip LK, Guandique CK, et al. 2015. CCR2 antagonism alters brain macrophage polarization and ameliorates cognitive dysfunction induced by traumatic brain injury. *J Neurosci* 35:748-60
131. Morganti JM, Riparip LK, Rosi S. 2016. Call Off the Dog(ma): M1/M2 Polarization Is Concurrent following Traumatic Brain Injury. *PLoS One* 11:e0148001

132. Mukherjee S, Arisi GM, Mims K, Hollingsworth G, O'Neil K, Shapiro LA. 2020. Neuroinflammatory mechanisms of post-traumatic epilepsy. *J Neuroinflammation* 17:193
133. Mychasiuk R, Farran A, Angoa-Perez M, Briggs D, Kuhn D, Esser MJ. 2014. A novel model of mild traumatic brain injury for juvenile rats. *J Vis Exp*
134. Nampiaparampil DE. 2008. Prevalence of chronic pain after traumatic brain injury: a systematic review. *Jama* 300:711-9
135. National Academies of Sciences E, and Medicine. 2019. Diagnosis and Assessment of Traumatic Brain Injury. In *Evaluation of the Disability Determination Process for Traumatic Brain Injury in Veterans*. Washington (DC). Number of.
136. Nieves MD, Furmanski O, Doiughty ML. 2020. Host Sex and Transplanted Human Induced Pluripotent Stem Cell Phenotype Interact to Influence Sensorimotor Recovery in a Mouse Model of Cortical Contusion Injury. *Brain Research* In press
137. O'Connor CA, Cernak I, Vink R. 2003. Interaction between anesthesia, gender, and functional outcome task following diffuse traumatic brain injury in rats. *J Neurotrauma* 20:533-41
138. Paterno R, Folweiler KA, Cohen AS. 2017. Pathophysiology and Treatment of Memory Dysfunction After Traumatic Brain Injury. *Curr Neurol Neurosci Rep* 17:52
139. Pearn ML, Niesman IR, Egawa J, Sawada A, Almenar-Queralt A, et al. 2017. Pathophysiology Associated with Traumatic Brain Injury: Current Treatments and Potential Novel Therapeutics. *Cell Mol Neurobiol* 37:571-85
140. Peron S, Droguerre M, Debarbieux F, Ballout N, Benoit-Marand M, et al. 2017. A Delay between Motor Cortex Lesions and Neuronal Transplantation Enhances Graft Integration and Improves Repair and Recovery. *J Neurosci* 37:1820-34
141. Petrisko TJ, Bloemer J, Pinky PD, Srinivas S, Heslin RT, et al. 2020. Neuronal CXCL10/CXCR3 Axis Mediates the Induction of Cerebral Hyperexcitability by Peripheral Viral Challenge. *Front Neurosci* 14:220
142. Putatunda R, Bethea JR, Hu WH. 2018. Potential immunotherapies for traumatic brain and spinal cord injury. *Chin J Traumatol* 21:125-36
143. Radomski KL, Zhou Q, Yi KJ, Doughty ML. 2013. Cortical contusion injury disrupts olfactory bulb neurogenesis in adult mice. *BMC Neurosci* 14:142
144. Rais Y, Zviran A, Geula S, Gafni O, Chomsky E, et al. 2013. Deterministic direct reprogramming of somatic cells to pluripotency. *Nature* 502:65-70
145. Rais Y, Zviran A, Geula S, Gafni O, Chomsky E, et al. 2015. Corrigendum: Deterministic direct reprogramming of somatic cells to pluripotency. *Nature* 520:710
146. Rao HM, Talkar T, Ciccarelli G, Nolan M, O'Brien A, et al. 2020. Sensorimotor conflict tests in an immersive virtual environment reveal subclinical impairments in mild traumatic brain injury. *Sci Rep* 10:14773
147. Rauen K, Reichelt L, Probst P, Schapers B, Muller F, et al. 2020. Quality of life up to 10 years after traumatic brain injury: a cross-sectional analysis. *Health Qual Life Outcomes* 18:166
148. Rigon A, Turkstra L, Mutlu B, Duff M. 2016. The female advantage: sex as a possible protective factor against emotion recognition impairment following traumatic brain injury. *Cogn Affect Behav Neurosci* 16:866-75
149. Roth TL, Nayak D, Atanasijevic T, Koretsky AP, Latour LL, McGavern DB. 2014. Transcranial amelioration of inflammation and cell death after brain injury. *Nature* 505:223-8

150. Rowe RK, Ellis GI, Harrison JL, Bachstetter AD, Corder GF, et al. 2016. Diffuse traumatic brain injury induces prolonged immune dysregulation and potentiates hyperalgesia following a peripheral immune challenge. *Mol Pain* 12
151. Rubin TG, Lipton ML. 2019. Sex Differences in Animal Models of Traumatic Brain Injury. *J Exp Neurosci* 13:1179069519844020
152. Rui P, Kang K. 2017. National Hospital Ambulatory Medical Care Survey: 2017 emergency department summary tables. In *National Center for Health Statistics*, p. 15. Available from: https://www.cdc.gov/nchs/data/nhamcs/web_tables/2017_ed_web_tables-508.pdf
153. Russo MV, McGavern DB. 2016. Inflammatory neuroprotection following traumatic brain injury. *Science* 353:783-5
154. Saber M, Kokiko-Cochran O, Puntambekar SS, Lathia JD, Lamb BT. 2017. Triggering Receptor Expressed on Myeloid Cells 2 Deficiency Alters Acute Macrophage Distribution and Improves Recovery after Traumatic Brain Injury. *J Neurotrauma* 34:423-35
155. Sandsmark DK, Bashir A, Wellington CL, Diaz-Arrastia R. 2019. Cerebral Microvascular Injury: A Potentially Treatable Endophenotype of Traumatic Brain Injury-Induced Neurodegeneration. *Neuron* 103:367-79
156. Sandsmark DK, Elliott JE, Lim MM. 2017. Sleep-Wake Disturbances After Traumatic Brain Injury: Synthesis of Human and Animal Studies. *Sleep* 40
157. Sawada M, Suzumura A, Itoh Y, Marunouchi T. 1993. Production of interleukin-5 by mouse astrocytes and microglia in culture. *Neurosci Lett* 155:175-8
158. Schaar KL, Brenneman MM, Savitz SI. 2010. Functional assessments in the rodent stroke model. *Exp Transl Stroke Med* 2:13
159. Schwartz M. 2000. Beneficial autoimmune T cells and posttraumatic neuroprotection. *Ann N Y Acad Sci* 917:341-7
160. Selya AS, Rose JS, Dierker LC, Hedeker D, Mermelstein RJ. 2012. A Practical Guide to Calculating Cohen's f(2), a Measure of Local Effect Size, from PROC MIXED. *Front Psychol* 3:111
161. Semple BD, Bye N, Rancan M, Ziebell JM, Morganti-Kossmann MC. 2010. Role of CCL2 (MCP-1) in traumatic brain injury (TBI): evidence from severe TBI patients and CCL2-/- mice. *J Cereb Blood Flow Metab* 30:769-82
162. Semple BD, Bye N, Ziebell JM, Morganti-Kossmann MC. 2010. Deficiency of the chemokine receptor CXCR2 attenuates neutrophil infiltration and cortical damage following closed head injury. *Neurobiology of disease* 40:394-403
163. Sergio LE, Gorbet DJ, Adams MS, Dobney DM. 2020. The Effects of Mild Traumatic Brain Injury on Cognitive-Motor Integration for Skilled Performance. *Front Neurol* 11:541630
164. Shafa M, Yang F, Fellner T, Rao MS, Baghbaderani BA. 2018. Human-Induced Pluripotent Stem Cells Manufactured Using a Current Good Manufacturing Practice-Compliant Process Differentiate Into Clinically Relevant Cells From Three Germ Layers. *Front Med (Lausanne)* 5:69
165. Sharma A, Sane H, Kulkarni P, Yadav J, Gokulchandran N, et al. 2015. Cell therapy attempted as a novel approach for chronic traumatic brain injury - a pilot study. *Springerplus* 4:26
166. Sharma R, Khristov V, Rising A, Jha BS, Dejene R, et al. 2019. Clinical-grade stem cell-derived retinal pigment epithelium patch rescues retinal degeneration in rodents and pigs. *Science translational medicine* 11

167. Shechter R, London A, Varol C, Raposo C, Cusimano M, et al. 2009. Infiltrating blood-derived macrophages are vital cells playing an anti-inflammatory role in recovery from spinal cord injury in mice. *PLoS Med* 6:e1000113
168. Sheriff FG, Hinson HE. 2015. Pathophysiology and clinical management of moderate and severe traumatic brain injury in the ICU. *Semin Neurol* 35:42-9
169. Shiozaki T, Hayakata T, Tasaki O, Hosotubo H, Fuijita K, et al. 2005. Cerebrospinal fluid concentrations of anti-inflammatory mediators in early-phase severe traumatic brain injury. *Shock* 23:406-10
170. Shlosberg D, Benifla M, Kaufer D, Friedman A. 2010. Blood-brain barrier breakdown as a therapeutic target in traumatic brain injury. *Nat Rev Neurol* 6:393-403
171. Shultz SR, McDonald SJ, Vonder Haar C, Meconi A, Vink R, et al. 2017. The potential for animal models to provide insight into mild traumatic brain injury: Translational challenges and strategies. *Neurosci Biobehav Rev* 76:396-414
172. Siebold L, Obenaus A, Goyal R. 2018. Criteria to define mild, moderate, and severe traumatic brain injury in the mouse controlled cortical impact model. *Exp Neurol* 310:48-57
173. Simon DW, McGeachy MJ, Bayir H, Clark RS, Loane DJ, Kochanek PM. 2017. The far-reaching scope of neuroinflammation after traumatic brain injury. *Nat Rev Neurol* 13:171-91
174. Siva Sai Sujith Sajja B, Tenn C, McLaws LJ, VandeVord P. 2014. IL-5; a diffuse biomarker associated with brain inflammation after blast exposure. *Biomed Sci Instrum* 50:375-82
175. Skardelly M, Gaber K, Burdack S, Scheidt F, Hilbig H, et al. 2011. Long-term benefit of human fetal neuronal progenitor cell transplantation in a clinically adapted model after traumatic brain injury. *J Neurotrauma* 28:401-14
176. Smith PF, Renner RM, Haslett SJ. 2016. Compositional data in neuroscience: If you've got it, log it! *J Neurosci Methods* 271:154-9
177. Sorensen TL, Trebst C, Kivisakk P, Klaege KL, Majmudar A, et al. 2002. Multiple sclerosis: a study of CXCL10 and CXCR3 co-localization in the inflamed central nervous system. *J Neuroimmunol* 127:59-68
178. Spani CB, Braun DJ, Van Eldik LJ. 2018. Sex-related responses after traumatic brain injury: Considerations for preclinical modeling. *Front Neuroendocrinol* 50:52-66
179. Springer JE, Prajapati P, Sullivan PG. 2018. Targeting the mitochondrial permeability transition pore in traumatic central nervous system injury. *Neural Regen Res* 13:1338-41
180. Steinbeck JA, Choi SJ, Mrejeru A, Ganat Y, Deisseroth K, et al. 2015. Optogenetics enables functional analysis of human embryonic stem cell-derived grafts in a Parkinson's disease model. *Nat Biotechnol* 33:204-9
181. Steinbeck JA, Studer L. 2015. Moving stem cells to the clinic: potential and limitations for brain repair. *Neuron* 86:187-206
182. Stocchetti N, Zanier ER. 2016. Chronic impact of traumatic brain injury on outcome and quality of life: a narrative review. *Crit Care* 20:148
183. Stuart DG, Hultborn H. 2008. Thomas Graham Brown (1882--1965), Anders Lundberg (1920-), and the neural control of stepping. *Brain Res Rev* 59:74-95
184. Su Y, Fan W, Ma Z, Wen X, Wang W, et al. 2014. Taurine improves functional and histological outcomes and reduces inflammation in traumatic brain injury. *Neuroscience* 266:56-65
185. Sulhan S, Lyon KA, Shapiro LA, Huang JH. 2020. Neuroinflammation and blood-brain barrier disruption following traumatic brain injury: Pathophysiology and potential therapeutic targets. *J Neurosci Res* 98:19-28

186. Sullivan KA, Kempe CB, Edmed SL, Bonanno GA. 2016. Resilience and Other Possible Outcomes After Mild Traumatic Brain Injury: a Systematic Review. *Neuropsychol Rev* 26:173-85
187. Sun AX, Yuan Q, Tan S, Xiao Y, Wang D, et al. 2016. Direct Induction and Functional Maturation of Forebrain GABAergic Neurons from Human Pluripotent Stem Cells. *Cell Rep* 16:1942-53
188. Tajiri N, Acosta SA, Shahaduzzaman M, Ishikawa H, Shinozuka K, et al. 2014. Intravenous transplants of human adipose-derived stem cell protect the brain from traumatic brain injury-induced neurodegeneration and motor and cognitive impairments: cell graft biodistribution and soluble factors in young and aged rats. *J Neurosci* 34:313-26
189. Takahashi K, Tanabe K, Ohnuki M, Narita M, Ichisaka T, et al. 2007. Induction of pluripotent stem cells from adult human fibroblasts by defined factors. *Cell* 131:861-72
190. Takamiya M, Fujita S, Saigusa K, Aoki Y. 2007. Simultaneous detections of 27 cytokines during cerebral wound healing by multiplexed bead-based immunoassay for wound age estimation. *J Neurotrauma* 24:1833-44
191. Tasci A, Okay O, Gezici AR, Ergun R, Ergungor F. 2003. Prognostic value of interleukin-1 beta levels after acute brain injury. *Neurol Res* 25:871-4
192. Taylor CJ, Peacock S, Chaudhry AN, Bradley JA, Bolton EM. 2012. Generating an iPSC bank for HLA-matched tissue transplantation based on known donor and recipient HLA types. *Cell Stem Cell* 11:147-52
193. Tennant KA, Adkins DL, Donlan NA, Asay AL, Thomas N, et al. 2011. The organization of the forelimb representation of the C57BL/6 mouse motor cortex as defined by intracortical microstimulation and cytoarchitecture. *Cereb Cortex* 21:865-76
194. Thelin EP, Tajsic T, Zeiler FA, Menon DK, Hutchinson PJA, et al. 2017. Monitoring the Neuroinflammatory Response Following Acute Brain Injury. *Front Neurol* 8:351
195. Thompson LH, Bjorklund A. 2015. Reconstruction of brain circuitry by neural transplants generated from pluripotent stem cells. *Neurobiology of disease* 79:28-40
196. Tucker LB, Fu AH, McCabe JT. 2016. Performance of Male and Female C57BL/6J Mice on Motor and Cognitive Tasks Commonly Used in Pre-Clinical Traumatic Brain Injury Research. *J Neurotrauma* 33:880-94
197. Tweedie D, Karnati HK, Mullins R, Pick CG, Hoffer BJ, et al. 2020. Time-dependent cytokine and chemokine changes in mouse cerebral cortex following a mild traumatic brain injury. *Elife* 9
198. Uchino H, Minamikawa-Tachino R, Kristian T, Perkins G, Narazaki M, et al. 2002. Differential neuroprotection by cyclosporin A and FK506 following ischemia corresponds with differing abilities to inhibit calcineurin and the mitochondrial permeability transition. *Neurobiology of disease* 10:219-33
199. Utagawa A, Truettner JS, Dietrich WD, Bramlett HM. 2008. Systemic inflammation exacerbates behavioral and histopathological consequences of isolated traumatic brain injury in rats. *Exp Neurol* 211:283-91
200. Vaughan LE, Ranganathan PR, Kumar RG, Wagner AK, Rubin JE. 2018. A mathematical model of neuroinflammation in severe clinical traumatic brain injury. *J Neuroinflammation* 15:345
201. Villapol S, Loane DJ, Burns MP. 2017. Sexual dimorphism in the inflammatory response to traumatic brain injury. *Glia* 65:1423-38
202. von Leden RE, Parker KN, Bates AA, Noble-Haeusslein LJ, Donovan MH. 2019. The emerging role of neutrophils as modifiers of recovery after traumatic injury to the developing brain. *Exp Neurol* 317:144-54

203. Waldron J, Lecanu L. 2011. Age and sex differences in neural stem cell transplantation: a descriptive study in rats. *Stem Cells Cloning* 4:25-37
204. Walsh JT, Hendrix S, Boato F, Smirnov I, Zheng J, et al. 2015. MHCII-independent CD4+ T cells protect injured CNS neurons via IL-4. *J Clin Invest* 125:699-714
205. Wang C, Iashchishyn IA, Kara J, Fodera V, Vetri V, et al. 2019. Proinflammatory and amyloidogenic S100A9 induced by traumatic brain injury in mouse model. *Neurosci Lett* 699:199-205
206. Wang Z, Luo Y, Chen L, Liang W. 2017. Safety of neural stem cell transplantation in patients with severe traumatic brain injury. *Exp Ther Med* 13:3613-8
207. Wanner IB, Anderson MA, Song B, Levine J, Fernandez A, et al. 2013. Glial scar borders are formed by newly proliferated, elongated astrocytes that interact to corral inflammatory and fibrotic cells via STAT3-dependent mechanisms after spinal cord injury. *J Neurosci* 33:12870-86
208. Ware JB, Dolui S, Duda J, Gaggi N, Choi R, et al. 2020. Relationship of Cerebral Blood Flow to Cognitive Function and Recovery in Early Chronic Traumatic Brain Injury. *J Neurotrauma*
209. Wattananit S, Tornero D, Graubardt N, Memanishvili T, Monni E, et al. 2016. Monocyte-Derived Macrophages Contribute to Spontaneous Long-Term Functional Recovery after Stroke in Mice. *J Neurosci* 36:4182-95
210. Weckbach S, Neher M, Losacco JT, Bolden AL, Liudmila Kulik MAF, et al. 2012. Challenging the role of adaptive immunity in neurotrauma: Rag1(-/-) mice lacking mature B and T cells do not show neuroprotection after closed head injury. *Neurotrauma* 10:1233-42
211. Wennersten A, Meier X, Holmin S, Wahlberg L, Mathiesen T. 2004. Proliferation, migration, and differentiation of human neural stem/progenitor cells after transplantation into a rat model of traumatic brain injury. *J Neurosurg* 100:88-96
212. Williams G, Morris ME, Schache A, McCrory P. 2009. Observational gait analysis in traumatic brain injury: accuracy of clinical judgment. *Gait Posture* 29:454-9
213. Wilson L, Stewart W, Dams-O'Connor K, Diaz-Arrastia R, Horton L, et al. 2017. The chronic and evolving neurological consequences of traumatic brain injury. *Lancet Neurol* 16:813-25
214. Winkler EA, Minter D, Yue JK, Manley GT. 2016. Cerebral Edema in Traumatic Brain Injury: Pathophysiology and Prospective Therapeutic Targets. *Neurosurg Clin N Am* 27:473-88
215. Wofford KL, Loane DJ, Cullen DK. 2019. Acute drivers of neuroinflammation in traumatic brain injury. *Neural Regen Res* 14:1481-9
216. Woitowich NC, Beery A, Woodruff T. 2020. A 10-year follow-up study of sex inclusion in the biological sciences. *Elife* 9
217. Woodcock T, Morganti-Kossmann MC. 2013. The role of markers of inflammation in traumatic brain injury. *Front Neurol* 4:18
218. Wright DW, Yeatts SD, Silbergleit R, Palesch YY, Hertzberg VS, et al. 2014. Very early administration of progesterone for acute traumatic brain injury. *N Engl J Med* 371:2457-66
219. Wu S, FitzGerald KT, Giordano J. 2018. On the Viability and Potential Value of Stem Cells for Repair and Treatment of Central Neurotrauma: Overview and Speculations. *Front Neurol* 9:602

220. Xiong Y, Mahmood A, Chopp M. 2018. Current understanding of neuroinflammation after traumatic brain injury and cell-based therapeutic opportunities. *Chin J Traumatol* 21:137-51
221. Xu L, Ryu J, Hiel H, Menon A, Aggarwal A, et al. 2015. Transplantation of human oligodendrocyte progenitor cells in an animal model of diffuse traumatic axonal injury: survival and differentiation. *Stem cell research & therapy* 6:93
222. Yan Y, Shin S, Jha BS, Liu Q, Sheng J, et al. 2013. Efficient and rapid derivation of primitive neural stem cells and generation of brain subtype neurons from human pluripotent stem cells. *Stem cells translational medicine* 2:862-70
223. Yu S, Kaneko Y, Bae E, Stahl CE, Wang Y, et al. 2009. Severity of controlled cortical impact traumatic brain injury in rats and mice dictates degree of behavioral deficits. *Brain Res* 1287:157-63
224. Yuan F, Fang KH, Cao SY, Qu ZY, Li Q, et al. 2015. Efficient generation of region-specific forebrain neurons from human pluripotent stem cells under highly defined condition. *Sci Rep* 5:18550
225. Yuan T, Liao W, Feng NH, Lou YL, Niu X, et al. 2013. Human induced pluripotent stem cell-derived neural stem cells survive, migrate, differentiate, and improve neurologic function in a rat model of middle cerebral artery occlusion. *Stem cell research & therapy* 4:73
226. Zeiler FA, McFadyen C, Newcombe VFJ, Synnot A, Donoghue EL, et al. 2019. Genetic Influences on Patient-Oriented Outcomes in Traumatic Brain Injury: A Living Systematic Review of Non-Apolipoprotein E Single-Nucleotide Polymorphisms. *J Neurotrauma*
227. Zhang ZX, Guan LX, Zhang K, Zhang Q, Dai LJ. 2008. A combined procedure to deliver autologous mesenchymal stromal cells to patients with traumatic brain injury. *Cytotherapy* 10:134-9
228. Zibara K, Ballout N, Mondello S, Karnib N, Ramadan N, et al. 2019. Combination of drug and stem cells neurotherapy: Potential interventions in neurotrauma and traumatic brain injury. *Neuropharmacology* 145:177-98